Elevated Phosphate-Induced Cell Signaling through Phosphate Transporter PiT-1 in Vascular Smooth Muscle Cells

Nicholas W. Chavkin

A dissertation submitted in partial fulfillment of the requirements for the degree of

Doctor of Philosophy

University of Washington

2016

Chair
Cecilia Giachelli

Committee Members
Deok-Ho Kim
Suzie Pun
Marta Scatena

Program Authorized to Offer Degree
Bioengineering

University of Washington

Abstract

Elevated Phosphate-Induced Cell Signaling through Phosphate Transporter PiT-1 in Vascular Smooth Muscle Cells

Nicholas W. Chavkin

Chairperson of the Supervisory Committee:
Professor Cecilia M. Giachelli
Department of Bioengineering

Vascular calcification (VC) is prevalent in chronic kidney disease and elevated serum inorganic phosphate (Pi) is a recognized risk factor. The type III sodium-dependent phosphate transporter, PiT-1, is required for elevated Pi-induced osteochondrogenic differentiation and matrix mineralization in vascular smooth muscle cells (VSMCs). However, the molecular mechanism(s) by which PiT-1 promotes these processes is unclear. The research presented in this thesis addresses the role of PiT-1 in vascular calcification mechanisms. First, the Pi concentration required to induce osteochondrogenic differentiation and matrix mineralization of mouse VSMCs was found to be much greater than that required for maximal Pi uptake, suggesting a signaling function of PiT-1 that was independent of Pi transport. Next, Pi transport-independent functions of PiT-1 were found to promote responses to elevated Pi in VSMCs, including ERK1/2 phosphorylation, osteochondrogenic differentiation, and matrix mineralization. Finally, elevated Pi was found to induce binding between PiT-1 and RapGEF1 in VSMCs, and RapGEF1 was required for elevated Pi-induced ERK1/2 phosphorylation through a Rap1/B-Raf/Mek1/2 pathway that promotes VSMC phenotype change. Together, the data presented here shows that elevated Pi promotes PiT-1 binding to RapGEF1 and ERK1/2

phosphorylation through Rap1/B-Raf/Mek1/2, which induces osteochondrogenic differentiation and matrix mineralization of VSMCs.

TABLE OF CONTENTS

LIST OF FIGURES

LIST OF TABLES

Acknowledgements

I could not have finished this dissertation without the support and guidance from all of my colleagues, friends, and family. Everyone has given me outstanding advice, without which I would not have been able to present this work.

First, I would like to acknowledge my advisor, Ceci Giachelli. Five years ago, she gave me the opportunity to start working on a project about a phosphate transporter. Along the way she has guided me through everything about my project, but also taught me to think more critically, ask the right questions, and design ways to answer those questions. She has been everything that I could want in a mentor.

Each lab member who has been in the Giachelli Lab while I've been working here has also helped me immensely. I'd like to thank Mei Speer, Liz Soberg, Hsueh Ying, and Manuela Borges, for teaching me numerous lab techniques, guidance through troubleshooting difficult assays, and helping me define my research goals and aims. My undergraduate student, Kadin Brooks, has helped with multiple experiments and pushed me to be more knowledgeable on my own project and a better mentor to those I get to teach and train. Two postdoctoral researchers, Matt Crouthamel and Mary Wallingford, have always been willing to listen to my data, help interpret findings, and guide the next steps. Mary has also been extremely helpful with career planning and looking at the big picture. And I'd like to thank all of the graduate students and research scientists who have been in the lab while I've been here and have talked and listened

through many experiments: Ice Buranaphatthana, Ted Chen, Jia Jun Chia, Jesse McClellan, Stephanie Miller, Ngoc Nguyen, and Cameron Rementer.

Finally, I'd like to thank my family for their support. My parents, Mary Lidstrom and Charles Chavkin, have always been there for me with love and advice. My brother, Ted Chavkin, has been more help than he realizes, and is always willing to listen to my research and ideas. And lastly and most importantly, my wife, Zoe, who had known that I wanted to go to grad school before I did, who offers constant love and support for everything I do, and without whom this would not have been possible.

Dedication

For Zoe, my inspiration

CHAPTER 1

INTRODUCTION

1.1 Clinical Significance

Vascular Calcification

Vascular calcification is the inappropriate deposition of bone mineral in the form of calcium phosphate crystals into the soft tissue of the vasculature, which disrupts normal vascular function. Prevalence of vascular calcification in the United States is extremely high and increases with age, with coronary artery calcium present in 9.6% of adults aged 33-45 and 50% of adults aged 45-84 [1,2]. Healthy vascular tissue is elastic and can respond to pressure differences from each heartbeat. However, normal elastic function is disrupted with calcification, which decreases tissue function and compliance leading to increased pulse wave velocity [3,4], valve regurgitation [5], and plaque instability [6,7]. All of these outcomes are correlated with an increased risk of cardiovascular morbidity and mortality [8–14].

There are three main locations where vascular calcification occurs: heart valves, arterial intimal layers, and arterial medial layers. Calcification of heart valves causes irreversible valve failure that blocks heart valves from properly opening and closing, leading to increased risk of death [9,15]. Arterial intimal calcification is mineral in the lumen of an artery, and this occurs mainly in atherosclerotic plaques. Classical risk factors for intimal calcification include old age, diabetes, smoking, high cholesterol diets, hypertension, and chronic kidney disease [16,17].

Mineralization of atherosclerotic plaques has been positively correlated with increased plaque instability [18,19], which leads to plaque rupture, thrombosis, and possible embolism associated with myocardial infarction or stroke. Arterial medial calcification occurs in the medial layer of the arterial wall and is associated with old age, diabetes, and chronic kidney disease [20,21]. Although initially believed to be non-detrimental, medial calcification is now positively correlated with increased pulse wave velocity and cardiovascular morbidity and mortality [22–25]. All three of these types of vascular calcification will inhibit vascular tissue function and lead to an increased risk of death.

Chronic Kidney Disease

Both arterial intimal calcification and arterial medial calcification are highly prevalent in patients with Chronic Kidney Disease (CKD). In normal kidney function, specific small molecules are filtered from the blood to the kidneys through glomeruli and into nephrons, where some of the small molecules are re-absorbed back into the blood and others are excreted as urine. CKD is a disease of the kidneys where the Glomerular Filtration Rate (GFR) is reduced, which leads to less filtration of the blood and more blood toxins present. CKD progresses from Stage 1 to Stage 5 as defined by a patient's reduction in GFR, and by Stage 5 the patient is in End Stage Renal Disease (ESRD) and will require hemodialysis to replace the kidney filtration function. Interestingly, arterial calcification is extremely prevalent in patients with pre-dialysis CKD and end-stage renal disease requiring dialysis [26,27]. This increase in arterial calcification prevalence is also correlated with an increase in cardiovascular mortality. Cardiovascular mortality is 10-30 times greater in CKD patients than age-matched controls [28,29]. Patients with CKD are more likely to die from cardiovascular disease than start dialysis [30]. Even on

dialysis, arterial calcification strongly predicts mortality. One clinical study following patients in ESRD showed that presence of arterial medial calcification or arterial intimal calcification reduced 5-year patient survival to 50% and 23%, respectively, compared to a 5-year survival of 90% for patients in ESRD with no arterial calcification [31]. Patients with CKD also show a decrease in bone density, prompting the American Society of Nephrology to re-classify CKD as Chronic Kidney Disease-Mineral Bone Disorder (CKD-MBD) [32], which more accurately describes the effects of kidney disease on bone mineral.

Hyperphosphatemia

Vascular calcification in CKD-MBD is associated with hyperphosphatemia, which is the increased concentration of inorganic phosphate (Pi) in patient blood serum and highly prevalent in CKD-MBD. Pi is an essential molecule that is the backbone of DNA, RNA, and plasma membrane lipids. Pi is required for the ability of ATP to store energy, and addition of Pi to proteins can promote cell signaling cascades and change enzyme activity. Along with calcium, Pi also makes up hydroxyapatite, which is the mineral found in vascular calcification and bone. Most of the inorganic phosphate in the body is in the bone (85%), with some in other tissues (14%) and a very small portion in extracellular fluid (1%) [33]. Since Pi is so important to many biological functions, Pi concentration in blood is strictly regulated by the intestines and the kidneys. People eat around 900mg of Pi per day in a western diet through the intestines, and healthy kidneys filter out enough of the ingested Pi to keep a stable blood serum Pi concentration of 1.0 mM Pi [32,34–37]. However, increase in serum Pi concentration is associated with vascular calcification. In patients with CKD-MBD, serum Pi concentration was directly correlated to degree of vascular calcification [38–41]. These clinical studies have been

reproduced in a mouse model where a 5/6 nephrectomy surgery causes uremia, a high Pi diet causes hyperphosphatemia, and arterial medial calcification is present [42]. Additionally, hyperphosphatemia in the general population have been associated with higher risk for vascular calcification [43–45].

Patients with CKD-MBD are at high risk of hyperphosphatemia due to declining kidney function. Multiple studies on Pi concentration and Pi homeostasis hormones have elucidated the complicated mechanism leading to hyperphosphatemia in CKD-MBD. In early-stage CKD-MBD, kidney filtration is slightly reduced, leading to decreased Pi filtration into the nephrons. However, Pi homeostasis hormones are upregulated to counteract this possible imbalance. Fibroblast Growth Factor 23 (FGF-23) and Parathyroid Hormone (PTH) are upregulated, which internalizes and inhibits the function of the type II sodium-dependent Pi transporter, NaPi-IIa, that would normally transport Pi back into the blood [46,47]. Down-regulation of 1,25-dihydroxyvitamin D will inhibit intestinal absorption of Pi by blocking the intestinal type II sodium-dependent Pi transporter, NaPi-IIb [48]. With less Pi re-absorption in nephrons, more Pi is excreted in urine and Pi levels are maintained in the normal range. As CKD-MBD progresses to later stages, further hormonal imbalances occur. The hormone Klotho, which is normally a required co-factor for FGF-23 activation, is down-regulated in late-stage CKD and promotes renal Pi retention and increased serum Pi [49]. High levels of FGF-23 also promote bone remodeling, which brings Pi from bone crystal into the blood and further promotes elevated serum Pi [47]. Eventually, Pi hormones cannot compensate for the reduction in kidney filtration, and the result is hyperphosphatemia. Indeed, hyperphosphatemia is a strong predictor of cardiovascular morbidity and mortality in the CKD-MBD population [50–52].

Current Treatments

Although current treatments for treating CKD-MBD target kidney disease progression and hyperphosphatemia, these treatments lack efficacy to prevent vascular calcification. One method is to limit the progression of CKD, which will sustain kidney function to maintain Pi homeostasis. Hypertension-controlling drugs, such as angiotensin-converting enzyme inhibitors (ACEi), have been used at the onset of CKD to limit kidney damage from high blood pressure [53]. However, recent studies have called this treatment into question [54,55], and current clinical trials are ongoing to re-evaluate ACEi treatment in CKD patients [56]. Sodium thiosulfate is another vasodilator that can bind calcium and has been shown to inhibit vascular calcification in an animal model, but this also caused low bone density of the animals and clinical trials are proceeding cautiously [57,58]. Another method of eliminating elevated Pi from the blood is hemodialysis, but hemodialysis does not block vascular calcification. Removal of Pi by hemodialysis is not very efficient since Pi binds tightly to H_2O and inhibits its movement through dialysis membranes [59], and hemodialysis also promotes vascular calcification through induction of vascular smooth muscle cell apoptosis [60]. Pi binders can be prescribed to CKD patients to limit hyperphosphatemia. Pi binders work by binding Pi in the intestinal tract so that it cannot be ingested into the blood [61]. There are two current types of Pi binders: calcium containing Pi binders and non-calcium containing Pi binders. Unfortunately, calcium containing Pi binders, such as Calcium acetate, promote coronary artery calcification, and non-calcium containing Pi binders, such as Sevelamer, have not consistently inhibited the progression of vascular calcification [62]. The last resort for end-stage renal disease patients is for a kidney transplant to increase kidney filtration, but cardiovascular mortality is still 2-5 times more

prevalent in kidney transplants patients compared to the general population [29]. Therefore, there is a strong need for a treatment that can target progression of vascular calcification on a cellular level.

1.2 Vascular smooth muscle cells

Vascular smooth muscle cell biology

The main type of cell in arteries and arterioles is a vascular smooth muscle cell (VSMC). The medial layer of arteries and arterioles is comprised of VSMCs and extracellular matrix components, mainly elastin and collagen. The primary function of VSMCs is to control vascular lumen size through sustained muscle contraction. VSMCs can contract through smooth muscle-specific myosin and actin interactions induced by calcium binding to calmodulin, which creates a weaker but sustained muscle contraction when compared to striated skeletal muscle [63]. Greater contraction will decrease lumen size (vasoconstriction) and less contraction will increase lumen size (vasodilation). Vasoconstriction and vasodilation are controlled by the renin angiotensin system, where the kidneys respond to low or high blood pressure by secreting more or less of the enzyme renin, which converts angiotensinogen to angiotensin I that is converted to angiotensin II and promotes constriction of VSMCs [64]. The lumen size will regulate blood flow through the vasculature, and both blood pressure and tissue blood flow can be controlled through VSMC contraction [65]. In addition to lumen size, VSMCs assist in maintaining vascular elasticity. The extracellular matrix in arteries and arterioles is made up of elastin fibers that expand with pressure and collagen fibers that maintain structural stability between the extracellular matrix and the VSMCs [66]. Strong interactions between VSMCs, elastin, and

collagen are required for vascular tissue compliance, which is essential in dampening the pulse wave velocity from each heartbeat [4].

Role of vascular smooth muscle cells in vascular calcification

Vascular calcification is now understood to be an active mineral deposition process regulated, in part, by VSMCs. In patients with arterial medial calcification, the mineral deposits appear in the extracellular matrix adjacent to VSMCs [67]. Around the mineral deposits, elastic lamina is degraded [42,68] and apoptotic cell bodies are present [69]. Upregulation of bone- and cartilage-related transcription factors and proteins is observed in VSMCs before mineral deposition occurs and is hypothesized to be one mechanism of mineral deposition [60]. Both bone and cartilage are often found in vascular calcification [70,71]. Together, these clinical data suggest that active cellular mechanisms promote mineral formation in arteries. Through many *in vitro* and *in vivo* studies in mineralization environments, the process in which VSMCs promote mineralization is now better understood.

One proposed mechanism in which VSMCs promote mineralization is through osteochondrogenic phenotype change. In multiple arterial diseases, VSMCs have shown plasticity and are able to differentiate from a 'contractile' state to a 'synthetic' state [72]. Healthy arteries consist of contractile, quiescent VSMCs that function to maintain vascular tone, but diseases vasculature can have synthetic VSMCs that can proliferate, migrate, degrade extracellular matrix, and promote mineralization [73]. Consistent in all VSMC phenotype change is a decrease in smooth muscle-specific genes, such as smooth muscle 22 alpha (SM22α), smooth muscle myosin heavy chain (SM-MHC), and smooth muscle alpha actin (SMα-actin)

[73]. Specifically in VSMCs that promote mineralization, osteochondrogenic-specific transcription factors and genes are up-regulated, such as runt-related transcription factor 2 (Runx2), alkaline phosphatase (ALP), osteopontin (OPN), osteocalcin (OCN), and osterix (OSX) [74]. This was nicely shown by Speer *et al*. in a murine lineage tracing study that used SM22α-specific Cre recombinase expression with an *in vivo* model of arterial medial calcification to identify aortic VSMCs in areas of mineralization that had lost smooth muscle-specific genes and gained osteochondrogenic-specific genes [75]. Down-regulation of smooth muscle-specific genes and up-regulation of osteochondrogenic-related genes is consistent with osteochondrogenic differentiation of VSMCs.

Cell signaling through ERK1/2 in VSMCs and matrix mineralization

Cell signaling through extracellular signal-related kinase 1 and 2 (ERK1 and ERK2) promote osteochondrogenic differentiation in VSMCs. ERK1 and ERK2 are cell signal transduction kinases in the mitogen-activated protein kinase (MAPK) family [76]. They are activated by phosphorylation from the mitogen-activated protein kinase kinases Mek1 and Mek2 [76], and can phosphorylate many different down-stream transcription factors, including ETS domain-containing protein (Elk-1) and the osteochondrogenic transcript factor Runx2 [77,78]. Phosphorylated Elk-1 binds to the smooth muscle promoter, myocardin, and blocks the promoter complex of myocardin and serum response factor (SRF) from binding to the smooth muscle DNA promotor sequence, effectively inhibiting smooth muscle-specific gene transcription [79]. Phosphorylated Runx2 binds to the osteochondrogenic DNA promotor sequence, OSE-2, which results in up-regulation of osteochondrogenic genes [80]. Indeed, in calcifying VSMCs, ERK1 and ERK2 phosphorylation is increased, and inhibition of ERK1 and ERK2 phosphorylation

with a small molecule inhibitor will decrease Runx2 phosphorylation, Elk-1 phosphorylation, and down-stream osteochondrogenic differentiation in calcifying VSMCs [74]. These data suggest that ERK1 and ERK2 are required for osteochondrogenic differentiation of VSMCs.

One mechanism in which osteochondrogenic differentiation of VSMCs promotes active mineralization is through secretion of calcification-competent matrix vesicles. Normally, VSMCs secrete matrix vesicles through the exosome pathway that contain calcification inhibitors, such as Fetuin-A and Matrix Gla Protein (MGP), and lack calcification promotors [81,82]. However, osteochondrogenic differentiation of VSMCs leads to a change in the protein contents of these matrix vesicles. These calcification-competent matrix vesicles lack calcification inhibitors and contain calcification promotors, such as ALP [82]. Calcification-competent matrix vesicles initiate calcification before secretion by creating small nucleation sites of calcium-phosphate mineral [83]. Once secreted, ALP hydrolyzes the potent calcification inhibitor pyrophosphate, which will promote mineral growth from the nucleation sites [84]. Also, these mineralization-competent matrix vesicles can initiate mineralization with Annexin-V nucleation sites on the outside of the membranes [82]. Once VSMCs are induced to an osteochondrogenic phenotype, secretion of calcification-competent matrix vesicles leads to vascular calcification.

Effects of elevated Pi VSMC phenotype and matrix mineralization

Elevated Pi induces VSMC osteochondrogenic differentiation and matrix mineralization. As shown in multiple *in vitro* studies, culturing VSMCs in elevated Pi media (greater than 2.2 mM Pi) will induce matrix mineralization compared to VSMCs cultured in normal Pi (1.0 mM Pi)

[85]. Additionally, VSMCs in elevated Pi media have increased Erk1/2 phosphorylation, undergo osteochondrogenic differentiation [74], and secrete mineralization-competent matrix vesicles [86]. These results have also been shown through *in vivo* murine models of chronic kidney disease. C57BL/6 mice given uremia through a 5/6 nephrectomy procedure and fed a high Pi diet show increased serum Pi and robust arterial medial calcification [42]. Arterial VSMCs in this model also undergo osteochondrogenic differentiation. Taken with clinical data, these results strongly suggest that hyperphosphatemia drives arterial medial calcification by induction of VSMC osteochondrogenic differentiation and active matrix mineralization.

1.3 Phosphate transporters

Type III sodium-dependent phosphate transporters

Pi is primarily moved through cell membranes through sodium-dependent Pi transporters. In order to have a larger concentration of intracellular Pi over extracellular Pi, all sodium-dependent Pi transporters use the inward sodium gradient created by the sodium-potassium ATPase to co-transport sodium and Pi ions [87]. The sodium-potassium ATPase pumps out three sodium ions per ATP used, so the sodium-dependent Pi transporters are indirect active transporters to move Pi against the concentration gradient.

Mammals have three types of sodium-dependent Pi transporters, labeled types I, II, and III. The type I transporters are of the SLC17 family, and they are mainly expressed in the proximal tubule of the kidney and the sinusoidal membrane of the liver [88]. The type II transporters are of the SLC34 family, and their main functionality is in the intestines for Pi ingestion and in the kidneys

for Pi re-absorption [89]. The type III transporters are SLC20A1 (PiT-1) and SLC20A2 (PiT-2). PiT-1 and PiT-2 are thought to play a more general role in intracellular Pi homeostasis [89]. The PiT proteins are described as high-affinity low-capacity transporters, meaning that rate of Pi transport is maximal at a low Pi concentration. Functionally, this results in Pi being transported through the PiT proteins as quickly as possible at normal Pi concentrations.

PiT-1 and PiT-2 also play important roles in embryonic development, and knock out mice have revealed tissue specific roles. The PiT-1 knock-out mouse was generated through a Lox/Cre recombinase strategy where pLox DNA sites were inserted into introns around exons 3 and 4 of the PiT-1 gene, and expression of Cre recombinase will delete exons 3 and 4 to generate an early stop codon [90]. The transgenic PiT-1 global knock-out phenotype is embryonically lethal in mice due to a defect in vascular maturation [90]. PiT-1 global deletion was also found to inhibit terminal B-cell differentiation and lead to severe anemia [91]. The PiT-2 global knock-out is sub-viable with smaller litter sizes probably due in part to placentation defects [92]. Placental vascular calcification is associated with maternal morbidity and a pre-eclampsia phenotype in these mice [92]. The PiT-2 global knockout mice that do survive show devere brain calcification, hydrocephalus, and have reduced bone mineral density [93]. The underlying mechanism for this phenotype is currently being investigated.

PiT-1 required for mineralization

The type III Pi transporter PiT-1 is required for elevated Pi-induced matrix mineralization in VSMCs. Li *et al*. used a short hairpin RNA approach to silence PiT-1 mRNA in an immortalized human newborn vascular smooth muscle cell line [94]. Silencing of PiT-1 mRNA

reduced protein and decreased sodium-dependent Pi uptake in the human VSMCs by about 50%. The results showed that human VSMCs lacking PiT-1 expression deposited around 50% less mineral after incubation in elevated Pi for 7, 10, and 14 days compared to scramble controls. Additionally, overexpression of mouse PiT-1 mRNA in the PiT-1 knock-down human VSMCs rescued the decrease in elevated Pi-induced mineralization. Upstream of mineralization, PiT-1 silencing inhibited osteochondrogenic differentiation as measured by a reduction in both Runx2 and OPN mRNA. These data suggest that PiT-1 plays a critical role in elevated Pi-induced transcriptional changes in VSMCs that leads to phenotype switching and eventual matrix mineralization. However, the mechanism for PiT-1 mediated osteochondrogenic differentiation and matrix mineralization was not elucidated in this study. PiT-1 silencing did not affect apoptosis and blocking apoptosis with the chemical inhibitor zVAD did not affect elevated Pi-induced mineralization, suggesting that apoptosis was not the mechanism for increased matrix mineralization. The research goals and results presented in this dissertation aim to elucidate the mechanism of PiT-1 mediated promotion of matrix mineralization and VSMC phenotype change.

1.4 Summary of Background and Significance

In conclusion, growing evidence suggest that hyperphosphatemia in chronic kidney disease patients induces arterial medial calcification through active mineral deposition by VSMCs. Elevated Pi causes osteochondrogenic differentiation in cultured VSMCs through the ERK1/2 cell signaling pathway and eventually leads to promotion of matrix mineralization. PiT-1 is required for elevated Pi-induced osteochondrogenic differentiation and matrix mineralization in cultured VSMC. However, the mechanism in which PiT-1 signals ERK1/2 phosphorylation in

response to elevated Pi and promotes VSMC matrix mineralization is unclear. A better understanding of this pathway could lead to therapeutics that inhibit vascular calcification by blocking the VSMC response to Pi.

1.5 Hypothesis and Specific Aims of Dissertation

The main purpose of this project was to elucidate the role of PiT-1 in elevated Pi-induced cell signaling, osteochondrogenic differentiation, and matrix mineralization in VSMCs. **The hypothesis was that PiT-1 promotes elevated Pi-induced matrix mineralization in VSMCs through both Pi uptake-dependent function and Pi uptake-independent function. Independent of Pi uptake, elevated Pi promotes PiT-1 binding to RapGEF1, leading to downstream ERK1/2 activation and VSMC phenotype change.** Three specific aims were completed to test this hypothesis. In specific aim #1, the Pi concentration dependence for matrix mineralization versus Pi uptake in VSMCs was investigated. In specific aim #2, Pi transport-independent function of PiT-1 was investigated to determine a role in elevated Pi-induced ERK1/2 cell signaling, osteochondrogenic differentiation, and matrix mineralization. In specific aim #3, adaptor proteins in the elevated Pi-induced cell signaling pathway from PiT-1 to ERK1/2 were investigated.

1.6 Outline of Dissertation Content

The following chapters detail the research goals, methods, and results of each specific aim individually. Chapter 2 describes that the Pi concentration required to promote ERK1/2

phosphorylation, osteochondrogenic differentiation, and matrix mineralization is much larger than the Pi concentration with maximal Pi uptake into VSMCs. Pi transport through PiT-1 alone cannot explain the role of PiT-1 in VSMC mineralization. Chapter 3 then identifies that Pi uptake-independent functions of PiT-1 can promote ERK1/2 phosphorylation leading to osteochondrogenic differentiation. Both Pi uptake-dependent and uptake-independent functions of PiT-1 promote mineralization. Chapter 4 further elucidates the PiT-1 cell signaling function leading to ERK1/2 activation through interacting partner RapGEF1 and down-stream adaptor proteins Rap1, B-Raf, and Mek1/2. Chapter 5 outlines the conclusions of this research and future directions of interest.

1.7 Notes to Chapter 1

1 Bild DE, Detrano R, Peterson D, Guerci A, Liu K, Shahar E, *et al.* Ethnic differences in coronary calcification: the Multi-Ethnic Study of Atherosclerosis (MESA). *Circulation* 2005; 111:1313–20.

2 Loria CM, Liu K, Lewis CE, Hulley SB, Sidney S, Schreiner PJ, *et al.* Early Adult Risk Factor Levels and Subsequent Coronary Artery Calcification. The CARDIA Study. *J Am Coll Cardiol* 2007; 49:2013–2020.

3 Kullo IJ, Bielak LF, Turner ST, Sheedy PF, Peyser PA. Aortic Pulse Wave Velocity Is Associated With the Presence and Quantity of Coronary Artery Calcium: A Community-Based Study. *Hypertension* 2006; 47:174–179.

4 Willum-Hansen T, Staessen JA, Torp-Pedersen C, Rasmussen S, Thijs L, Ibsen H, *et al.* Prognostic value of aortic pulse wave velocity as index of arterial stiffness in the general population. *Circulation* 2006; 113:664–70.

5 Koos R, Mahnken AH, Dohmen G, Brehmer K, Günther RW, Autschbach R, *et al.* Association of aortic valve calcification severity with the degree of aortic regurgitation after transcatheter aortic valve implantation. *Int J Cardiol* 2011; 150:142–145.

6 Fitzgerald PJ, Ports TA, Yock PG. Contribution of localized calcium deposits to dissection after angioplasty. An observational study using intravascular ultrasound. *Circulation* 1992; 86:64–70.

7 Burke AP, Taylor A, Farb A, Malcom GT, Virmani R. Coronary calcification: insights from sudden coronary death victims. *Zeitschrift für Kardiol* 2000; 89 Suppl 2:49–53.

8 Davies MJ, Thomas AC. Plaque fissuring--the cause of acute myocardial infarction,

sudden ischaemic death, and crescendo angina. *Br Heart J* 1985; 53:363–73.

9 Otto CM, Burwash IG, Legget ME, Munt BI, Fujioka M, Healy NL, *et al.* Prospective study of asymptomatic valvular aortic stenosis. Clinical, echocardiographic, and exercise predictors of outcome. *Circulation* 1997; 95:2262–70.

10 Burke AP, Farb A, Malcom GT, Liang Y, Smialek JE, Virmani R, *et al.* Plaque Rupture and Sudden Death Related to Exertion in Men With Coronary Artery Disease. *JAMA* 1999; 281:921.

11 Dujardin KS, Enriquez-Sarano M, Schaff H V, Bailey KR, Seward JB, Tajik AJ. Mortality and morbidity of aortic regurgitation in clinical practice. A long-term follow-up study. *Circulation* 1999; 99:1851–7.

12 Otto CM, Lind BK, Kitzman DW, Gersh BJ, Siscovick DS. Association of Aortic-Valve Sclerosis with Cardiovascular Mortality and Morbidity in the Elderly. *http://dx.doi.org/101056/NEJM199907153410302* 1999.

13 Meaume S, Benetos A, Henry OF, Rudnichi A, Safar ME. Aortic Pulse Wave Velocity Predicts Cardiovascular Mortality in Subjects >70 Years of Age. *Arterioscler Thromb Vasc Biol* 2001; 21:2046–2050.

14 Sutton-Tyrrell K, Najjar SS, Boudreau RM, Venkitachalam L, Kupelian V, Simonsick EM, *et al.* Elevated aortic pulse wave velocity, a marker of arterial stiffness, predicts cardiovascular events in well-functioning older adults. *Circulation* 2005; 111:3384–90.

15 Butany J, Collins MJ, Demellawy DEI, Nair V, Israel N, Leong SW, *et al.* Morphological and clinical findings in 247 surgically excised native aortic valves. *Can J Cardiol* 2005; 21:747–55.

16 Stenvinkel P, Heimbürger O, Paultre F, Diczfalusy U, Wang T, Berglund L, *et al.* Strong

association between malnutrition, inflammation, and atherosclerosis in chronic renal failure. *Kidney Int* 1999; 55:1899–1911.

17 Allison MA, Criqui MH, Wright CM. Patterns and Risk Factors for Systemic Calcified Atherosclerosis. *Arterioscler Thromb Vasc Biol* 2004; 24:331–336.

18 Maldonado N, Kelly-Arnold A, Vengrenyuk Y, Laudier D, Fallon JT, Virmani R, *et al.* A mechanistic analysis of the role of microcalcifications in atherosclerotic plaque stability: potential implications for plaque rupture. *Am J Physiol Heart Circ Physiol* 2012; 303:H619–28.

19 Detrano R, Guerci AD, Carr JJ, Bild DE, Burke G, Folsom AR, *et al.* Coronary calcium as a predictor of coronary events in four racial or ethnic groups. *N Engl J Med* 2008; 358:1336–45.

20 Everhart JE, Pettitt DJ, Knowler WC, Rose FA, Bennett PH. Medial arterial calcification and its association with mortality and complications of diabetes. *Diabetologia* 1987; 31:16–23.

21 Leskinen Y, Salenius JP, Lehtimäki T, Huhtala H, Saha H. The prevalence of peripheral arterial disease and medial arterial calcification in patients with chronic renal failure: Requirements for diagnostics. *Am J Kidney Dis* 2002; 40:472–479.

22 BEADENKOPF WG, DAOUD AS, LOVE BM. CALCIFICATION IN THE CORONARY ARTERIES AND ITS RELATIONSHIP TO ARTERIOSCLEROSIS AND MYOCARDIAL INFARCTION. *Am J Roentgenol Radium Ther Nucl Med* 1964; 92:865–71.

23 Witteman JM, Kok F, Van Saase JCM, Valkenburg H. AORTIC CALCIFICATION AS A PREDICTOR OF CARDIOVASCULAR MORTALITY. *Lancet* 1986; 328:1120–1122.

24 Wilson PW, Kauppila LI, O'Donnell CJ, Kiel DP, Hannan M, Polak JM, *et al.* Abdominal aortic calcific deposits are an important predictor of vascular morbidity and mortality. *Circulation* 2001; 103:1529–34.

25 Vliegenthart R, Hollander M, Breteler MMB, van der Kuip DAM, Hofman A, Oudkerk M, *et al.* Stroke is associated with coronary calcification as detected by electron-beam CT: the Rotterdam Coronary Calcification Study. *Stroke* 2002; 33:462–5.

26 Raggi P, Boulay A, Chasan-Taber S, Amin N, Dillon M, Burke SK, *et al.* Cardiac calcification in adult hemodialysis patients. *J Am Coll Cardiol* 2002; 39:695–701.

27 Toussaint ND, Lau KK, Strauss BJ, Polkinghorne KR, Kerr PG. Associations between vascular calcification, arterial stiffness and bone mineral density in chronic kidney disease. *Nephrol Dial Transplant* 2008; 23:586–93.

28 Sarnak MJ. Cardiovascular complications in chronic kidney disease. *Am J Kidney Dis* 2003; 41:11–17.

29 Foley RN, Parfrey PS, Sarnak MJ. Clinical epidemiology of cardiovascular disease in chronic renal disease. *Am J Kidney Dis* 1998; 32:S112–9.

30 Shulman NB, Ford CE, Hall WD, Blaufox MD, Simon D, Langford HG, *et al.* Prognostic value of serum creatinine and effect of treatment of hypertension on renal function. Results from the hypertension detection and follow-up program. The Hypertension Detection and Follow-up Program Cooperative Group. *Hypertens (Dallas, Tex 1979)* 1989; 13:I80–93.

31 London GM, Guérin AP, Marchais SJ, Métivier F, Pannier B, Adda H. Arterial media calcification in end-stage renal disease: impact on all-cause and cardiovascular mortality. *Nephrol Dial Transplant* 2003; 18:1731–40.

32 Moe S, Drüeke T, Cunningham J, Goodman W, Martin K, Olgaard K, *et al.* Definition, evaluation, and classification of renal osteodystrophy: A position statement from Kidney Disease: Improving Global Outcomes (KDIGO). *Kidney Int* 2006; 69:1945–1953.

33 Penido MGMG, Alon US. Phosphate homeostasis and its role in bone health. *Pediatr Nephrol* 2012; 27:2039–48.

34 Burnett S-AM, Gunawardene SC, Bringhurst FR, Jüppner H, Lee H, Finkelstein JS. Regulation of C-Terminal and Intact FGF-23 by Dietary Phosphate in Men and Women. *J Bone Miner Res* 2006; 21:1187–1196.

35 Murer H, Hernando N, Forster I, Biber J. Regulation of Na/Pi transporter in the proximal tubule. *Annu Rev Physiol* 2003; 65:531–42.

36 Cross HS, Debiec H, Peterlik M. Mechanism and regulation of intestinal phosphate absorption. *Miner Electrolyte Metab* 1990; 16:115–24.

37 Kestenbaum B, Belozeroff V. Mineral metabolism disturbances in patients with chronic kidney disease. *Eur J Clin Invest* 2007; 37:607–22.

38 Russo D, Miranda I, Ruocco C, Battaglia Y, Buonanno E, Manzi S, *et al.* The progression of coronary artery calcification in predialysis patients on calcium carbonate or sevelamer. *Kidney Int* 2007; 72:1255–61 ST – The progression of coronary artery c.

39 Block GA, Hulbert-Shearon TE, Levin NW, Port FK. Association of serum phosphorus and calcium x phosphate product with mortality risk in chronic hemodialysis patients: a national study. *Am J Kidney Dis* 1998; 31:607–17.

40 Maréchal C, Coche E, Goffin E, Dragean A, Schlieper G, Nguyen P, *et al.* Progression of Coronary Artery Calcification and Thoracic Aorta Calcification in Kidney Transplant Recipients. *Am J Kidney Dis* Published Online First: 2011. doi:S0272-6386(11)01195-4

[pii] 10.1053/j.ajkd.2011.07.019 LA - ENG

41 Goldsmith DJ, Covic A, Sambrook PA, Ackrill P. Vascular calcification in long-term haemodialysis patients in a single unit: a retrospective analysis. *Nephron* 1997; 77:37–43 ST – Vascular calcification in long–term ha.

42 Pai A, Leaf EM, El-Abbadi M, Giachelli CM. Elastin degradation and vascular smooth muscle cell phenotype change precede cell loss and arterial medial calcification in a uremic mouse model of chronic kidney disease. *Am J Pathol* 2011; 178:764–73.

43 Dhingra R, Sullivan LM, Fox CS, Wang TJ, D'Agostino Sr. RB, Gaziano JM, *et al.* Relations of serum phosphorus and calcium levels to the incidence of cardiovascular disease in the community. *Arch Intern Med* 2007; 167:879–85.

44 Kestenbaum BR, Adeney KL, de Boer IH, Ix JH, Shlipak MG, Siscovick DS. Incidence and progression of coronary calcification in chronic kidney disease: the Multi-Ethnic Study of Atherosclerosis. *Kidney Int* 2009; 76:991–8.

45 Tonelli M, Curhan G, Pfeffer M, Sacks F, Thadhani R, Melamed ML, *et al.* Relation between alkaline phosphatase, serum phosphate, and all-cause or cardiovascular mortality. *Circulation* 2009; 120:1784–92.

46 Hruska KA, Mathew S, Lund R, Qiu P, Pratt R. Hyperphosphatemia of chronic kidney disease. *Kidney Int* 2008; 74:148–57.

47 Isakova T, Wahl P, Vargas GS, Gutiérrez OM, Scialla J, Xie H, *et al.* Fibroblast growth factor 23 is elevated before parathyroid hormone and phosphate in chronic kidney disease. *Kidney Int* 2011; 79:1370–8.

48 Levin A, Bakris GL, Molitch M, Smulders M, Tian J, Williams LA, *et al.* Prevalence of abnormal serum vitamin D, PTH, calcium, and phosphorus in patients with chronic kidney

disease: results of the study to evaluate early kidney disease. *Kidney Int* 2007; 71:31–8.

49 Koh N, Fujimori T, Nishiguchi S, Tamori A, Shiomi S, Nakatani T, *et al.* Severely reduced production of klotho in human chronic renal failure kidney. *Biochem Biophys Res Commun* 2001; 280:1015–20.

50 Noordzij M, Korevaar JC, Bos WJ, Boeschoten EW, Dekker FW, Bossuyt PM, *et al.* Mineral metabolism and cardiovascular morbidity and mortality risk: peritoneal dialysis patients compared with haemodialysis patients. *Nephrol Dial Transpl* 2006; 21:2513–20 ST – Mineral metabolism and cardiovascula.

51 Tentori F, Blayney MJ, Albert JM, Gillespie BW, Kerr PG, Bommer J, *et al.* Mortality risk for dialysis patients with different levels of serum calcium, phosphorus, and PTH: the Dialysis Outcomes and Practice Patterns Study (DOPPS). *Am J Kidney Dis* 2008; 52:519–30.

52 Block GA, Klassen PS, Lazarus JM, Ofsthun N, Lowrie EG, Chertow GM. Mineral metabolism, mortality, and morbidity in maintenance hemodialysis. *J Am Soc Nephrol* 2004; 15:2208–18.

53 Casas JP, Chua W, Loukogeorgakis S, Vallance P, Smeeth L, Hingorani AD, *et al.* Effect of inhibitors of the renin-angiotensin system and other antihypertensive drugs on renal outcomes: systematic review and meta-analysis. *Lancet* 2005; 366:2026–2033.

54 Ahmed AK, Kamath NS, El Kossi M, El Nahas AM. The impact of stopping inhibitors of the renin-angiotensin system in patients with advanced chronic kidney disease. *Nephrol Dial Transplant* 2010; 25:3977–82.

55 Solbu MD, Jardine AG. "To block or not to block"; whether to continue renin–angiotensin–aldosterone system blockade in advanced chronic kidney disease. *Nephrol*

Dial Transplant 2015; 31:gfv351.

56 Bhandari S, Ives N, Brettell EA, Valente M, Cockwell P, Topham PS, *et al.* Multicentre randomized controlled trial of angiotensin-converting enzyme inhibitor/angiotensin receptor blocker withdrawal in advanced renal disease: the STOP-ACEi trial. *Nephrol Dial Transplant* 2016; 31:255–61.

57 Pasch A, Schaffner T, Huynh-Do U, Frey BM, Frey FJ, Farese S. Sodium thiosulfate prevents vascular calcifications in uremic rats. *Kidney Int* 2008; 74:1444–53 ST – Sodium thiosulfate prevents vascular.

58 Mathews SJ, de Las Fuentes L, Podaralla P, Cabellon A, Zheng S, Bierhals A, *et al.* Effects of sodium thiosulfate on vascular calcification in end-stage renal disease: a pilot study of feasibility, safety and efficacy. *Am J Nephrol* 2011; 33:131–8 ST – Effects of sodium thiosulfate on vascu.

59 Cupisti A, Gallieni M, Rizzo MA, Caria S, Meola M, Bolasco P. Phosphate Control in Dialysis. *Int J Nephrol Renovasc Dis* 2013; 6:193–205.

60 Shroff RC, McNair R, Figg N, Skepper JN, Schurgers L, Gupta A, *et al.* Dialysis accelerates medial vascular calcification in part by triggering smooth muscle cell apoptosis. *Circulation* 2008; 118:1748–57.

61 Hutchison AJ, Smith CP, Brenchley PEC. Pharmacology, efficacy and safety of oral phosphate binders. *Nat Rev Nephrol* 2011; 7:578–89.

62 Qunibi W, Moustafa M, Muenz LR, He DY, Kessler PD, Diaz-Buxo JA, *et al.* A 1-Year Randomized Trial of Calcium Acetate Versus Sevelamer on Progression of Coronary Artery Calcification in Hemodialysis Patients With Comparable Lipid Control: The Calcium Acetate Renagel Evaluation-2 (CARE-2) Study. *Am J Kidney Dis* 2008; 51:952–

965.

63 Murphy RA, Herlihy JT, Megerman J. Force-Generating Capacity and Contractile Protein Content of Arterial Smooth Muscle. *J Gen Physiol* 1974; 64:691–705.

64 Peach MJ. Renin-Angiotensin System: Biochemistry and Mechanisms of Action. *Physiol REVIE ws* 1977; 57.

65 Bohr DF, Webb RC. Vascular Smooth Muscle Function and Its Changes in Hypertension. *Am J Med* 1984; 77:3–16.

66 Gross L, Epstein EZ, Kugel MA. Histology of the Coronary Arteries and their Branches in the Human Heart. *Am J Pathol* 1934; 10:253–274.7.

67 Moe SM, O'Neill KD, Duan D, Ahmed S, Chen NX, Leapman SB, *et al.* Medial artery calcification in ESRD patients is associated with deposition of bone matrix proteins. *Kidney Int* 2002; 61:638–47.

68 Guérin AP, Pannier B, Métivier F, Marchais SJ, London GM. Assessment and significance of arterial stiffness in patients with chronic kidney disease. *Curr Opin Nephrol Hypertens* 2008; 17:635–641.

69 Proudfoot D, Skepper JN, Hegyi L, Bennett MR, Shanahan CM, Weissberg PL. Apoptosis regulates human vascular calcification in vitro: evidence for initiation of vascular calcification by apoptotic bodies. *Circ Res* 2000; 87:1055–62.

70 Hunt JL, Fairman R, Mitchell ME, Carpenter JP, Golden M, Khalapyan T, *et al.* Bone formation in carotid plaques: a clinicopathological study. *Stroke* 2002; 33:1214–9.

71 Mohler ER, Gannon F, Reynolds C, Zimmerman R, Keane MG, Kaplan FS. Bone formation and inflammation in cardiac valves. *Circulation* 2001; 103:1522–8.

72 Owens GK, Kumar MS, Wamhoff BR. Molecular Regulation of Vascular Smooth Muscle

Cell Differentiation in Development and Disease. 2004; :767–801.

73 Alexander MR, Owens GK. Epigenetic control of smooth muscle cell differentiation and phenotypic switching in vascular development and disease. *Annu Rev Physiol* 2012; 74:13–40.

74 Speer MY, Li X, Hiremath PG, Giachelli CMC-P 2895022. Runx2/Cbfa1, but not loss of myocardin, is required for smooth muscle cell lineage reprogramming toward osteochondrogenesis. *J Cell Biochem* 2010; 110:935–47.

75 Speer MY, Yang H-YY, Brabb T, Leaf E, Look A, Lin W-LL, *et al.* Smooth muscle cells give rise to osteochondrogenic precursors and chondrocytes in calcifying arteries. *Circ Res* 2009; 104:733–41.

76 Cargnello M, Roux PP. Activation and function of the MAPKs and their substrates, the MAPK-activated protein kinases. *Microbiol Mol Biol Rev* 2011; 75:50–83.

77 Cruzalegui FH, Cano E, Treisman R. ERK activation induces phosphorylation of Elk-1 at multiple S/T-P motifs to high stoichiometry.

78 Ge C, Xiao G, Jiang D, Yang Q, Hatch NE, Roca H, *et al.* Identification and Functional Characterization of ERK/MAPK Phosphorylation Sites in the Runx2 Transcription Factor. *J Biol Chem* 2009; 284:32533–32543.

79 Yoshida T, Sinha S, Dandré F, Wamhoff BR, Hoofnagle MH, Kremer BE, *et al.* Myocardin is a key regulator of CArG-dependent transcription of multiple smooth muscle marker genes. *Circ Res* 2003; 92:856–64.

80 Ducy P, Zhang R, Geoffroy V, Ridall AL, Karsenty G. Osf2/Cbfa1: A Transcriptional Activator of Osteoblast Differentiation. *Cell* 1997; 89:747–754.

81 Reynolds JL, Skepper JN, McNair R, Kasama T, Gupta K, Weissberg PL, *et al.*

Multifunctional roles for serum protein fetuin-a in inhibition of human vascular smooth muscle cell calcification. *J Am Soc Nephrol* 2005; 16:2920–30.

82 Kapustin AN, Shanahan CM. Calcium Regulation of Vascular Smooth Muscle Cell-Derived Matrix Vesicles. *Trends Cardiovasc Med* Published Online First: 15 August 2012. doi:10.1016/j.tcm.2012.07.009

83 Kapustin AN, Chatrou MLL, Drozdov I, Zheng Y, Davidson SM, Soong D, *et al.* Vascular Smooth Muscle Cell Calcification Is Mediated by Regulated Exosome Secretion. *Circ Res* 2015; 116:1312–1323.

84 Lomashvili KA, Garg P, Narisawa S, Millan JL, O'Neill WC. Upregulation of alkaline phosphatase and pyrophosphate hydrolysis: potential mechanism for uremic vascular calcification. *Kidney Int* 2008; 73:1024–30.

85 Shanahan CM, Crouthamel MH, Kapustin A, Giachelli CM. Arterial calcification in chronic kidney disease: key roles for calcium and phosphate. *Circ Res* 2011; 109:697–711 ST – Arterial calcification in chronic ki.

86 Reynolds JL, Joannides AJ, Skepper JN, McNair R, Schurgers LJ, Proudfoot D, *et al.* Human vascular smooth muscle cells undergo vesicle-mediated calcification in response to changes in extracellular calcium and phosphate concentrations: a potential mechanism for accelerated vascular calcification in ESRD. *J Am Soc Nephrol* 2004; 15:2857–67.

87 Werner A, Dehmelt L, Nalbant P. Na+-dependent phosphate cotransporters: the NaPi protein families. *J Exp Biol* 1998; 201:3135–42.

88 Reimer RJ. SLC17: a functionally diverse family of organic anion transporters. *Mol Aspects Med* 2013; 34:350–9.

89 Virkki L V, Biber J, Murer H, Forster IC. Phosphate transporters: a tale of two solute

carrier families. *Am J Physiol Renal Physiol* 2007; 293:F643–54.

90 Festing MH, Speer MY, Yang H-Y, Giachelli CM. Generation of mouse conditional and null alleles of the type III sodium-dependent phosphate cotransporter PiT-1. *Genesis* 2009; 47:858–63.

91 Liu L, Sánchez-Bonilla M, Crouthamel M, Giachelli C, Keel S. Mice lacking the sodium-dependent phosphate import protein, PiT1 (SLC20A1), have a severe defect in terminal erythroid differentiation and early B-cell development. *Exp Hematol* Published Online First: 30 January 2013. doi:10.1016/j.exphem.2013.01.004

92 Wallingford MC, Gammill HS, Giachelli CM. Slc20a2 deficiency results in fetal growth restriction and placental calcification associated with thickened basement membranes and novel CD13 and lamininα1 expressing cells. *Reprod Biol* 2016; 16:13–26.

93 Wallingford MC, Chia J, Leaf EM, Borgeia S, Chavkin NW, Sawangmake C, *et al.* SLC20A2 deficiency in mice leads to elevated phosphate levels in cerbrospinal fluid and glymphatic pathway-associated arteriolar calcification, and recapitulates human idiopathic basal ganglia calcification. *Brain Pathol* Published Online First: 29 January 2016. doi:10.1111/bpa.12362

94 Li X, Yang H-YY, Giachelli CM. Role of the sodium-dependent phosphate cotransporter, Pit-1, in vascular smooth muscle cell calcification. *Circ Res* 2006; 98:905–12.

CHAPTER 2

SEPARATION BETWEEN PI CONCENTRATIONS REQUIRED FOR PIT-1 TRANSPORT AND ELEVATED PI-INDUCED EFFECTS ON VSMCS

Chapter published in similar form as part of: "Phosphate uptake-independent signaling functions of the type III sodium-dependent phosphate transporter, PiT-1, in vascular smooth muscle cells." Chavkin NW, Chia J, Crouthamel MH, Giachelli CM. Experimental Cell Research. 2015 Apr 10;333(1):39-48.

2.1 Introduction

The functions of PiT-1 that promote elevated Pi-induced mineralization are unclear. One well-understood function of PiT-1 is Pi uptake, which is required for elevated Pi-induced mineralization. However, studies have presented data suggesting that the kinetics of Pi uptake do not explain the elevated Pi-induced effects on VSMCs. Villa-Bellosta *et al.* showed that sodium-dependent Pi uptake did not change when rat aortic VSMCs were induced to calcify with PDGF, TNF-α, or Pi [1]. Other studies have also characterized Pi uptake kinetics of PiT-1 and questioned the role of Pi uptake in VSMC matrix mineralization [2]. A separation between Pi uptake into VSMCs and Pi required for VSMC mineralization would suggest a role of PiT-1 in mineralization that is not dependent on Pi transport.

Pi-uptake independent functions of PiT-1 have recently been discovered and show that other functions of PiT-1 may exist. A PiT-1 protein with a single point mutation that does not transport Pi has been shown to promote cellular proliferation in HeLa cells [3]. A PiT-1 protein with a different point mutation that still inhibited Pi transport could inhibit apoptosis induced by tumor necrosis factor α (TNF-α) [4]. Also supporting the hypothesis of Pi uptake-independent PiT-1 function, B-cells that had a differentiation defect in PiT-1 null mice did not show a difference in Pi uptake [5]. Other studies suggest that PiT-1 may play a role in ERK1/2 phosphorylation. Knock-down of PiT-1 mRNA with siRNA in proliferating chondrocytes showed a reduction in elevated Pi-induced ERK1/2 phosphorylation, and knock-down of PiT-2 mRNA did not show the same result [6]. A cell signaling function of PiT-1 may play a role in mineralization.

These results suggest that PiT-1 may have a role in cell functions independent of Pi uptake, and that these functions may be a result of an ERK1/2 cell signaling pathway. **The present aim will test the hypothesis that Pi concentrations required for ERK1/2 phosphorylation, osteochondrogenic differentiation, and matrix mineralization are well above the Michaelis-Menten rate constant of sodium-dependent Pi uptake in VSMCs**. To test this, sodium-dependent Pi uptake kinetic parameters in VSMCs will be determined. Varying Pi concentrations will be tested to induce matrix mineralization and osteochondrogenic differentiation, and compared to Pi uptake kinetics. Finally, elevated Pi-induced ERK1/2 phosphorylation will be tested in control and PiT-1-deficient VSMCs to see whether PiT-1 is required for elevated Pi-induced ERK1/2 phosphorylation.

2.2 Materials and Methods

Cell isolation and maintenance

Primary medial VSMCs were isolated from aortas of wild-type C57BL/6 (WT VSMC), PiT-1 flox/flox C57BL/6 (PiT-1 fl/fl VSMC), and PiT-1 flox/flox SM22αCre C57BL/6 (PiT-1 ΔSM VSMC) mice as previously described [7]. Briefly, aortas were removed from 4-5 week old mice, the medial layer was isolated and digested in collagen and elastin, and the primary (P0) VSMCs were incubated in T-25 flasks at 37O C and 5% CO2 with Dulbecco's Modified Eagle Medium (DMEM, Life Technologies, 11995) supplemented with 20% Fetal Bovine Serum (FBS, HyClone), 1% antibiotic/antimycotic, 1% glutamine, and 1% non-essential amino acids (Life Technologies). VSMCs were passaged and maintained at 37O C and 5% CO2 in normal growth media DMEM supplemented with 10% FBS and 1% antibiotic/antimycotic.

Pi uptake assay

Pi uptake was measured as previously described [8]. Briefly, VSMCs were seeded into 12-well tissue culture plates and incubated with radiolabeled H333PO4 (Perkin Elmer) and un-labeled potassium phosphate in either sodium-containing Earle's Balanced Salt Solution (EBSS) or sodium-free, choline-containing EBSS. VSMCs were incubated for 20 minutes, lysate was collected, and radioactive counts were recorded in OptiFluor (Perkin Elmer) using a LS 6500 Beckman liquid scintillation counter. Sodium- dependent Pi uptake was calculated by subtracting uptake in choline containing media from total uptake in sodium containing media, and normalized to incubation time and protein concentration of the cell lysate, quantified by

Bicinchoninic Acid assay (Thermo Scientific). Michaelis-Menten kinetic parameters were determined by non-linear regression.

Calcification assay

Calcification was determined as previously described [8]. Briefly, VSMCs were grown in 6-well tissue culture plates in normal growth media until 70-80% confluent, then VSMCs were incubated with DMEM supplemented with 5% FBS, 1% antibiotic/antimycotic, and Na2PO4/NaPO4 (pH = 7.4) to varying Pi concentrations. After 8 days, calcium was extracted with 0.6 N HCl at 4oC overnight. Calcium concentration was determined by the O-Cresolphthalein method using the Calcium Reagent Set (Teco Diagnostics). Protein lysate was collected in 0.2 N NaOH. Protein concentration was determined by Bicinchoninic Acid assay. Calcium data was normalized to protein data.

Real-time quantitative PCR

Collection of mRNA was performed with RNeasy Mini Kit (Qiagen) following manufacturer's protocol. Real-time quantitative PCR (Q-PCR) was performed with primers listed (Table 1). All Q-PCR gene counts were normalized to 18S gene counts and quantified using the quantitative ΔΔCt method.

Quantification of Pi-induced phosphorylated ERK1/2

VSMCs were grown in 6-well tissue culture plates in normal growth media. At 70-80% confluence, cells were washed twice with PBS and incubated in Pi-free DMEM (Life Technologies, 11971) supplemented with 1% FBS and 1% antibiotic/antimycotic. After 24

hours, media was aspirated and VSMCs were incubated in Pi-free DMEM supplemented with 1% FBS, 1% antibiotic/antimycotic, and Na2PO4/NaPO4 (pH = 7.4) to varying Pi concentrations. After 5 or 15 minutes of incubation, VSMCs were washed three times with ice-cold PBS, and cell lysate was collected using lysate buffer (0.1 mM Tris pH 6.8 2% SDS) with added protease inhibitors and phosphatase inhibitors. Protein was loaded at 10ug/lane into 10% SDS-PAGE gels, transferred to PVDF membranes, and analyzed by immunoblot. Primary phosphorylated ERK1/2 and total ERK1/2 antibodies (Cell Signaling Technology) and secondary HRP-conjugated goat anti-rabbit antibody (Jackson ImmunoResearch) were used with Western Lighting (ECL) substrate to expose the protein signal. ImageJ software (NIH, Bethesda, MD) was used to quantify the densitometry of the bands.

Statistical analysis

SPSS software v16.0 (SPSS, Chicago, IL) was used to perform Student t-tests to compare means of two individual groups, and one-way ANOVA with post-hoc Tukey test to compare means of three or more individual groups. Linear regression to determine variable correlation and nonlinear regression to determine Michaelis-Menten parameters were performed using STATA version 12 (StataCorp). A p-value of less than 0.05 was considered statistically significant.

2.3 Results

Michaelis-Menten kinetic parameters of Pi uptake in VSMCs

To determine the concentration-dependent effects of Pi on wild-type mouse aortic VSMCs, we examined sodium-dependent Pi uptake over a range of Pi concentrations. Similar to previous

findings [2,7,9], the rate of sodium dependent Pi uptake in wild-type VSMCs increased at Pi concentrations between 0.03 mM to 0.1 mM, and saturated at 0.5 mM, consistent with high-affinity low-capacity Pi transport (Fig. 2.1). Michaelis-Menten parameters Vmax (maximal velocity of Pi uptake) and Km (Pi concentration at half of Vmax velocity) were calculated by non-linear regression. Sodium-dependent Pi uptake of primary wild-type VSMCs showed a Vmax of 0.369±0.035 pmol Pi/(ug Protein*min) and Km of 0.113±0.032 mM. . These values are also consistent with high-affinity low-capacity Pi transport and suggest that velocity of Pi uptake through PiT-1 is maximal below 0.5mM Pi.

Pi concentrations required to induce matrix mineralization are well above Pi uptake Km

Elevated Pi induces VSMCs to mineralize, but the concentrations required for mineralization are not well characterized. A large difference between Pi concentrations required for mineralization and the Pi uptake kinetics calculated above may suggest a different regulatory mechanism for mineralization. Primary wild-type VSMCs were cultured in different Pi concentrations for 8 days, and calcification of the matrix was quantified in each Pi concentration. Significant VSMC matrix mineralization was observed only at Pi concentrations at or above 2.4 mM compared to negligible amounts of calcification at 1.0mM Pi (Fig. 2.2). The Pi concentration required for mineralization is much higher than 0.5mM Pi, where Pi uptake through PiT-1 is maximal.

Elevated Pi well above Pi transport Km is required for phenotype change

Elevated Pi-induced matrix mineralization is initiated and promoted through osteochondrogenic differentiation. However, the Pi concentration required to induce osteochondrogenic differentiation is unclear. To assess this, primary wild-type VSMCs were incubated in varying

concentrations of Pi, RNA was collected at day 4, and osteochondrogenic differentiation was assessed by a decrease in SM22α mRNA and an increase in OPN mRNA. In VSMCs, OPN mRNA expression was significantly increased and SM22α mRNA expression was significantly decreased at a Pi concentration of 2.6 mM compared to 1.0 mM (Fig. 2.3A and 2.3B). Importantly, PiT-1 mRNA levels were not significantly increased across the same range of Pi concentrations (Fig. 2.3C), suggesting that an increase in the amount of PiT-1 made by VSMCs was not responsible for the Pi concentration dependence observed for VSMC calcification and osteochondrogenic phenotype change.

PiT-1 deficiency eliminates Pi-induced ERK1/2 phosphorylation in VSMCs

ERK1/2 phosphorylation was previously shown to be important for elevated Pi-induced osteochondrogenic differentiation of VSMCs [20]. To investigate the concentration of Pi required to induce ERK1/2 phosphorylation and the role of PiT-1 in elevated Pi-induced ERK1/2 phosphorylation in VSMCs, control primary VSMCs (PiT-1 fl/fl VSMCs) and VSMCs lacking PiT-1 expression (PiT-1 ΔSM VSMCs) were isolated, induced with varying Pi concentrations, and ERK1/2 phosphorylation was assessed. Elevated Pi induced ERK1/2 phosphorylation in PiT-1 fl/fl VSMCs in a dose- and time-dependent manner (Fig 2.4). A 2-fold increase in ERK1/2 phosphorylation was observed in VSMCs treated with 3.0 mM for 15 min compared to 1.0 mM Pi treatment. Elevated sodium sulfate did not induce ERK1/2 phosphorylation in VSMCs, suggesting that this response was specific to elevated Pi and not a generalized response to increased anions. In contrast, Pi-induced ERK1/2 phosphorylation at 3.0 mM Pi was greatly diminished in VSMCs from PiT-1 ΔSM, and no induction between 3.0 mM and 1.0 mM Pi was observed (Figure 2). Finally, there was no difference between ERK1/2 phosphorylation in

response to either 0.5 mM or 1.0 mM Pi in either cell line. These data suggest Pi concentrations around 3.0mM Pi are required for elevated Pi-induced ERK1/2 phosphorylation, and that PiT-1 is required for elevated Pi-induced ERK1/2 phosphorylation. Additionally, Pi concentrations around maximal Pi uptake (0.5mM and 1.0mM Pi) had no difference in ERK1/2 phosphorylation.

2.4 Discussion

The data presented support a large separation between sodium-dependent Pi uptake through PiT-1 and elevated Pi-induced effects on VSMCs. Pi uptake has the most variation between Pi concentrations of 0.03mM and 0.1mM, but by 0.5mM Pi the velocity of Pi uptake into VSMCs has reached maximum potential. This is in contrast to the concentration of Pi required for matrix mineralization in VSMCs, which is 2.4mM Pi or greater to show significant mineralization. Additionally, a Pi concentration of 2.6mM was required for significant osteochondrogenic differentiation as measured by decreased SM22α and increased OPN, which suggested a signaling function responsible for elevated Pi-induced effects. ERK1/2 phosphorylation was increased at 3.0mM Pi, but not 1.0mM Pi or 0.5mM Pi, in VSMCs. As PiT-1 had not previously been linked to ERK1/2 phosphorylation in VSMCs, it was very interesting to find that PiT-1 deletion in VSMCs eliminated elevated Pi-induced ERK1/2 phosphorylation. Together, the data suggest that a Pi uptake-independent mechanism through PiT-1 may be responsible for ERK1/2 phosphorylation, osteochondrogenic differentiation, and matrix mineralization.

PiT-1 has been identified as a potential Pi sensor in previous studies and review articles. These findings were mainly performed while studying bone formation, as Pi transport has been suggested to play an important role in hydroxyapatite formation in bone tissue [10]. Proliferating chondrocytes were found to induce ERK1/2 phosphorylation in the presence of elevated Pi, and PiT-1 siRNA eliminated this ERK1/2 induction [6]. The authors of this study suggested that PiT-1 may play a role in Pi sensing because of this link to ERK1/2 phosphorylation in proliferating chondrocytes. A review article published in 2010 shows support for a possible Pi sensing mechanism involving PiT-1 and ERK1/2 that could relay systemic, local, and cellular signals to promote bone formation [11]. However, none of these articles suggest a specific mechanism or a cell signaling pathway that could support the hypothesis that PiT-1 is a Pi sensor. The data do support a possible connection between PiT-1 and ERK1/2.

There are also multiple functional similarities between PiT-1 and ERK1/2. Beck et al. showed that PiT-1 silencing reduced cell proliferation, and that overexpression of a Pi uptake-deficient PiT-1 mutant could rescue this process in HeLa cells [3]. Also, Salaun et al. showed that a Pi uptake-deficient PiT-1 mutant reduced the rate of apoptosis in HeLa cells treated with Tumor Necrosis Factor-α [4]. Finally, PiT-1 regulation of hematopoietic stem cell differentiation was found to be Pi uptake-independent [5,12]. However, none of those studies identified the cell signaling pathway required for transport-independent PiT-1 functions. Our findings suggest that ERK1/2 cell signaling is required for the PiT-1 response to elevated Pi, and further studies are warranted to confirm Pi uptake-independent functions and investigate adaptor proteins that are responsible for PiT-1 signaling through ERK1/2. Since ERK kinases have been implicated in control of proliferation, apoptosis, and differentiation [13–15], it is interesting to speculate that

the PiT-1 driven ERK1/2 signaling pathway that we have identified here might be involved in these processes as well.

In conclusion, Pi uptake-independent PiT-1 functions that promote ERK1/2 phosphorylation may lead to osteochondrogenic differentiation and matrix mineralization and Pi concentrations well above maximal Pi uptake. This hypothesis would help explain the separation between Pi concentrations required for Pi uptake and matrix mineralization.

Gene	Primer Sequence (5' to 3')	Accession Number
OPN	F: TGAGGTCAAAGTCTAGGAGTTTCC R: TTAGACTCACCGCTCTTCATGTG P: *FAM*–TTCTGATGAACAGTATCCTG–*MGB*	NM_009263
SM22α	F: GACTGACATGTTCCAGACTGTTGAC R: CAAACTGCCCAAAGCCATTAG P: *FAM*–TGAAGGTAAGGATATGGCAGC–*MGB*	NM_011526
PiT-1	F:TTCCTTGTTCGTGCGTTCATC R:AATTGGTAAAGCTCGTAAGCCATT P:*FAM*-CCGTAAGGCAGATCC-*MGB*	NM_015747
PiT-2	F:GACCGTGGAAACGCTAATGG R: CTCAGGAAGGACGCGATCAA P:*FAM*-CATGGTTGGTTCAGCTG-*MGB*	NM_011394

Table 2.1. Real-time Q-PCR primers and probes. Primers and probes used in Q-PCR are listed here with the gene name and accession number. Q-PCR probes are FAM-reporters with MGB quenchers. F = Forward primer; R = Reverse primer; P = Probe.

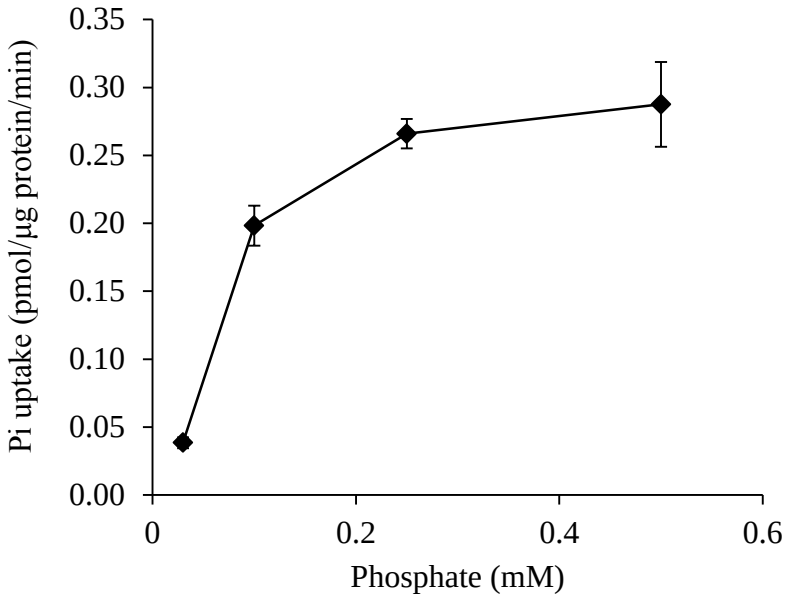

Figure 2.1. Pi uptake in WT VSMCs. Sodium-dependent Pi uptake was measured at different Pi concentrations (0.03 mM to 0.5 mM Pi) in VSMCs isolated from wild-type C57BL/6 mice (WT VSMCs) and normalized to protein concentration for each sample and assay time.

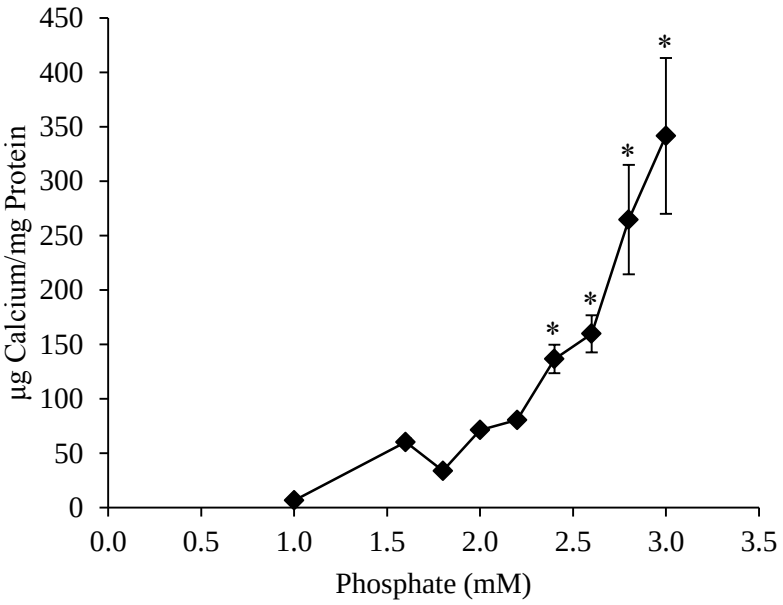

Figure 2.2. Calcification of WT VSMCs in varying Pi concentrations. Calcium deposition of WT VSMCs was quantified after 8 days of incubated in various Pi concentrations. Statistically significant differences from 1.0 mM Pi data are indicated by * = $P<0.05$ as measured by One-way ANOVA post-hoc Tukey analysis.

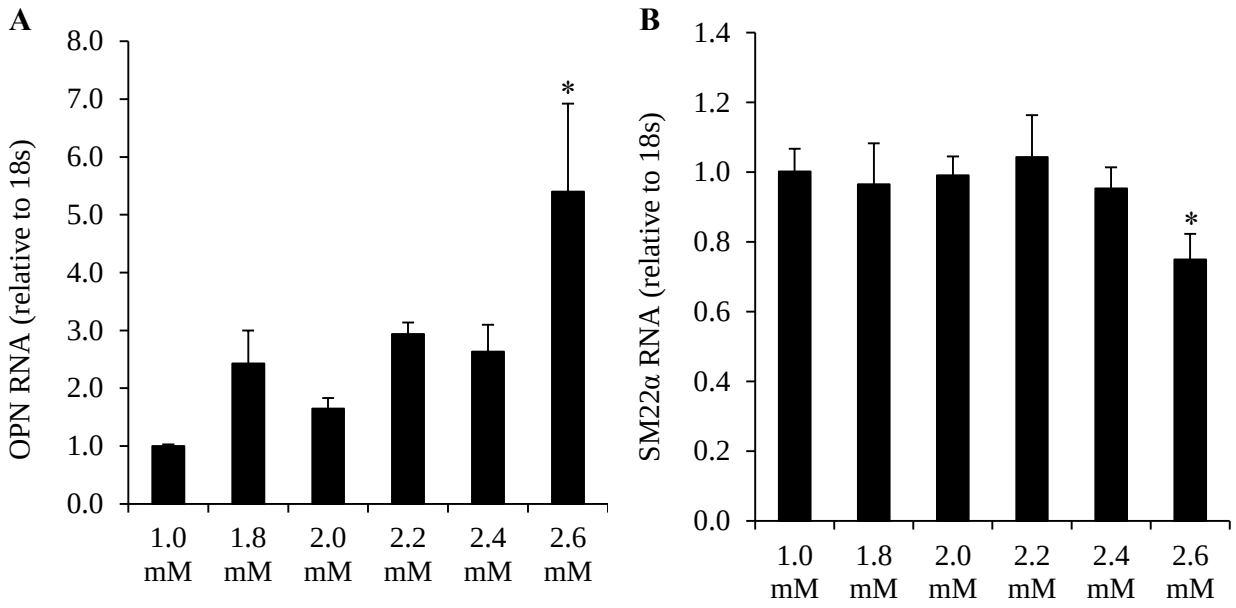

Figure 2.3. Osteochondrogenic differentiation of WT VSMCs in varying Pi concentrations. RNA lysate of WT VSMCs was collected after 6 days of Pi induction, and then (A) OPN and (B) SM22α were quantified by Q-PCR. Data are presented as mean ± standard deviation (S.D.), n = 3 for all data points. Statistically significant differences from 1.0 mM Pi data are indicated by * = $P<0.05$ as measured by One-way ANOVA post-hoc Tukey analysis.

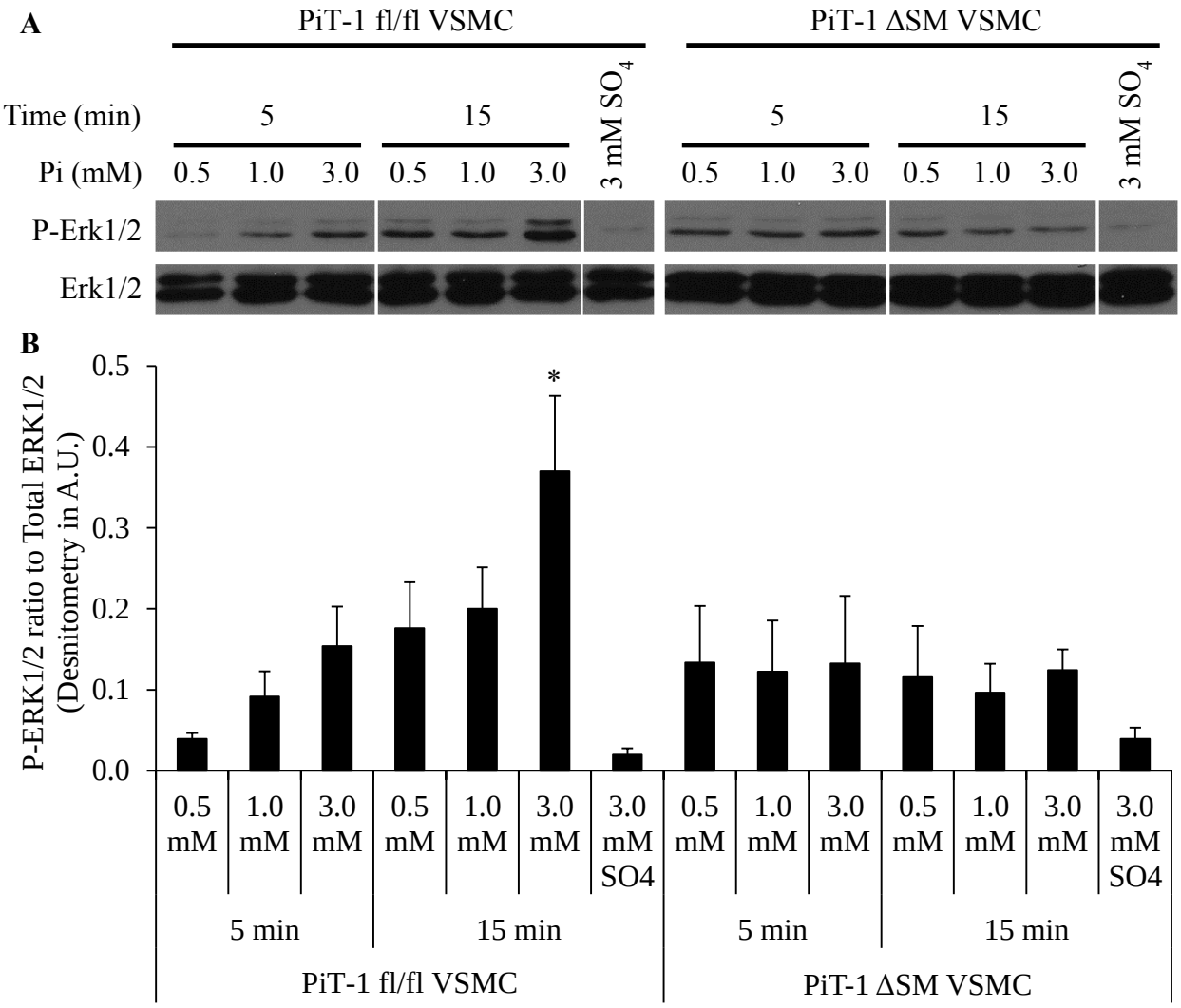

Figure 2.4. PiT-1 is required for Pi-induced ERK1/2 phosphorylation in VSMCs. (A) Pi induction of p-ERK1/2 and total ERK1/2 were visualized by Western blot analysis by incubating PiT-1 fl/fl and PiT-1 ΔSM VSMCs in 0.5 mM Pi, 1.0 mM Pi, 3.0 mM Pi, or 3.0 mM Sodium sulfate for 5 or 15 minutes. (B) Densitometry was used to quantify the immunoblot images and shown as the ratio of P-ERK1/2 to Total ERK1/2. Western blot is representative of three experiments with similar results, and quantification is represented as mean ± S.D., n = 3 for all data points. Statistically significant differences from all other data from the same cell line is indicated by * = $P<0.05$ as measured by One-way ANOVA post-hoc Tukey analysis.

2.5 Notes to Chapter 2

1 Villa-Bellosta R, Levi M, Sorribas V. Vascular smooth muscle cell calcification and SLC20 inorganic phosphate transporters: effects of PDGF, TNF-alpha, and Pi. *Pflugers Arch* 2009; 458:1151–61.

2 Villa-Bellosta R, Bogaert YE, Levi M, Sorribas V. Characterization of phosphate transport in rat vascular smooth muscle cells: implications for vascular calcification. *Arterioscler Thromb Vasc Biol* 2007; 27:1030–6.

3 Beck L, Leroy C, Salaün C, Margall-Ducos G, Desdouets C, Friedlander GC-P. Identification of a novel function of PiT1 critical for cell proliferation and independent of its phosphate transport activity. *J Biol Chem* 2009; 284:31363–74.

4 Salaün C, Leroy C, Rousseau A, Boitez V, Beck L, Friedlander GC-P. Identification of a novel transport-independent function of PiT1/SLC20A1 in the regulation of TNF-induced apoptosis. *J Biol Chem* 2010; 285:34408–18.

5 Liu L, Sánchez-Bonilla M, Crouthamel M, Giachelli C, Keel S. Mice lacking the sodium-dependent phosphate import protein, PiT1 (SLC20A1), have a severe defect in terminal erythroid differentiation and early B-cell development. *Exp Hematol* Published Online First: 30 January 2013. doi:10.1016/j.exphem.2013.01.004

6 Kimata M, Michigami T, Tachikawa K, Okada T, Koshimizu T, Yamazaki M, *et al.* Signaling of extracellular inorganic phosphate up-regulates cyclin D1 expression in proliferating chondrocytes via the Na+/Pi cotransporter Pit-1 and Raf/MEK/ERK pathway. *Bone* 2010; 47:938–947.

7 Crouthamel MH, Lau WL, Leaf EM, Chavkin NW, Wallingford MC, Peterson DF, *et al.*

Sodium-Dependent Phosphate Cotransporters and Phosphate-Induced Calcification of Vascular Smooth Muscle Cells: Redundant Roles for PiT-1 and PiT-2. *Arterioscler Thromb Vasc Biol* 2013; 33:2625–2632.

8 Jono S, McKee MD, Murry CE, Shioi a., Nishizawa Y, Mori K, *et al.* Phosphate Regulation of Vascular Smooth Muscle Cell Calcification. *Circ Res* 2000; 87:e10–e17.

9 Li X, Yang H-YY, Giachelli CM. Role of the sodium-dependent phosphate cotransporter, Pit-1, in vascular smooth muscle cell calcification. *Circ Res* 2006; 98:905–12.

10 Penido MGMG, Alon US. Phosphate homeostasis and its role in bone health. *Pediatr Nephrol* 2012; 27:2039–48.

11 Khoshniat S, Bourgine A, Julien M, Weiss P, Guicheux J, Beck L. The emergence of phosphate as a specific signaling molecule in bone and other cell types in mammals. *Cell Mol Life Sci* 2011; 68:205–18 ST – The emergence of phosphate as a speci.

12 Forand A, Beck L, Leroy C, Rousseau A, Boitez V, Cohen I, *et al.* EKLF-driven PIT1 expression is critical for mouse erythroid maturation in vivo and in vitro. *Blood* 2013; 121:666–78.

13 Meloche S, Pouysségur J. The ERK1/2 mitogen-activated protein kinase pathway as a master regulator of the G1- to S-phase transition. *Oncogene* 2007; 26:3227–39.

14 Wada T, Penninger JM. Mitogen-activated protein kinases in apoptosis regulation. *Oncogene* 2004; 23:2838–49.

15 Roskoski R. ERK1/2 MAP kinases: Structure, function, and regulation. *Pharmacol Res* 2012; 66:105–143.

CHAPTER 3

PHOSPHATE UPTAKE-INDEPENDENT PIT-1 FUNCTIONS PROMOTE ELEVATED PHOSPHATE INDUCED ERK1/2 PHOSPHORYLATION, PHENOTYPE CHANGE, AND MATRIX MINERALIZATION IN VSMCS

Chapter published in similar form as part of: "Phosphate uptake-independent signaling functions of the type III sodium-dependent phosphate transporter, PiT-1, in vascular smooth muscle cells." Chavkin NW, Chia JJ, Crouthamel MH, Giachelli CM. Experimental Cell Research. 2015 Apr 10;333(1):39-48.

3.1 Introduction

PiT-1 has been the key focus of many other studies looking at functions other than phosphate transport. The first known function of PiT-1 was as a membrane receptor for the Gibbon ape leukemia virus, which gave the first name for PiT-1 as the gibbon ape leukemia virus receptor 1 (GLVR-1) [1]. The phosphate transport function of PiT-1 was published in 1996 [2]. As PiT-1 RNA was found in all tissues, PiT-1 was thought to be responsible for intracellular phosphate homeostasis. This is in contrast to other sodium-dependent phosphate transporters which have specific expression patterns and play more specific roles in the intestines and kidneys.

Although it is clear that elevated Pi directly induces VSMC calcification through PiT-1, the molecular mechanisms by which PiT-1 facilitates this process are still unclear. Furthermore, as

described in Chapter 2, the concentration of Pi that induces matrix calcification (>2mM) in VSMCs is much higher than that required for maximal Pi uptake by PiT-1 in VSMCs (~0.5mM). Previous literature also describes Pi uptake-independent functions of PiT-1. This suggests that PiT-1 might have a signaling function independent of Pi uptake that promotes elevated Pi-induced effects. **We hypothesize that Pi uptake-independent functions of PiT-1 promote elevated Pi-induced ERK1/2 phosphorylation, osteochondrogenic differentiation, and matrix mineralization.** To address this possibility, effects of elevated Pi were carefully examined in VSMC expressing wild-type and transport-deficient PiT-1 mutants. Our findings indicate that PiT-1 has both phosphate uptake-dependent and phosphate uptake-independent functions in VSMC related to VC.

3.2 Materials and Methods

Site-directed mutagenesis of mouse PiT-1 cDNA

A pLXIN vector containing wild-type mouse PiT-1 cDNA (PiT-1 WT), that was previously created [3], was used as the template for site-directed mutagenesis (QuikChange, Agilent Technologies). Primers were designed (QuikChange Primer Design Program, Agilent Technologies) to create Pi uptake deficient mutants (PiT-1-E74K, PiT-1-S132A, PiT-1-S623A) as shown in Table 3.1. Sequencing by the University of Washington Sequencing Center confirmed gene sequence.

Retroviral infection of primary mouse VSMCs

PiT-1 ΔSM VSMCs were transduced as previously described [3] with pLXIN vectors containing wild-type, Pi uptake-deficient PiT-1 mutants, or control (vector alone). Briefly, the pLXIN vectors were transfected into Ecotropic Phoenix Packaging Cell Lines (ATCC, SD 3444) with Lipofectamine 2000 (Life Technologies) to create retrovirus-conditioned media, which was used to infect PiT-1 ΔSM VSMCs. VSMCs were selected and maintained in 200 ug/mL G418 (Sigma).

Real-time quantitative PCR

Collection of mRNA was performed with RNeasy Mini Kit (Qiagen) following manufacturer's protocol. Real-time quantitative PCR (Q-PCR) was performed with primers listed (Table 2.1). All Q-PCR gene counts were normalized to 18S gene counts and quantified using the quantitative ΔΔCt method.

Immunocytochemistry of PiT-1 ΔSM VSMCs expressing PiT-1 constructs

PiT-1 ΔSM VSMCs transduced as described above were grown in Nunc Lab-Tek Permanox 4-well chamber slides (Sigma) in growth media until 70-80% confluent. VSMCs were washed with PBS and fixed with 100% MeOH at -20^0 C for 20 minutes. Fixed cells were washed with PBS and probed for PiT-1 with a rabbit anti-mouse PiT-1 antibody primary (lab generated serum) and DyLight 549-Conjugated AffiniPure Donkey Anti-Rabbit IgG secondary (Jackson ImmunoResearch, final 1.5 µg/mL concentration). Cells were counterstained with DAPI at 1µg/mL for 5 minutes, mounted with ProLong Gold Antifade (Life Technologies), and imaged with a Nikon E800 Upright Microscope.

Pi uptake assay

Pi uptake was measured as previously described [4]. Briefly, VSMCs were seeded into 12-well tissue culture plates and incubated with radiolabeled H333PO4 (Perkin Elmer) and un-labeled potassium phosphate in either sodium-containing Earle's Balanced Salt Solution (EBSS) or sodium-free, choline-containing EBSS. VSMCs were incubated for 20 minutes, lysate was collected, and radioactive counts were recorded in OptiFluor (Perkin Elmer) using a LS 6500 Beckman liquid scintillation counter. Sodium- dependent Pi uptake was calculated by subtracting uptake in choline containing media from total uptake in sodium containing media, and normalized to incubation time and protein concentration of the cell lysate, quantified by Bicinchoninic Acid assay (Thermo Scientific). Michaelis-Menten kinetic parameters were determined by non-linear regression.

Quantification of Pi-induced phosphorylated ERK1/2

VSMCs were grown in 6-well tissue culture plates in normal growth media. At 70-80% confluence, cells were washed twice with PBS and incubated in Pi-free DMEM (Life Technologies, 11971) supplemented with 1% FBS and 1% antibiotic/antimycotic. After 24 hours, media was aspirated and VSMCs were incubated in Pi-free DMEM supplemented with 1% FBS, 1% antibiotic/antimycotic, and Na_2PO_4/$NaPO_4$ (pH = 7.4) to varying Pi concentrations. After 5 or 15 minutes of incubation, VSMCs were washed three times with ice-cold PBS, and cell lysate was collected using lysate buffer (0.1 mM Tris pH 6.8 2% SDS) with added protease inhibitors and phosphatase inhibitors. Protein was loaded at 10ug/lane into 10% SDS-PAGE gels, transferred to PVDF membranes, and analyzed by immunoblot. Primary phosphorylated ERK1/2 and total ERK1/2 antibodies (Cell Signaling Technology) and secondary HRP-

conjugated goat anti-rabbit antibody (Jackson ImmunoResearch) were used with Western Lighting (ECL) substrate to expose the protein signal. ImageJ software (NIH, Bethesda, MD) was used to quantify the densitometry of the bands.

Calcification assay

Calcification was determined as previously described [4]. Briefly, VSMCs were grown in 6-well tissue culture plates in normal growth media until 70-80% confluent, then VSMCs were incubated with DMEM supplemented with 5% FBS, 1% antibiotic/antimycotic, and $Na_2PO_4/NaPO_4$ (pH = 7.4) to varying Pi concentrations. After 8 days, calcium was extracted with 0.6 N HCl at 4^oC overnight. Calcium concentration was determined by the O-Cresolphthalein method using the Calcium Reagent Set (Teco Diagnostics). Protein lysate was collected in 0.2 N NaOH. Protein concentration was determined by Bicinchoninic Acid assay. Calcium data was normalized to protein data.

Apoptosis assay

Apoptosis was determined through FITC-conjugated Annexin V flow cytometry using the FITC Annexin V Apoptosis Detection Kit (BD Pharmagen), following manufacturer's protocol. Briefly, VSMCs were gently trypsinized with 0.05% trypsin in versene for 5 minutes, and the FITC-conjugated Annexin V antibody and Propidium iodide were used to stain the suspended VSMCs. VSMCs undergoing apoptosis was defined as Annexin V positive and PI negative.

Statistical analysis

SPSS software v16.0 (SPSS, Chicago, IL) was used to perform Student t-tests to compare means of two individual groups, and one-way ANOVA with post-hoc Tukey test to compare means of three or more individual groups. Linear regression to determine variable correlation and nonlinear regression to determine Michaelis-Menten parameters were performed using STATA version 12 (StataCorp). A p-value of less than 0.05 was considered statistically significant.

3.3 Results

Generation and characterization of Pi uptake deficient PiT-1 mutants

Since Pi concentrations that induced matrix mineralization, osteochondrogenic differentiation, and ERK1/2 phosphorylation were well above the Km of Pi uptake by PiT-1, we considered that PiT-1 may be involved in cell signaling through a Pi uptake-independent pathway. To separate Pi uptake-dependent function from Pi uptake-independent function of PiT-1, transport deficient PiT-1 mutants were generated. Previous studies on human PiT-1 identified three amino acids critical to Pi uptake: E70, S128, S621 [5–7]. Point mutations of these amino acids inhibited Pi uptake through PiT-1 without affecting membrane localization [5–7]. Therefore, we generated the corresponding point mutations in mouse PiT-1: E74K, S132A, and S623A (Table 3.2). PiT-1 WT, PiT-1 transport-defective mutants (PiT-1-E74K, PiT-1-S132A, and PiT-1-S623A), and vector alone were expressed in VSMCs lacking PiT-1 (PiT-1 ΔSM VSMCs). Over-expression of these constructs in PiT-1 ΔSM VSMCs was confirmed by Q-PCR (Fig. 3.1A). Immunofluorescent histochemistry established that PiT-1 WT and mutant constructs were appropriately localized to the plasma membrane of transduced VSMCs (Fig. 3.1B). Since recent studies revealed an up-regulation of the related family member, PiT-2, when PiT-1 was deleted

from osteoblast or smooth muscle cells in vivo [8,9], PiT-2 RNA expression was examined in the engineered cell lines. PiT-1 overexpression in cultured primary VSMCs did not significantly alter PiT-2 mRNA expression levels (Fig. 3.1C).

Reduced Pi uptake kinetics of PiT-1 ΔSM VSMCs overexpressing PiT-1 transport deficient mutants

Rate of sodium-dependent Pi uptake was measured across a range of Pi concentrations in PiT-1 ΔSM VSMCs expressing either vector control, PiT-1 WT, or the mutant constructs PiT-1-E74K, PiT-1-S132A, or PiT-1-S623A (Fig. 3.2). As expected, overexpression of PiT-1 WT significantly increased the rate of sodium-dependent Pi uptake compared to vector control VSMCs at all Pi concentrations tested. The PiT-1-E74K mutant did not increase the rate of sodium-dependent Pi uptake compared to vector control, and VSMC containing this construct had the lowest Pi uptake rate of the three PiT-1 mutants. The PiT-1-S132A and PiT-1-S623A mutations had intermediate effects; Pi uptake rate was significantly less than VSMCs overexpressing PiT-1 WT at lower Pi concentrations, but similar to PiT-1 WT at higher Pi concentrations. These findings are consistent with calculated Pi uptake kinetic parameters of each cell line (Table 3.3). Maximal velocity (Vmax) of Pi uptake into the VSMCs expressing PiT-1 WT, PiT-1-S132A, and PiT-1-S623A were 0.881, 0.736, 0.950 pmol Pi/ug/min, respectively, and were two- to three-fold higher than cells expressing vector control or PiT-1-E74K (0.408, 0.290 pmol Pi/ug/min, respectively). Furthermore, sodium-independent Pi uptake was not different between the cell lines containing the different PiT-1 mutants (data not shown). Subsequent experiments utilized the PiT-1-E74K mutant since it showed the least ability to transport Pi among the PiT-1 mutant constructs tested.

Both PiT-1-WT and PiT-1-E74K promote elevated Pi-induced ERK1/2 phosphorylation

Pi-induced ERK1/2 phosphorylation mediated by PiT-1 is Pi uptake-independent

Since we found that PiT-1 was required for Pi-induced ERK1/2 phosphorylation in VSMCs, we investigated whether Pi transport by PiT-1 was required for this process. PiT-1 ΔSM VSMCs expressing vector control, PiT-1 WT, or PiT-1-E74K were treated with either normal (1.0 mM) or elevated (3.0 mM) Pi, and ERK1/2 phosphorylation was measured. As shown in Fig. 3.3, VSMCs expressing PiT-1 WT and PiT-1-E74K, but not vector control, both showed an increase in ERK1/2 phosphorylation in response to elevated Pi treatment. Incubation in 3.0 mM Pi increased ERK1/2 phosphorylation by 34% in PiT-1 WT and 30% in PiT-1-E74K VSMCs compared to 1.0 mM Pi treatment. This result suggests that ERK1/2 signaling mediated by elevated Pi through PiT-1 was Pi uptake-independent.

Pi uptake-independent PiT-1 function promotes Pi-induced osteochondrogenic differentiation.

Both PiT-1-WT and PiT-1-E74K promote elevated Pi-induced osteochondrogenic differentiation

Pi uptake-independent PiT-1 function promotes Pi-induced osteochondrogenic differentiation

In VSMCs, ERK1/2 phosphorylation is required for osteochondrogenic differentiation in response to elevated Pi [10]. To determine if Pi uptake-independent PiT-1 functions promote VSMC phenotype change via ERK1/2 phosphorylation, we examined RNA expression of the osteochondrogenic lineage marker, OPN, and smooth muscle lineage marker, SM22α, in VSMCs expressing vector control, PiT-1 WT, or PiT-1-E74K. Expression of either PiT-1 WT or PiT-1-E74K greatly reduced SM22α mRNA levels compared to vector control (Fig. 3.4A). This effect was observed even under normal Pi conditions, suggesting that increased PiT-1 expression,

independent of extracellular Pi levels, promotes down-regulation of SM22α. Furthermore, as shown in Figure 6, OPN was induced to a greater extent in VSMCs expressing PiT-1 WT and PiT-1-E74K compared to vector control (Fig. 3.4B). Down-regulation of SM22α and up-regulation of OPN is consistent with increased VSMC osteochondrogenic differentiation in VSMCs expressing PiT-1 WT or PiT-1-E74K.

PiT-1 promotes VSMC matrix mineralization via Pi uptake-dependent and Pi uptake-independent processes

PiT-1 expression has previously been shown to be required for elevated Pi-induced VSMC matrix mineralization [3], but whether Pi uptake through PiT-1 was required for this activity has not been determined. To address this, VSMCs expressing vector control, PiT-1 WT, or PiT-1-E74K were induced to mineralize with elevated Pi. Elevated Pi (2.6 mM) promoted calcification of all three VSMC lines compared to normal Pi conditions (1.0 mM). To rule out potential effects of PiT-1 on cell death in response to elevated Pi, apoptosis rates in vector control, PiT-1 WT, and PiT-1-E74K expressing VSMCs in normal and elevated Pi conditions were measured. Rates of apoptosis were less than 5% in all conditions tested, and elevated Pi did not induce apoptosis compared to normal Pi conditions (Fig. 3.5C).

While VSMCs expressing PiT-1 WT showed the greatest induction, PiT-1-E74K expressing VSMCs also showed significantly greater mineralization than vector control VSMCs (Fig. 3.5A). Furthermore, VSMCs expressing PiT-1-S132A and PiT-1-S623A (mutants with intermediate phosphate uptake properties) mineralized more than VSMC expressing PiT-1-E74K (Fig. 3.5B). Though statistically significant, matrix mineralization in VSMCs was poorly correlated with

calculated Vmax values of VSMC Pi uptake (R2 = 0.25) (Fig. 3.5D), suggesting that PiT-1 functions besides phosphate uptake contribute to maximal VSMC matrix mineralization.

3.4 Discussion

The present study addressed the hypothesis that PiT-1 mediates both phosphate uptake-dependent and -independent functions important for Pi-induced calcification in VSMC. Transduction with both WT and transport deficient PiT-1 mutants restored Pi-inducible ERK1/2 phosphorylation in PiT-1 deficient VSMC. Moreover, VSMC osteochondrogenic differentiation was similar in VSMC expressing WT and transport deficient PiT-1 mutants. Finally, Pi transport-deficient mutants enhanced VSMC calcification, though at lower levels than PiT-1 WT. These data suggest that PiT-1 signaling through ERK1/2 and downstream regulation of osteochondrogenic gene expression occurs via a Pi uptake-independent pathway, and that both Pi uptake-dependent and -independent processes play a role in promoting Pi-induced calcification.

The importance of ERK1/2 phosphorylation in osteochondrogenic differentiation and matrix mineralization of VSMCs in response to elevated Pi has been previously established [10–12]. In the present study, we extended these findings by determining that PiT-1 was required for Pi-induced ERK1/2 phosphorylation in VSMC. These results are consistent with findings in chondrocytes and HEK293 cells that showed decreased Pi-induced ERK1/2 phosphorylation following PiT-1 knock-down by siRNA [11,12]. Furthermore, our studies are the first to show that PiT-1 induction of ERK1/2 phosphorylation in VSMC in response to elevated Pi can occur in the absence of Pi uptake through PiT-1.

In addition to ERK1/2 phosphorylation, Pi-induced regulation of genes downstream of ERK1/2 signaling, including SM22α and OPN, was supported by both WT and transport-defective PiT-1. Additionally, we observed that overexpression of either PiT-1-WT or PiT-1-E74K caused down-regulation of SM22α in normal Pi conditions, suggesting that the PiT-1 signaling pathway might be active under normal Pi conditions when PiT-1 density is very high. Our findings of a signaling function for PiT-1 are consistent with growing evidence in several other cell types for transport-independent functions of PiT-1.

Although transport defective PiT-1 was able to support elevated Pi-induced ERK1/2 phosphorylation and osteochondrogenic differentiation at levels similar to WT PiT-1, this was not the case for VSMC matrix mineralization. Both Pi uptake-dependent and Pi uptake-independent functions of PiT-1 were required to promote maximal VSMC matrix mineralization. These findings suggest that Pi uptake-dependent and -independent mechanisms regulate distinct cellular functions in VSMCs that work in concert to promote matrix mineralization depending on the level of extracellular Pi. One possibility is that at normal ambient Pi of 1.0 mM, the Pi transport function of PiT-1 predominates, and allows Pi entry into VSMC for essential cell functions with excess Pi shed from the cell via efflux transporters or matrix vesicles [13–15]. In contrast, at high ambient Pi (>2.0 mM), PiT-1 activates ERK1/2 and drives osteochondrogenic phenotype change, thereby promoting the loading of matrix vesicles not only with Pi, but also with pro-calcific cargo making them “calcification competent”. The importance of Pi-loaded matrix vesicles in initiating VSMC mineralization has been extensively studied, and osteochondrogenic differentiation of VSMC has been shown to enhance formation of

calcification competent matrix vesicles by loading them with pro-calcific molecules such as alkaline phosphatase, and removing calcium mineral inhibitors including matrix GLA protein and Fetuin-A [14,15]. Clearly, further investigations are required to test these exciting possibilities, and to determine the molecular mechanism by which PiT-1 senses extracellular Pi levels.

In conclusion, our findings suggest that at extracellular Pi concentrations above physiological levels, PiT-1 acts as a phosphate sensor with cell signaling functions that regulate ERK kinase activity, VSMC osteochondrogenic differentiation, and calcification. This possibility would help explain the strikingly different Pi-dependence of phosphate uptake (maximal 0.5 mM) versus VSMC differentiation and calcification (occurring above 2.0 mM). Further studies to delineate the mechanisms by which PiT-1 acts as a Pi sensor are warranted, and will help identify new therapeutic targets for treatment of VC.

Gene	Primer Sequence (5' to 3')
PiT-1-E74K	F: CTTAGCTAGCATCTTCAAAACTGTGGGCTCCGC R: GCGGAGCCCACAGTTTTGAAGATGCTAGCTAAG
PiT-1-S132A	F: GCTTCGTTTTTGAAGCTTCCGATTGCTGGGACCCATTG R: CAATGGGTCCCAGCAATCGGAAGCTTCAAAAACGAAGC
PiT-1-S623A	F: ACATTGGCCTTCCCATCGCCACAACACATTGCAAA R: TTTGCAATGTGTTGTGGCGATGGGAAGGCCAATGT

Table 3.1. Site-directed mutagenesis primers. Primers and probes used in site-directed are listed here with the gene name. Primers used in site-directed mutagenesis have the desired mutation underlined.

Human PiT-1	Mouse PiT-1	Mutation
Glu70 (E70)	Glu74 (E74)	Glutamic acid → Lysine (E74K) [5]
Ser128 (S128)	Ser132 (S132)	Serine → Alanine (S132A) [6]
Ser621 (S621)	Ser623 (S623)	Serine → Alanine (S623A) [7]

Table 3.2. Essential PiT-1 amino acids and mutations that affect Pi transport. Mutations in human PiT-1 that were described in previous studies to be essential for Pi transport are listed with the corresponding amino acid in mouse PiT-1. The mutation described that inhibited Pi transport is listed with the annotation describing the mouse PiT-1 mutation.

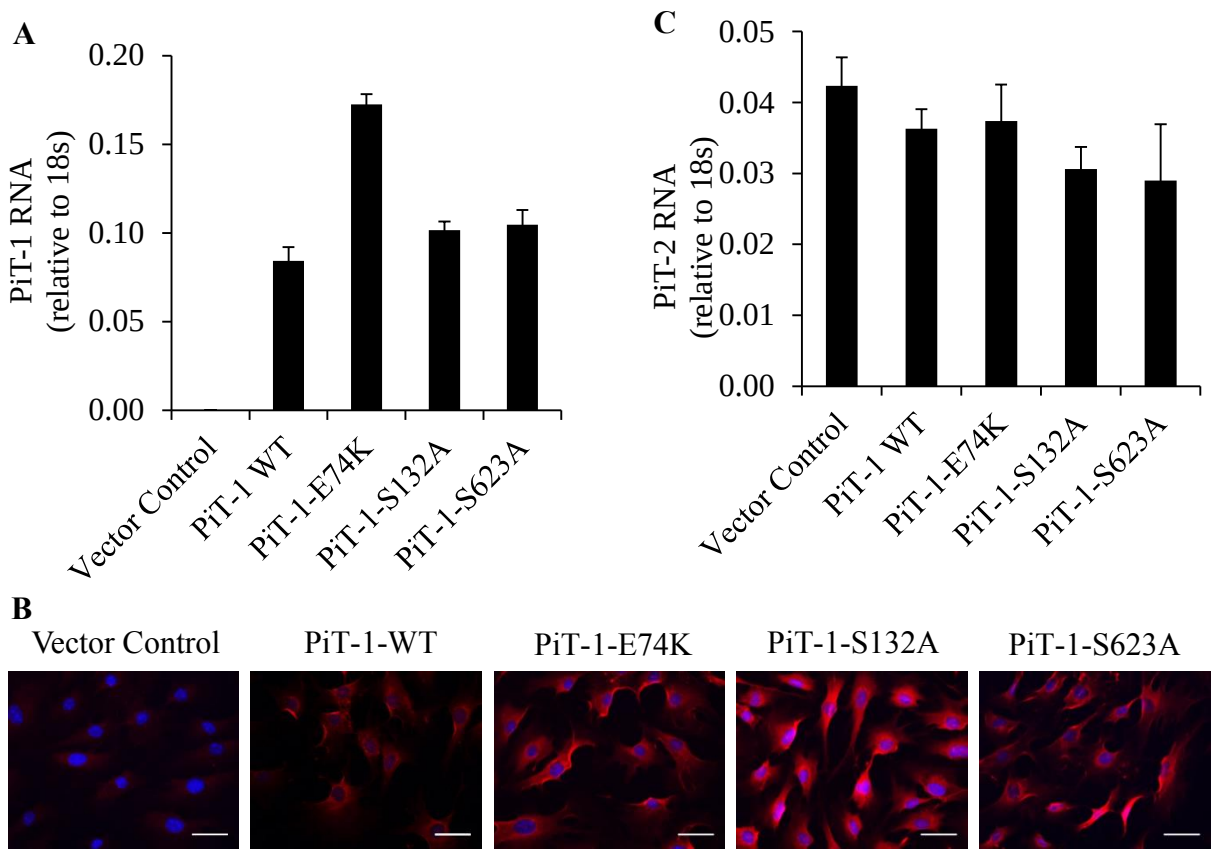

Figure 3.1. PiT-1 constructs transduced into PiT-1 ΔSM VSMCs are expressed and did not alter PiT-2 mRNA levels. (A) Q-PCR quantification of PiT-1 mRNA expression of PiT-1 ΔSM VSMCs transduced with vector control, PiT-1 WT, PiT-1-E74K, PiT-1-S132A, or PiT-1-S623A confirmed stable expression. (B) Immunocytochemical analysis of PiT-1 ΔSM VSMCs expressing Vector Control, PiT-1-WT, PiT-1-E74K, PiT-1-S132A, or PiT-1-S623A with primary PiT-1 antibody (red) and DAPI counterstain (blue) show expression of the PiT-1 WT, PiT-1-E74K, PiT-1-S132A, and PiT-1-S623A proteins, scale bar is 25 μm. (C) PiT-2 mRNA quantification by Q-PCR confirmed no significant effects on PiT-2 mRNA expression in any cell line. Data presented as mean ± S.D. (A,C) or representative images (B).

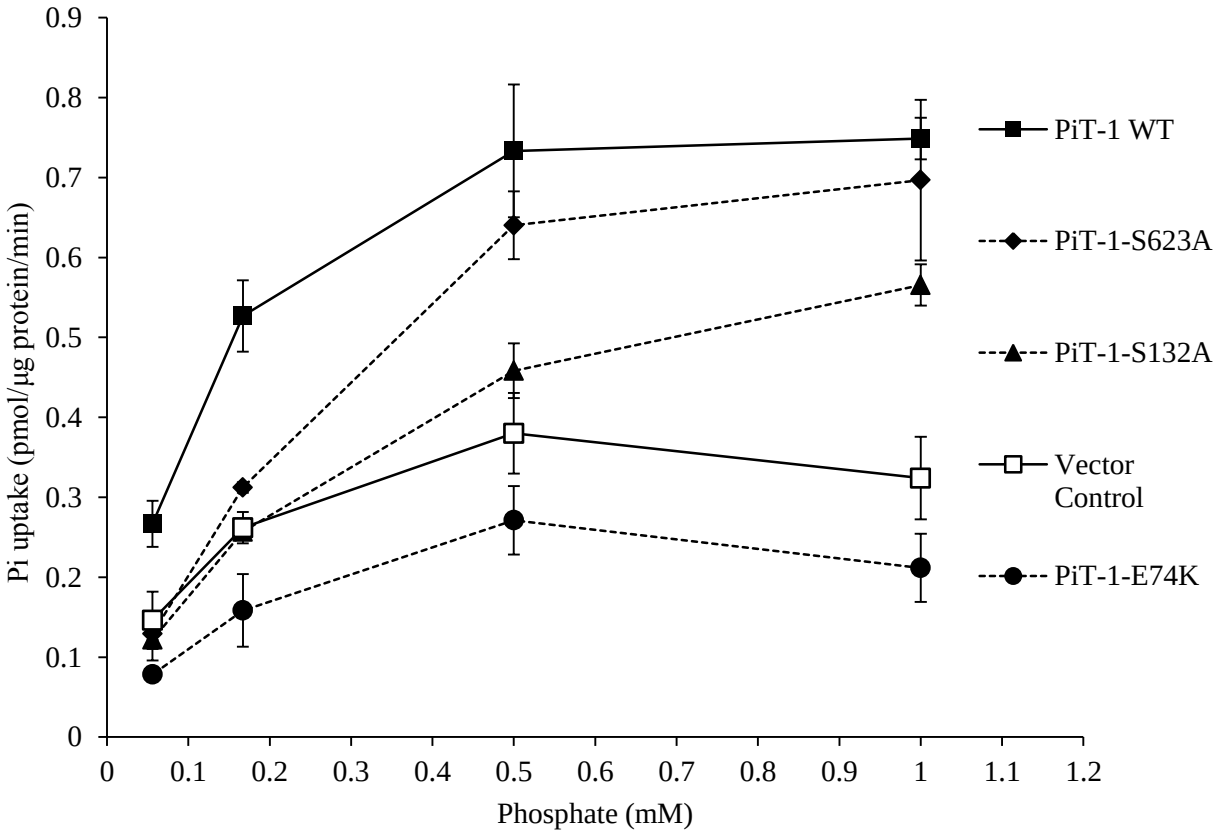

Figure 3.2. PiT-1 point mutations impair sodium-dependent Pi uptake in VSMCs. Sodium-dependent Pi uptake was quantified over a range of Pi concentrations in VSMCs expressing vector control, PiT-1 WT, PiT-1-E74K, PiT-1-S132A, or PiT-1-S623A. VSMC Pi uptake was measured over 20 minutes and normalized to time and VSMC protein content. Dashed connecting lines signify PiT-1 point mutation constructs. Data presented as mean ± S.D., n = 3 for all data points. Statistically significant differences between Vector Control and each PiT-1 construct at the same Pi concentration are indicated by * = $P<0.05$ as measured by One-way ANOVA post-hoc Tukey analysis.

Cell Line	Vmax (pmol/μg/min) ± S.E.	Km (mM) ± S.E.
Wild-type VSMC	0.369 ± 0.035	0.113 ± 0.032
Vector Control	0.408 ± 0.030	0.066 ± 0.024
PiT-1 WT	0.881 ± 0.035	0.102 ± 0.016
PiT-1-E74K	0.290 ± 0.032	0.097 ± 0.042
PiT-1-S132A	0.736 ± 0.031	0.303 ± 0.035
PiT-1-S623A	0.950 ± 0.008	0.308 ± 0.072

Table 3.3. Michaelis-Menten kinetic values of PiT-1 mutants. Kinetic values Vmax and Km were calculated based on Pi uptake data obtained for each VSMC line. Non-linear regression was performed and standard error was obtained using MATLAB software. Data is presented as mean ± S.E.

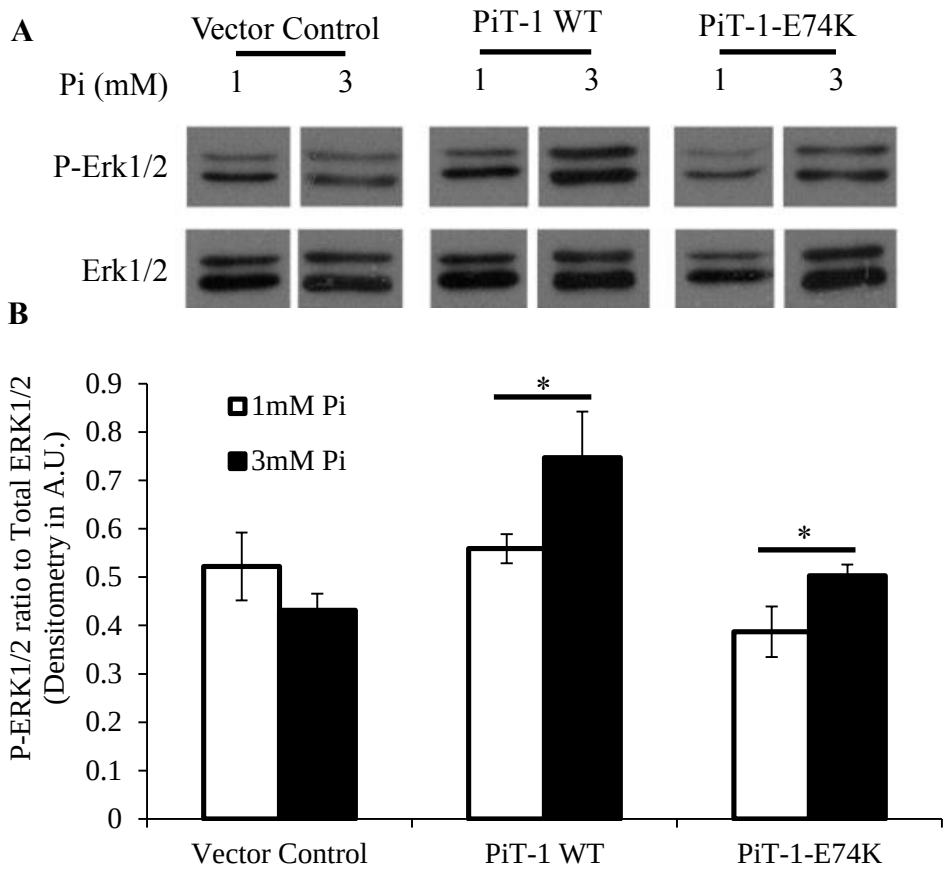

Figure 3.3. Elevated Pi induced ERK1/2 phosphorylation through Pi transport-independent PiT-1 function. (A) ERK1/2 phosphorylation was induced in PiT-1 ΔSM VSMCs expressing vector control, PiT-1 WT, or PiT-1-E74K with incubation in 1.0 mM or 3.0 mM Pi for 15 minutes. P-ERK1/2 and total ERK1/2 were visualized by western blot analysis. (B) Densitometry quantification of three independent experiments shows the ratio of P-ERK1/2 to Total ERK1/2. Data presented as a representative image (A) or mean ± S.D., n = 3 for all data points (B). Statistically significant differences between two independent means are indicated by * = $P<0.05$ as measured by student t-test.

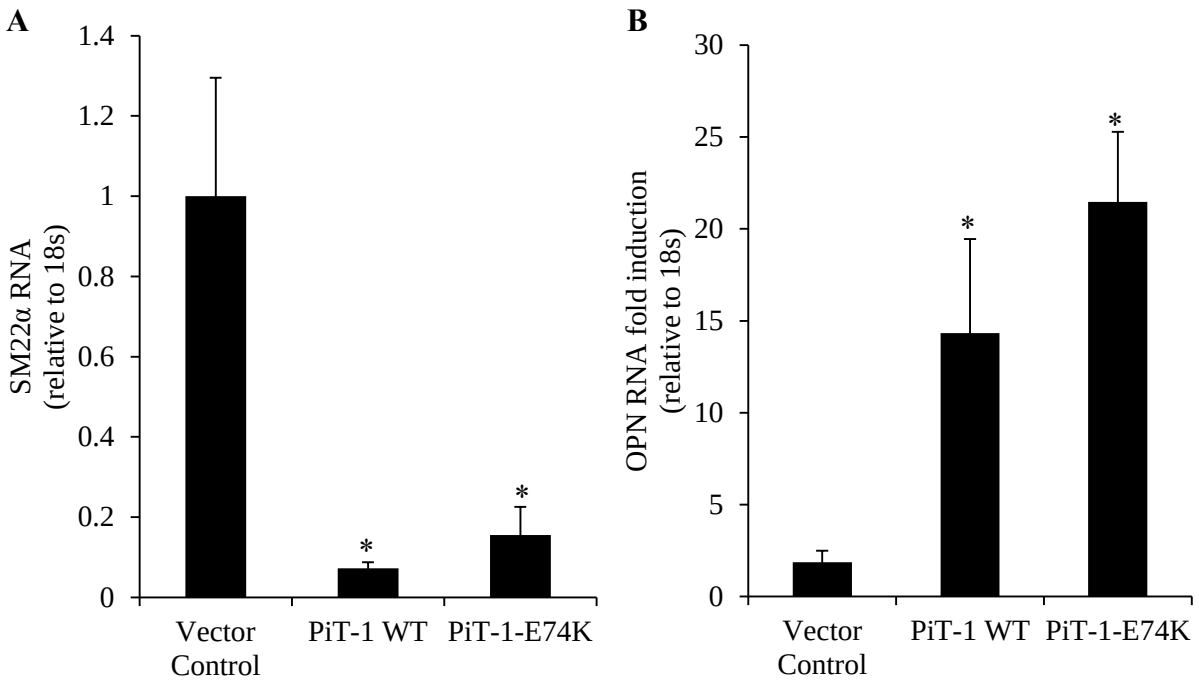

Figure 3.4. PiT-1 promotion of VSMC osteochondrogenic differentiation does not require Pi uptake. (A) SM22α RNA expression in PiT-1 ΔSM VSMCs expressing vector control, PiT-1 WT, or PiT-1-E74K was quantified by Q-PCR after incubation in 1.0 mM Pi for 4 days. (B) OPN RNA expression is presented as fold-induction of 2.6 mM Pi over 1.0 mM Pi after 4 days of incubation. Data presented as mean ± S.D., n = 3 for all data points. Statistically significant differences of means compared to vector control are indicated by * = $P<0.05$ as measured by One-way ANOVA post-hoc Tukey analysis.

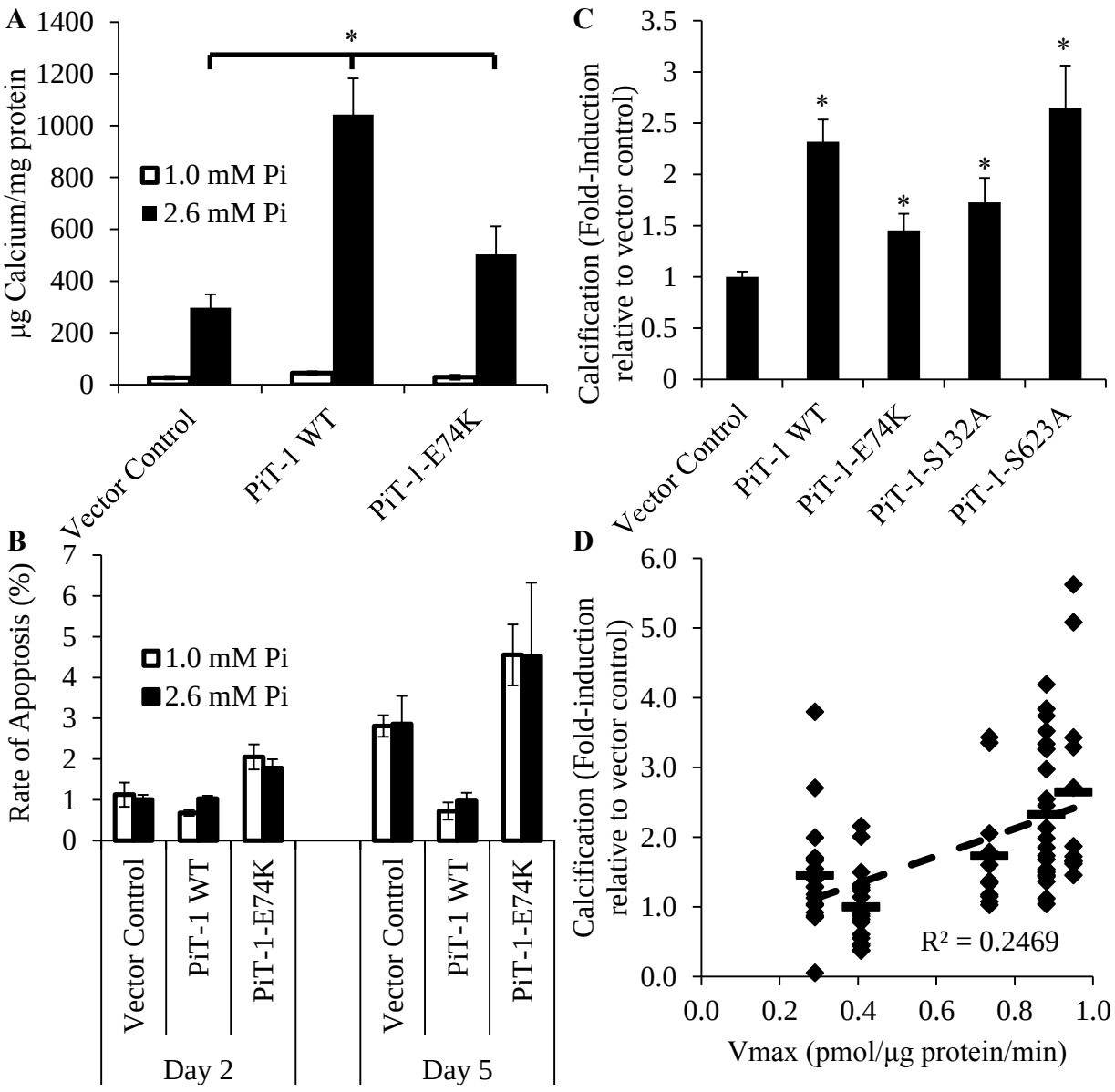

Figure 3.5. PiT-1 promotes VSMC matrix mineralization through both Pi uptake-dependent and -independent functions. (A) Matrix calcium content was quantified from PiT-1 ΔSM VSMCs expressing vector control, PiT-1 WT, or PiT-1-E74K that were induced to mineralize in normal Pi (1.0 mM) or elevated Pi (2.6 mM) for 8 days. (B) Rate of apoptosis was determined after incubation in normal or elevated Pi for 2 or 5 days. (C) Calcification was quantified of PiT-1 ΔSM VSMCs expressing vector control, PiT-1 WT, PiT-1-E74K, PiT-1-S132A, or PiT-1-S623A, and data is presented as fold-induction over vector control for each experiment by cell line. (D) Correlation analysis between calcification and calculated sodium-dependent Pi uptake Vmax parameter for each cell line is presented. Data is presented as mean ± S.D. (A-C), or as single points for linear regression (D). Statistically significant differences between indicated means (A) or compared to vector control (C) are indicated by * = $P<0.05$, determined by One-way ANOVA post-hoc Tukey analysis.

3.5 Notes to Chapter 3

1 Johann S V, Gibbons JJ, O'Hara BC-P. GLVR1, a receptor for gibbon ape leukemia virus, is homologous to a phosphate permease of Neurospora crassa and is expressed at high levels in the brain and thymus. *J Virol* 1992; 66:1635–40 ST – GLVR1, a receptor for gibbon ape leu.

2 Kavanaugh MP, Kabat D. Identification and characterization of a widely expressed phosphate transporter/retrovirus receptor family. *Kidney Int* 1996; 49:959–63 ST – Identification and characterization o.

3 Li X, Yang H-YY, Giachelli CM. Role of the sodium-dependent phosphate cotransporter, Pit-1, in vascular smooth muscle cell calcification. *Circ Res* 2006; 98:905–12.

4 Jono S, McKee MD, Murry CE, Shioi a., Nishizawa Y, Mori K, *et al.* Phosphate Regulation of Vascular Smooth Muscle Cell Calcification. *Circ Res* 2000; 87:e10–e17.

5 Bøttger P, Pedersen LC-P. Mapping of the minimal inorganic phosphate transporting unit of human PiT2 suggests a structure universal to PiT-related proteins from all kingdoms of life. *BMC Biochem* 2011; 12:21.

6 Beck L, Leroy C, Salaün C, Margall-Ducos G, Desdouets C, Friedlander GC-P. Identification of a novel function of PiT1 critical for cell proliferation and independent of its phosphate transport activity. *J Biol Chem* 2009; 284:31363–74.

7 Salaün C, Leroy C, Rousseau A, Boitez V, Beck L, Friedlander GC-P. Identification of a novel transport-independent function of PiT1/SLC20A1 in the regulation of TNF-induced apoptosis. *J Biol Chem* 2010; 285:34408–18.

8 Crouthamel MH, Lau WL, Leaf EM, Chavkin NW, Wallingford MC, Peterson DF, *et al.*

Sodium-Dependent Phosphate Cotransporters and Phosphate-Induced Calcification of Vascular Smooth Muscle Cells: Redundant Roles for PiT-1 and PiT-2. *Arterioscler Thromb Vasc Biol* 2013; 33:2625–2632.

9 Bourgine A, Pilet P, Diouani S, Source S, Lesoeur J, Beck-Cormier S, *et al.* Mice with hypomorphic expression of the sodium-phosphate cotransporter PiT1/Slc20a1 have an unexpected normal bone mineralization. *PLoS One* 2013; 8:e65979.

10 Speer MY, Yang H-YY, Brabb T, Leaf E, Look A, Lin W-LL, *et al.* Smooth muscle cells give rise to osteochondrogenic precursors and chondrocytes in calcifying arteries. *Circ Res* 2009; 104:733–41.

11 Kimata M, Michigami T, Tachikawa K, Okada T, Koshimizu T, Yamazaki M, *et al.* Signaling of extracellular inorganic phosphate up-regulates cyclin D1 expression in proliferating chondrocytes via the Na+/Pi cotransporter Pit-1 and Raf/MEK/ERK pathway. *Bone* 2010; 47:938–947.

12 Yamazaki M, Ozono K, Okada T, Tachikawa K, Kondou H, Ohata Y, *et al.* Both FGF23 and extracellular phosphate activate Raf/MEK/ERK pathway via FGF receptors in HEK293 cells. *J Cell Biochem* 2010; 111:1210–1221.

13 Ito M, Haito S, Furumoto M, Uehata Y, Sakurai A, Segawa H, *et al.* Unique uptake and efflux systems of inorganic phosphate in osteoclast-like cells. *Am J Physiol Cell Physiol* 2007; 292:C526–34.

14 Reynolds JL, Joannides AJ, Skepper JN, McNair R, Schurgers LJ, Proudfoot D, *et al.* Human vascular smooth muscle cells undergo vesicle-mediated calcification in response to changes in extracellular calcium and phosphate concentrations: a potential mechanism for accelerated vascular calcification in ESRD. *J Am Soc Nephrol* 2004; 15:2857–67.

15 Kapustin AN, Davies JD, Reynolds JL, McNair R, Jones GT, Sidibe A, *et al.* Calcium regulates key components of vascular smooth muscle cell-derived matrix vesicles to enhance mineralization. *Circ Res* 2011; 109:e1–12.

CHAPTER 4

ELEVATED PHOSPHATE-INDUCED CELL SIGNALING THROUGH PIT-1 REQUIRES RAPGEF1

Chapter to be published in similar form as: "Rap1 guanine nucleotide exchange factor, RapGEF1, is required for sodium-dependent phosphate transporter PiT-1 mediated phosphate signaling through ERK1/2 and inhibition of smooth muscle 22 alpha in vascular smooth muscle cells." Chavkin NW, Brooks KE, Lund SM, Soberg EM, Wallingford MC, Giachelli CM. *In preparation*.

4.1 Introduction

Inorganic phosphate (Pi) is an essential molecule required almost every cellular function, including membrane stability, nucleic acid polymerization, and enzyme activation. Pi is also a main component of hydroxyapatite crystal in bone mineral [1]. Systemic phosphate homeostasis maintains serum Pi concentration around 1.0mM through a balance of Pi intake through the intestines and Pi excretion through the kidneys, with the hormones FGF-23, Vitamin D, PTH, and Klotho playing an important role in regulating Pi homeostasis [2,3]. Pathologies that dysregulate systemic Pi homeostasis can affect bone mineral deposition. Patients with late-stage chronic kidney disease have hyperphosphatemia (concentrations greater than 1.46mM Pi) that leads to arterial medial calcification and have a greatly increased risk of cardiovascular morbidity and mortality [4–6]. Elevated serum Pi in hyperphosphatemia promotes active

mineral deposition by vascular smooth muscle cells (VSMCs), leading to matrix mineralization in the medial layer of arteries [2]. This process is initiated by elevated Pi-induced ERK1/2 phosphorylation that leads to down-regulation of VSMC genes such as smooth muscle 22 alpha (SM22α), consistent with VSMC phenotype change [7,8]. However, the mechanism in which elevated Pi promotes VSMC phenotype change is unclear.

The main phosphate transporters in VSMCs are SLC20A1 (PiT-1) and SLC20A2 (PiT-2) [9]. PiT-1 and PiT-2 are type III sodium-dependent phosphate co-transporters that use the inward sodium gradient to transport two sodium ions for every one inorganic phosphate ion into the cell [10]. These transporters are thought to play a role in intracellular Pi homeostasis [10]. In VSMCs, PiT-1 has been shown to be required for elevated Pi-induced matrix mineralization and VSMC phenotype change [9]. However, PiT-1 is a high-affinity low-capacity transporter, and the concentration of Pi required to induce matrix mineralization is well above the concentration with maximal Pi uptake [11,12]. In a previous study, we had shown that a Pi uptake-independent function of PiT-1 was required for elevated Pi-induced ERK1/2 phosphorylation that leads to VSMC phenotype change [12]. These results suggested a cell signaling pathway from PiT-1 to ERK1/2 that is induced by elevated Pi and leads to down-regulation of smooth muscle genes.

A potential adaptor protein that binds to PiT-1 is Rap1 guanine nucleotide exchange factor (RapGEF1). A previous study investigated protein interactions in human liver lysates by a high-throughput yeast-two-hybrid assay and found that PiT-1 and RapGEF1 are interacting partners, however this was not tested in a low-throughput method [13]. RapGEF1 is an activator of the small GTPase Rap1 [14]. RapGEF1 is required for ERK1/2 phosphorylation in specific

pathways involving Rap1 activation and down-stream B-Raf and MEK1/2 phosphorylation [14,15]. That same cell pathway resulted in phosphorylation of Elk-1 [15], which is a transcription factor that inhibits the smooth muscle cell promoting transcription factor, Myocardin, from binding to smooth muscle-specific promoter regions and therefore inhibiting smooth muscle genes [16,17]. Together, these data suggest that RapGEF1 may play a role in PiT-1 mediated ERK1/2 phosphorylation and VSMC phenotype change. **The research presented here tests the hypothesis that RapGEF1 binds to PiT-1 in VSMCs and is required for elevated Pi-induced ERK1/2 phosphorylation and down-regulation of smooth muscle genes.** In order to test this hypothesis, RapGEF1 and PiT-1 protein binding was investigated and siRNA directed towards RapGEF1 was used to examine effects of RapGEF1 mRNA knock-down in VSMCs.

4.2 Materials and Methods

Cell culture and maintenance

Human new-born VSMCs (HNBSMCs) used in experiments were previously published [9]. HNBSMCs were passaged and maintained in Dulbecco's Modified Eagle Medium (DMEM, Gibco Life Technologies, Cat#11995) supplemented with 15% Fetal Bovine Serum (FBS, HyClone), 1% penicillin/1% streptomycin (Life Technologies). Primary medial VSMCs were isolated from aortas of wild-type C57BL/6 mice (WT VSMC) as previously described [12]. Briefly, aortas were removed from 4-5 week old mice, the medial layer was isolated and digested in collagen and elastin, and the primary (P0) VSMCs were incubated in DMEM supplemented with 20% FBS, 1% antibiotic/antimycotic, 1% glutamine, and 1% non-essential amino acids

(Life Technologies). VSMCs were passaged and maintained in DMEM supplemented with 10% FBS and 1% antibiotic/antimycotic. Experiments used primary VSMCs between P5 and P9.

Co-immunoprecipitation

Co-immunoprecipitation experiments were performed with the Pierce Crosslink Magnetic IP/Co-IP Kit (Pierce), according to the protocol. Briefly, HNBSMCs were cultured in 6-well plates and incubated for 15 minutes in NH buffer (20mM HEPES pH 7.5, 150mM NaCl) with phosphate ($Na_2PO_4/NaPO_4$ pH = 7.4) supplemented to either 1.0mM or 3.0mM, then cells were washed in NH buffer with either 1.0mM Pi or 3.0mM Pi and lysed in NH Lysate buffer (20mM HEPES pH 7.5, 150mM NaCl, 0.1% Triton-X100). Then, 5 µg of antibody against RapGEF1 (Rabbit polyclonal IgG anti-Rapgef1 C-19, Santa Cruz Biotechnologies) or IgG control (IgG from rabbit serum Cat#I5006, Sigma-Aldrich) were bound to magnetic beads, the antibody-bound beads were incubated with 100 µg of protein from HNBSMC lysate for 1 hour at room-temperature, then bound protein was eluted. Protein elution was run on a western blot and probed with an anti-PiT-1 antibody (Chicken anti-PiT-1, gift from Dr. Moshe Levi, UC Boulder).

RapGEF1 RNA silencing

WT VSMCs were seeded at $2.5x10^4$ cells per well in 6-well plates. 24 hours after seeding, siRNA directed towards RapGEF1 (Silencer Select s98950, Thermo Fischer Scientific) was administered as described in the Lipofectamine RNAiMAX protocol (Life Technologies). Briefly, 5 µL of 1mM siRNA was added to 250 µL Opti-MEM (Gibco Life Technologies, Cat#31985), 1.5 µL of RNAiMAX was added to another 250 µL Opti-MEM, these dilutions were mixed and incubated for 5 minutes, VSMCs were refed with 10% FBS DMEM containing

no antibiotics, and the 500 µL Opti-MEM dilution of siRNA and RNAiMAX was added to the VSMCs.

Quantitative PCR

RNA was quantified by Q-PCR. Specific genes were quantified using primers and probes directed towards RapGEF1 (TaqMan Cat#4331182, Thermo Fischer Scientific) or SM22α (forward: 5'-GACTGACATGTTCCAGACTGTTGAC-3', reverse: 5'-CAAACTGCCCAAAGCCATTAG-3', probe: FAM-5'-TGAAGGTAAGGATATGGCAGC-3'-MGB). Relative gene values were normalized to 18s ribosomal control values in each sample (Applied Biosystems), then normalized to control values in a delta-delta-18s method.

Fluorescent immunocytochemistry

Immunocytochemistry was performed by culturing either HNBSMCs or WT VSMCs on glass slides coated with poly-D-lysine. Cells were fixed with 4% paraformaldehyde and permeabilized with PBS containing 0.25% Triton-X100. Fixed cells were blocked with PBS-T containing 0.25% bovine serum albumin (BSA, Sigma-Aldrich) and 4% donkey serum (Jackson ImmunoResearch). Primary antibodies against RapGEF1 (Rabbit polyclonal IgG anti-Rapgef1 C-19, Santa Cruz Biotechnologies) or PiT-1 (Chicken anti-PiT-1, gift from Dr. Moshe Levi, UC Boulder) and fluorescent secondary antibodies against Rabbit IgG (Alexa 488-conjugated Donkey anti-Rabbit IgG, Jackson ImmunoResearch) or Chicken IgY (TRITC-conjugated Rabbit anti-Chicken IgY Novex, Life Technologies) were diluted in PBS-T containing 0.25% BSA and 2% donkey serum. Antibodies were incubated in succession to avoid cross signals. Slides were mounted with Prolong Gold Anti-fade Mountant (Prolong Thermo Fischer Scientific). Imaging

was performed with either a Nikon E800 Upright Microscope or a Leica SP8X Confocal Microscope.

Elevated Pi-induced ERK1/2 phosphorylation assay

ERK1/2 phosphorylation assay was performed as previously described [12]. Briefly, WT VSMCs were incubated in Pi-free DMEM (Gibco Life Technologies Cat#11971) supplemented with 1% FBS for 16 hours, then refed with Pi-free DMEM containing different concentrations of Pi, FBS, or $NaSO_4$ (Sigma-Aldrich). If inhibitors were used, then the inhibitors were either added during the first Pi-free DMEM with 1% FBS refeed or in Pi-free DMEM with 1% FBS at 1 hour before induction with different Pi concentrations. Cells were lysed after 15 minutes in Lysate Buffer (0.1 M Tris pH = 6.8, 2% SDS) with Protease Inhibitor Cocktail (Roche), PMSF (Sigma-Aldrich), and Halt Phosphatase Inhibitor Cocktail (Thermo Scientific). Lysates were run on a western blot with antibodies against phosphorylated ERK1/2 or total ERK1/2 (Cell Signaling Technologies). Protein bands were quantified by ImageJ densitometry analysis, and phosphorylated ERK1/2 was normalized to total ERK1/2 for each sample. ERK1/2 phosphorylation was also quantified by the Thermo Scientific Pierce ERK1/2 Colorimetric In-Cell ELISA Kit (Thermo Fischer). VSMCs were seeded in 96-well plates in growth media, refed with Pi-free DMEM with 1% FBS and incubated for 16 hours, refed with Pi-free DMEM with 1% FBS with added inhibitor and incubated for 1 hour, then refed with Pi-free DMEM containing added inhibitor and different concentrations of Pi, FBS, or $NaSO_4$. After different times, cells were fixed with 4% paraformaldehyde and the In-Cell ELISA Kit protocol was followed to obtain absorbance readings corresponding to amount of phosphorylated ERK1/2.

Statistical Analysis

SPSS software v16.0 (SPSS, Chicago, IL) was used to perform Student t-tests to compare means of two individual groups, and one-way ANOVA with post-hoc Tukey test to compare means of three or more individual groups. Linear regression to determine variable correlation and nonlinear regression to determine Michaelis-Menten parameters were performed using STATA version 12 (StataCorp). A p-value of less than 0.05 was considered statistically significant.

4.3 Results

Interaction between RapGEF1 and PiT-1 proteins in VSMCs increase with elevated Pi.

A previously published study had observed that PiT-1 and RapGEF1 could bind in a yeast-two-hybrid assay, but this binding had not been confirmed in mammalian cells. To investigate whether PiT-1 and RapGEF1 interact in VSMCs, fluorescent immunocytochemistry and co-immunoprecipitation were performed on PiT-1 and RapGEF1 proteins (Fig. 1). Immunocytochemistry on HNBSMCs was performed to visualize PiT-1 and RapGEF1 localization (Fig. 1A and 1B). DAPI staining was also performed to visualize nuclei (Fig. 1C). Both PiT-1 and RapGEF1 are expressed in cultured HNBSMCs with similar membrane and cytosol localization patterns. An overlay of PiT-1, RapGEF1, and DAPI staining shows possible co-staining locations throughout the cell (Fig. 1D). To confirm protein interactions between PiT-1 and RapGEF1 and to assess the effect of elevated Pi on these interactions, HNBSMCs were incubated in either normal 1.0mM Pi or elevated 3.0mM Pi for 15 minutes and co-immunoprecipitation was performed with a capture antibody against RapGEF1 and probing for PiT-1 by western blot (Fig 1E). A PiT-1 band was observed in both the 1.0mM Pi and 3.0mM Pi

after RapGEF1 capture, and no band was observed in the IgG capture negative control. Quantification of the PiT-1 band from three independent samples shows that more PiT-1 protein is present in 3.0mM Pi compared to 1.0mM Pi after co-immunoprecipitation with the RapGEF1 capture antibody (Fig. 1F). These data show that elevated Pi increases binding of RapGEF1 and PiT-1.

RNA silencing of RapGEF1 eliminates elevated Pi-induced ERK1/2 phosphorylation.

Pi uptake-independent function of PiT-1 is required for elevated Pi-induced ERK1/2 phosphorylation in VSMCs [12]. To investigate the role of RapGEF1 in elevated Pi-induced ERK1/2 phosphorylation, small interfering RNA was used to silence RapGEF1 mRNA (siRapGEF1), and then the effect of elevated Pi on phosphorylated ERK1/2 was assessed. Primary murine VSMCs transfected with siRapGEF1 showed a greater than 95% reduction in RapGEF1 mRNA compared to negative control siRNA (siNegative) at 2, 3, and 4 days after siRNA transfection (Fig. 2A). Protein reduction was also visible through fluorescent immunocytochemistry of RapGEF1 protein in siNegative and siRapGEF1 VSMCs (Fig. 2B and 2C). ERK1/2 phosphorylation was visualized by western blot in siNegative and siRapGEF1 VSMCs after induction with either 0.5mM, 1.0mM, or 3.0mM Pi (Fig. 2D). Densitometry quantification showed that ERK1/2 phosphorylation in siNegative VSMCs was increased 1.5-fold in 3.0mM Pi media over 1.0mM Pi media, but RapGEF1 siRNA eliminated this effect (Fig. 2E). Together, these data show that silencing RapGEF1 mRNA and protein eliminates elevated Pi-induced ERK1/2 phosphorylation in VSMCs.

Small molecule inhibitors against Rap1, B-Raf, or Mek1/2 eliminate elevated Pi-induced ERK1/2 phosphorylation.

RapGEF1 can lead to ERK1/2 phosphorylation through a Rap1/B-Raf/Mek1/2 cell signaling cascade [15]. To test this pathway in RapGEF1 mediated cell signaling through PiT-1 to ERK1/2, each step was inhibited and elevated Pi-induced ERK1/2 phosphorylation was assessed. Rap1, B-Raf, and Mek1/2 have small molecule inhibitors that can block activation of each one individually (GGTI298, GDC0879, and U0126, respectively). Serial dilutions of these inhibitors were tested (starting at 20μM GGTI298, 10μM GDC0879, and 20μM U0126) in the elevated Pi-induced ERK1/2 phosphorylation assay with primary murine VSMCs (Fig. 3A). VSMCs were incubated in Pi-free DMEM with each inhibitor (or 0.5% DMSO control) for 16 hours before elevated Pi induction. 3.0mM Pi induced ERK1/2 phosphorylation in the control treatment, but the highest concentrations of each inhibitor all blocked ERK1/2 phosphorylation. As the inhibitor was diluted, ERK1/2 phosphorylation increased to resemble the 3.0mM Pi control induction. The concentration of each inhibitor that blocked elevated Pi-induced ERK1/2 phosphorylation was tested with a 1 hour pre-incubation before elevated Pi induction (Fig. 3B). ERK1/2 phosphorylation was reduced in all of the inhibitor cases compared 3.0mM Pi induction in control treated VSMCs. Inhibitors against Rap1, B-Raf, and Mek1/2 all individually inhibit elevated Pi-induced ERK1/2 phosphorylation in VSMCs.

RNA silencing of RapGEF1 up-regulates mRNA SM22-alpha and eliminates elevated Pi-induced inhibition of SM22-alpha mRNA.

Downstream of ERK1/2 phosphorylation, PiT-1 mediated cell signaling inhibits SM22α expression in VSMCs consistent with VSMC phenotype change [12]. Therefore, changes in

SM22 α mRNA expression were investigated with RapGEF1 siRNA to assess the role of RapGEF1 in VSMC phenotype change. First, SM22α mRNA expression was quantified in growth media (DMEM with 10% FBS) in VSMCs treated with siNegative control or siRapGEF1. SM22α mRNA expression was increased by 5-fold 2 days after siRNA treatment and by 9-fold 3 days after siRNA treatment, but was reduced to control amount by day 4 (Fig 4A). Next, the role of RapGEF1 in SM22α mRNA inhibition by elevated Pi was assessed. SM22α mRNA expression was reduced in siNegative VSMCs after 4 days of incubation in 2.6mM Pi media (DMEM with 3% FBS) compared to 1.0mM Pi media, but siRapGEF1 eliminated SM22α reduction. RNA silencing of RapGEF1 eliminates PiT-1 mediated inhibition of SM22α expression.

4.4 Discussion

The results presented here show that RapGEF1 interacts with PiT-1 in VSMCs, and that PiT-1 mediated ERK1/2 cell signaling and VSMC phenotype change in response to elevated Pi requires RapGEF1. This signaling pathway goes through a Rap1/B-Raf/Mek1/2 cascade. Overall, the data suggest that elevated Pi initiates protein binding between PiT-1 and RapGEF1, which requires Rap1, B-Raf, and Mek1/2 to phosphorylate ERK1/2 and down-regulate smooth muscle-specific genes.

RapGEF1 has several known functions and mechanisms of activation. In mice, global deletion of RapGEF1 is embryonically lethal at E7.5 due to decreased cell adhesion of embryonic fibroblasts and decreased embryogenesis [18]. Other studies have also implicated RapGEF1-

meditated activation of Rap1 on cell adhesion function and ERK1/2 phosphorylation [15,19,20]. Most interesting to the results of this study, RapGEF1 was found to be required for vascular maturation of embryos [21]. That study found that transgenic mice hypomorphic for RapGEF1 died in embryo at age E11.5 due to vascular integrity defects, which is a strikingly similar phenotype to the PiT-1 global deletion mouse that is embryonically lethal at E14.5 and had vascular defects starting at E11.5 [22]. The signaling pathway and down-stream regulation of smooth muscle cell genes presented in the results may help explain the role of RapGEF1 in vascular maturation.

RapGEF1 localization also seems to play a large role in the activation of Rap1 and down-stream signaling proteins. A membrane localization signal attached to RapGEF1 was sufficient to activate Rap1 [14]. Furthermore, a previous study found that although Epac1 (a different Rap1 activator) does not normally lead to ERK1/2 phosphorylation, adding a membrane localization signal to Epac1 does lead to down-stream ERK1/2 phosphorylation after Rap1 activation [23]. Membrane localization of RapGEF1 could be the initiation mechanism for the cell signaling response to elevated Pi. RapGEF1 binding to PiT-1 on the cell membrane may be enough to initiate the cell signaling response to elevated Pi through ERK1/2 phosphorylation. This underlying mechanism could also suggest a role for PiT-1 and RapGEF1 signaling in mammalian cell Pi sensing.

In conclusion, the data presented here suggest that elevated Pi induces PiT-1 to bind to RapGEF1, initiating a cell signaling pathway through Rap1, B-Raf, and Mek1/2 to increase ERK1/2 phosphorylation and inhibit smooth muscle cell gene expression in VSMCs.

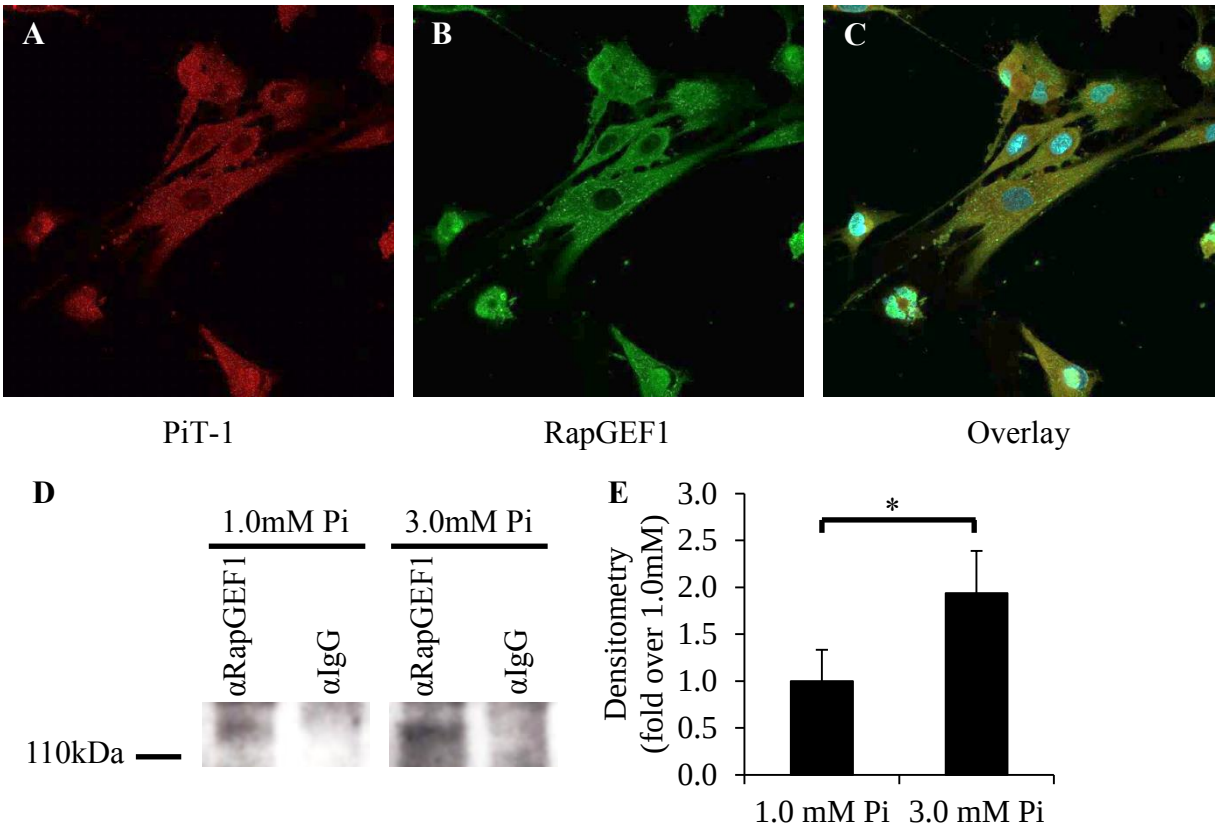

Figure 4.1. Visualization and quantification of RapGEF1 and PiT-1 interactions. Fluorescent immunocytochemistry of cultured HNBSMCs probing for A) PiT-1, B) RapGEF1, and combining the images with DAPI staining in D) as an overlay was performed. D) HNBSMCs incubated in either 1.0mM Pi or 3.0mM Pi for 15 minutes were lysed, co-immunoprecipitation was performed using a capture antibody against RapGEF1 or IgG control, and elution was run on a western blot and probed for PiT-1. A representative western blot of three independent samples is shown. E) The three independent samples were quantified by densitometry analysis. (* = $p<0.05$ by t-test).

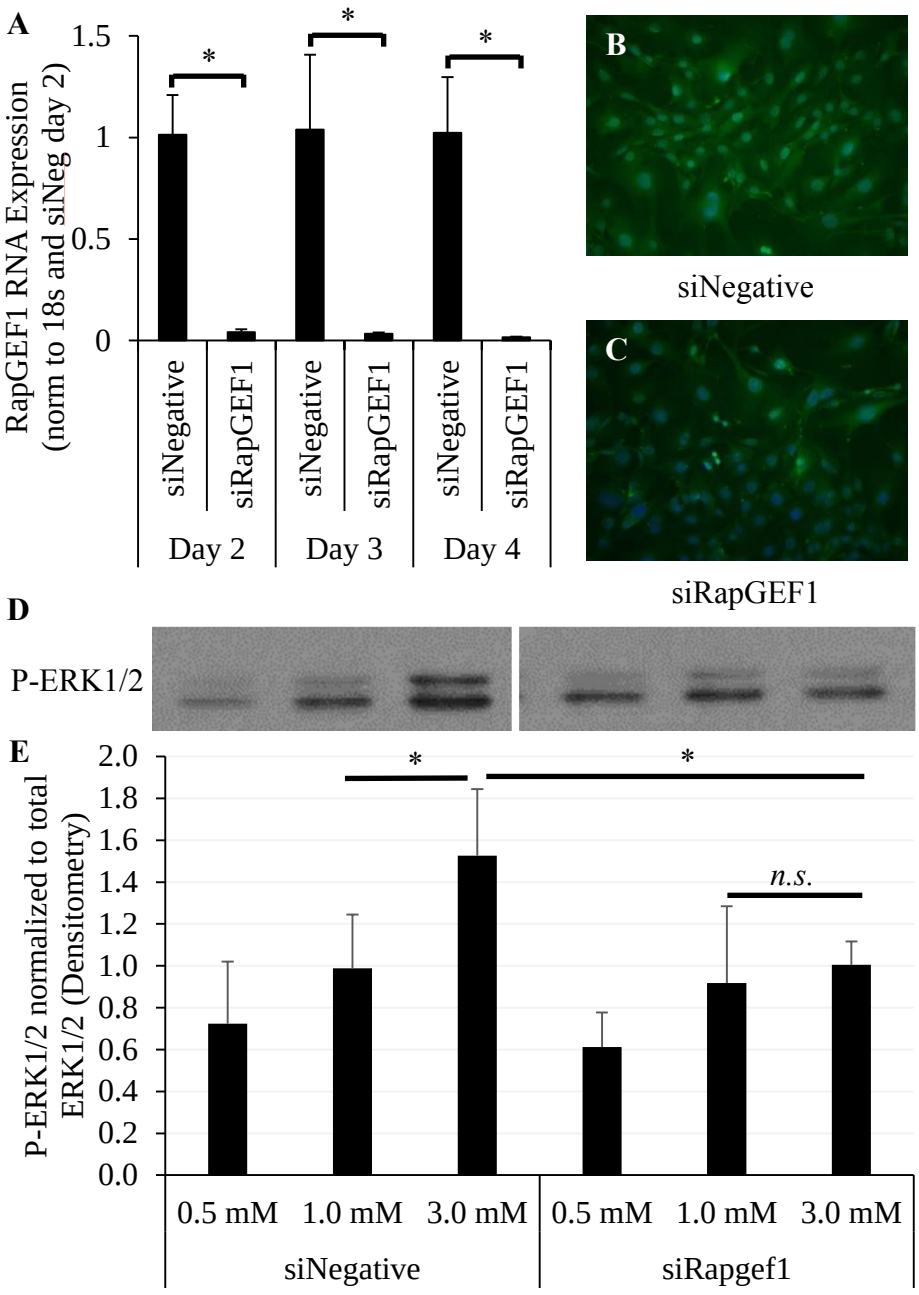

Figure 4.2 RapGEF1 silencing eliminates elevated Pi-induced ERK1/2 phosphorylation. Primary murine VSMCs were transfected with either RapGEF1 siRNA (siRapGEF1) or negative control siRNA (siNegative). A) RapGEF1 RNA was quantified with qRT-PCR on day 2, 3, and 4 after siRNA transfection. Immunocytochemistry probing for RapGEF1 (green) and staining for DAPI (blue) was used to visualize RapGEF1 protein in B) siNegative and C) siRapGEF1 VSMCs. D) Both siNegative and siRapGEF1 VSMCs were incubated in media containing either 0.5mM, 1.0mM, or 3.0mM Pi for 15 minutes ERK1/2 phosphorylation was visualized by western blot (representative image shown). E) Quantification of six independent samples was performed by densitometry analysis. (* = $p < 0.05$)

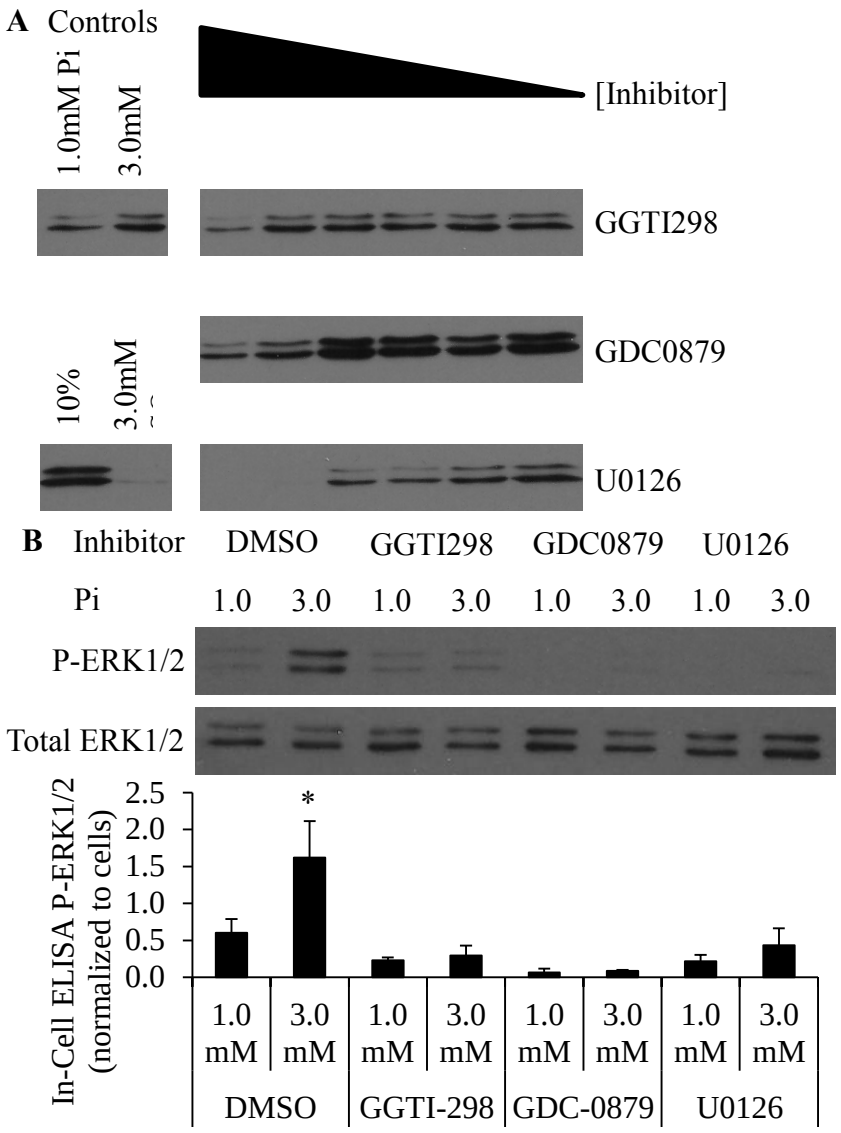

Figure 4.3. Inhibitors against Rap1, B-Raf, and Mek1/2 eliminate elevated Pi-induced ERK1/2 phosphorylation. Elevated Pi-induced ERK1/2 phosphorylation was assessed with small molecule inhibitors against activation of Rap1 (GGTI298), B-Raf (GDC0879), and Mek1/2 (U0126). A) Primary murine VSMCs were incubated in Pi-free DMEM with varying inhibitor concentrations for 16 hours starting at 20μM GGTI298, 10μM GDC0879, or 20μM U0126 and diluted serially with a dilution factor of 10, then induced with 3.0mM Pi (or given controls), and phosphorylated ERK1/2 was quantified by western blot. B) VSMCs were incubated in Pi-free DMEM overnight, then Pi-free DMEM with varying concentrations of inhibitors (20μM GGTI298, 10μM GDC0879, or 20μM U0126) for 1 hour, and induced with either 1.0mM or 3.0mM Pi, then ERK1/2 was visualized by western blot and quantified by In-Cell ELISA assay. (* = $p<0.05$)

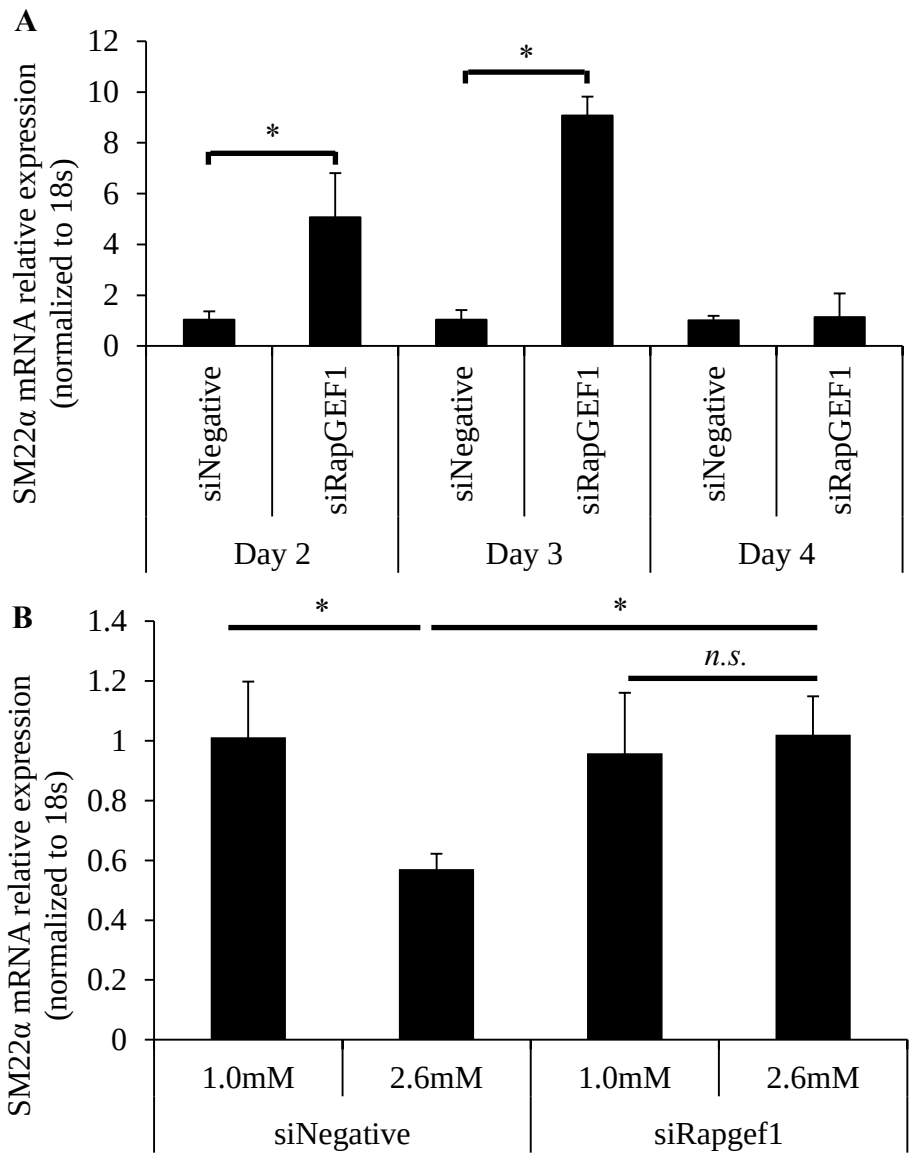

Figure 4.4. RapGEF1 silencing increases SM22α mRNA and eliminates elevated Pi-induced SM22α mRNA inhibition. A) SM22α mRNA expression was quantified at day 2, 3, and 4 post transfection with either siNegative or siRapGEF1. B) VSMCs were treated with either siNegative or siRapGEF1 and incubated for 4 days in 1.0mM Pi or 2.6mM Pi media and SM22α mRNA was quantified. (* = $p<0.05$)

4.5 Notes to Chapter 4

1 LeGeros RZ. Formation and transformation of calcium phosphates: relevance to vascular calcification. *Zeitschrift Kardiol* 2001; 90:III116–III124.

2 Shanahan CM, Crouthamel MH, Kapustin A, Giachelli CM. Arterial calcification in chronic kidney disease: key roles for calcium and phosphate. *Circ Res* 2011; 109:697–711 ST – Arterial calcification in chronic ki.

3 Penido MGMG, Alon US. Phosphate homeostasis and its role in bone health. *Pediatr Nephrol* 2012; 27:2039–48.

4 Tonelli M, Sacks F, Pfeffer M, Gao Z, Curhan G. Relation between serum phosphate level and cardiovascular event rate in people with coronary disease. *Circulation* 2005; 112:2627–33.

5 Block GA, Hulbert-Shearon TE, Levin NW, Port FK. Association of serum phosphorus and calcium x phosphate product with mortality risk in chronic hemodialysis patients: a national study. *Am J Kidney Dis* 1998; 31:607–17.

6 Adeney KL, Siscovick DS, Ix JH, Seliger SL, Shlipak MG, Jenny NS, *et al.* Association of serum phosphate with vascular and valvular calcification in moderate CKD. *J Am Soc Nephrol* 2009; 20:381–7.

7 Speer MY, Yang H-YY, Brabb T, Leaf E, Look A, Lin W-LL, *et al.* Smooth muscle cells give rise to osteochondrogenic precursors and chondrocytes in calcifying arteries. *Circ Res* 2009; 104:733–41.

8 Speer MY, Li X, Hiremath PG, Giachelli CMC-P 2895022. Runx2/Cbfa1, but not loss of myocardin, is required for smooth muscle cell lineage reprogramming toward

osteochondrogenesis. *J Cell Biochem* 2010; 110:935–47.

9 Li X, Yang H-YY, Giachelli CM. Role of the sodium-dependent phosphate cotransporter, Pit-1, in vascular smooth muscle cell calcification. *Circ Res* 2006; 98:905–12.

10 Virkki L V, Biber J, Murer H, Forster IC. Phosphate transporters: a tale of two solute carrier families. *Am J Physiol Renal Physiol* 2007; 293:F643–54.

11 Villa-Bellosta R, Levi M, Sorribas V. Vascular smooth muscle cell calcification and SLC20 inorganic phosphate transporters: effects of PDGF, TNF-alpha, and Pi. *Pflugers Arch* 2009; 458:1151–61.

12 Chavkin NW, Chia JJ, Crouthamel MH, Giachelli CM. Phosphate uptake-independent signaling functions of the type III sodium-dependent phosphate transporter, PiT-1, in vascular smooth muscle cells. *Exp Cell Res* 2015; 333:39–48.

13 Wang J, Huo K, Ma L, Tang L, Li D, Huang X, *et al.* Toward an understanding of the protein interaction network of the human liver. *Mol Syst Biol* 2011; 7:536.

14 Gotoh T, Hattori S, Nakamura S, Kitayama H, Noda M, Takai Y, *et al.* Identification of Rap1 as a target for the Crk SH3 domain-binding guanine nucleotide-releasing factor C3G. *Mol Cell Biol* 1995; 15:6746–6753.

15 Vossler MR, Yao H, York RD, Pan M-G, Rim CS, Stork PJ. cAMP Activates MAP Kinase and Elk-1 through a B-Raf- and Rap1-Dependent Pathway. *Cell* 1997; 89:73–82.

16 Yoshida T, Sinha S, Dandré F, Wamhoff BR, Hoofnagle MH, Kremer BE, *et al.* Myocardin is a key regulator of CArG-dependent transcription of multiple smooth muscle marker genes. *Circ Res* 2003; 92:856–64.

17 Kawai-Kowase K, Owens GK. Multiple repressor pathways contribute to phenotypic switching of vascular smooth muscle cells. *Am J Physiol Cell Physiol* 2007; 292:C59–69.

18 Ohba Y, Ikuta K, Ogura A, Matsuda J, Mochizuki N, Nagashima K, *et al.* Requirement for C3G-dependent Rap1 activation for cell adhesion and embryogenesis. *EMBO J* 2001; 20:3333–3341.

19 Arai A, Nosaka Y, Kohsaka H, Miyasaka N, Miura O, Hynes R, *et al.* CrkL activates integrin-mediated hematopoietic cell adhesion through the guanine nucleotide exchange factor C3G. *Blood* 1999; 93:3713–22.

20 Bos JL. Linking Rap to cell adhesion. *Curr Opin Cell Biol* 2005; 17:123–128.

21 Voss AK, Gruss P, Thomas T. The guanine nucleotide exchange factor C3G is necessary for the formation of focal adhesions and vascular maturation. *Development* 2003; 130:355–67.

22 Festing MH, Speer MY, Yang H-Y, Giachelli CM. Generation of mouse conditional and null alleles of the type III sodium-dependent phosphate cotransporter PiT-1. *Genesis* 2009; 47:858–63.

23 Wang Z, Dillon TJ, Pokala V, Mishra S, Labudda K, Hunter B, *et al.* Rap1-Mediated Activation of Extracellular Signal-Regulated Kinases by Cyclic AMP Is Dependent on the Mode of Rap1 Activation. *Mol Cell Biol* 2006; 26:2130–2145.

CHAPTER 5

CONCLUSIONS AND FUTURE STUDIES

5.1 Conclusions

In this dissertation, I provide evidence that PiT-1 promotes elevated Pi-induced ERK1/2 phosphorylation, osteochondrogenic differentiation, and matrix mineralization in VSMCs through Pi uptake-independent cell signaling functions initiated by binding with RapGEF1, causing a signaling cascade through Rap1/B-Raf/Mek1/2 that phosphorylates ERK1/2 and promotes VSMC phenotype change (Fig. 5.1).

These results suggest that PiT-1 may potentially play a role in Pi sensing in mammalian cells. Pi sensing has been described in *E. coli* and *S. cerevisiae* [1,2], but the exact mammalian cell Pi sensing pathway has not been discovered. However, elevated Pi causes both very quick and long-term changes to cells, suggesting that a Pi sensing and response mechanism exists and has not been accurately defined. Other investigators have suggested that PiT-1 may be important in Pi sensing in bone formation and phosphate homeostasis. Bergwitz *et al.* reviewed literature on Pi induction of ERK1/2 in different cell types and concluded that PiT-1 may be an important protein in Pi sensing in mammalian cells [3], but a mechanism was not presented. Miyamoto *et al.* also concluded in a review that PiT-1 and PiT-2 may play a role in Pi sensing related to bone formation and vascular calcification [4], but again a mechanism was not presented. One study also suggested that sodium-dependent Pi transporters could be responsible for Pi sensing in renal epithelial cells [5]. It is unclear if the pathway outlined in this dissertation is a specific response

in VSMCs to smooth muscle-specific genes, or if it could also affect osteoblasts, osteocytes, or chondrocytes. It is also unclear if these *in vitro* studies will translate to *in vivo* mechanism. A more ubiquitous function of this pathway and confirmation of this cell signaling pathway *in vivo* would suggest that PiT-1 is part of the mammalian cellular Pi sensing and response mechanism.

The response to elevated Pi through PiT-1 that promotes osteochondrogenic differentiation could be targeted with therapeutics in order to block the response to elevated Pi in VSMCs and inhibit vascular calcification. If this signaling pathway can be observed *in vivo*, then potential therapeutics could target this pathway to block vascular calcification. This is a very exciting proposal, as there are currently no drugs that can directly target vascular calcification. An ideal drug that targets vascular calcification would also be specific to VSMCs without adverse effects on bone formation, and this pathway may satisfy these criteria as it seems to be directed towards down-regulation of smooth muscle-specific genes. Additionally, there are other diseases that are initiated or progressed by down-regulation of smooth muscle-specific genes in VSMCs, such as atherosclerosis and restenosis [6,7]. These diseases may be inhibited by a drug that can promote smooth muscle-specific genes in VSMCs.

5.2 Future studies

Possible future studies extended from this project include investigating the specific mechanism in which PiT-1 responds to elevated Pi, possible drug targets, and testing therapies *in vivo*. These studies are outlined in this section.

One possible mechanism for PiT-1 response to elevated Pi is through monomerization. The data suggest that PiT-1 can sense and respond to elevated Pi, and this response would require a fast response. Previous studies show that the related phosphate transporter PiT-2 can oligomerize, and that elevated phosphate reduces this oligomerization [8]. The amino acid sequence of mouse PiT-2 is 65% identical to that of mouse PiT-1 by BLAST, suggesting that these proteins can function in similar manners in response to elevated extracellular Pi. An oligomerization response to different concentrations of Pi could be a fast response to changes in Pi required for initial Pi sensing. We hypothesize that elevated Pi induces PiT-1 monomers, which reveals an active binding site and initiates a signaling cascade through ERK1/2. This mechanism would work as a novel Pi sensor initiating a conformational change in PiT-1 that induces a cell signaling response.

A possible future study would be to test this hypothesis through protein interaction studies. Fluorescence-Lifetime Imaging Microscopy (FLIM) to quantitate Fluorescence Resonance Energy Transfer (FRET) would be used to visualize and quantitate PiT-1 dimerization in live cells. The FLIM-FRET method described in Dr. Levi's previously published work would be used to visualize and quantify PiT-1 dimerization [9,10]. Briefly, chromophore-conjugated PiT-1 protein would be overexpressed in PiT-1 ΔSM VSMCs and dimerization of the conjugated PiT-1 protein would be visualized by confocal fluorescent microscopy. This assay would be performed after incubation in a range of Pi concentrations (0 mM to 10 mM) for 60 minutes to determine the ability for elevated Pi to affect PiT-1 dimerization. This study would show if changing Pi concentration could change PiT-1 oligomerization state and suggest a mechanism for elevated Pi sensing in VSMCs.

Beyond mechanistic studies, future directions could also include testing different siRNA and small molecule inhibitors on the elevated Pi-induced ERK1/2 phosphorylation pathway to discover more drug targets and therapeutics. In order to investigate the inorganic phosphate signaling pathway to ERK1/2 in vascular smooth muscle cells, we have optimized an InCell ELISA assay (Pierce Biotechnology) that uses elevated inorganic phosphate to induce ERK1/2 phosphorylation in vascular smooth muscle cells. Briefly, mouse primary aortic vascular smooth muscle cells are grown and seeded into TC dishes. 48 hours after cell seeding, the cells are refed with phosphate-free culture media supplemented with 1% fetal bovine serum. 24 hours after this refeed, the cells are refed with the same media supplemented with experimental additions (different concentrations of sodium phosphate, positive control fetal bovine serum, or negative control sodium sulfate). In a 96-well plate, we have optimized this assay to detect differences in ERK1/2 phosphorylation between 0 mM phosphate and 0.5 mM phosphate, and a 6-fold increase between 1.0 mM phosphate and 3.0 mM Pi. We are most interested in the difference between 1.0 mM Pi and 3.0 mM Pi, as these concentrations are physiologically normal (1.0 mM) and hyperphosphatemic (3.0 mM) in patients. A high-throughput screen could test different siRNA or small molecule inhibitors on a much larger scale than presented in this project.

Positive siRNA and compounds would be confirmed and tested in elevated phosphate induction assays that have been well established in the Giachelli lab. First, the positives would be confirmed in a large format elevated phosphate-induced ERK1/2 phosphorylation assay that has been well characterized in lab. After these positives have been confirmed, we would use them to test their effectiveness in inhibition of vascular smooth muscle cell mineralization. To further

understand mechanistic changes driving mineralization, we would additionally investigate osteochondrogenic differentiation of VSMCs with the given siRNA or compound. Compounds or siRNA that inhibit elevated phosphate-induced ERK1/2 phosphorylation, osteochondrogenic differentiation, and matrix mineralization will be extremely valuable targets both in understanding vascular calcification and potential therapeutics for patients at risk for vascular calcification.

Currently, there are no drugs that can inhibit vascular calcification in patients. A compound or siRNA that can inhibit elevated Pi-induced ERK1/2 phosphorylation, osteochondrogenic differentiation, and matrix mineralization is an exemplary target to inhibit vascular calcification. Through this knowledge, we can plan follow-up in vivo studies using a mouse model with vascular calcification induced by renal ablation. The Giachelli lab has pioneered the renal ablation model to study CKD-induced arterial medial calcification [11]. This *in vivo* model is well characterized by our lab and has been used in paradigm-shifting investigations in vascular calcification mechanisms. A positive mechanism for inhibition of vascular calcification in this *in vivo* model would be a possible drug or lead to a possible drug that could inhibit vascular calcification in patients.

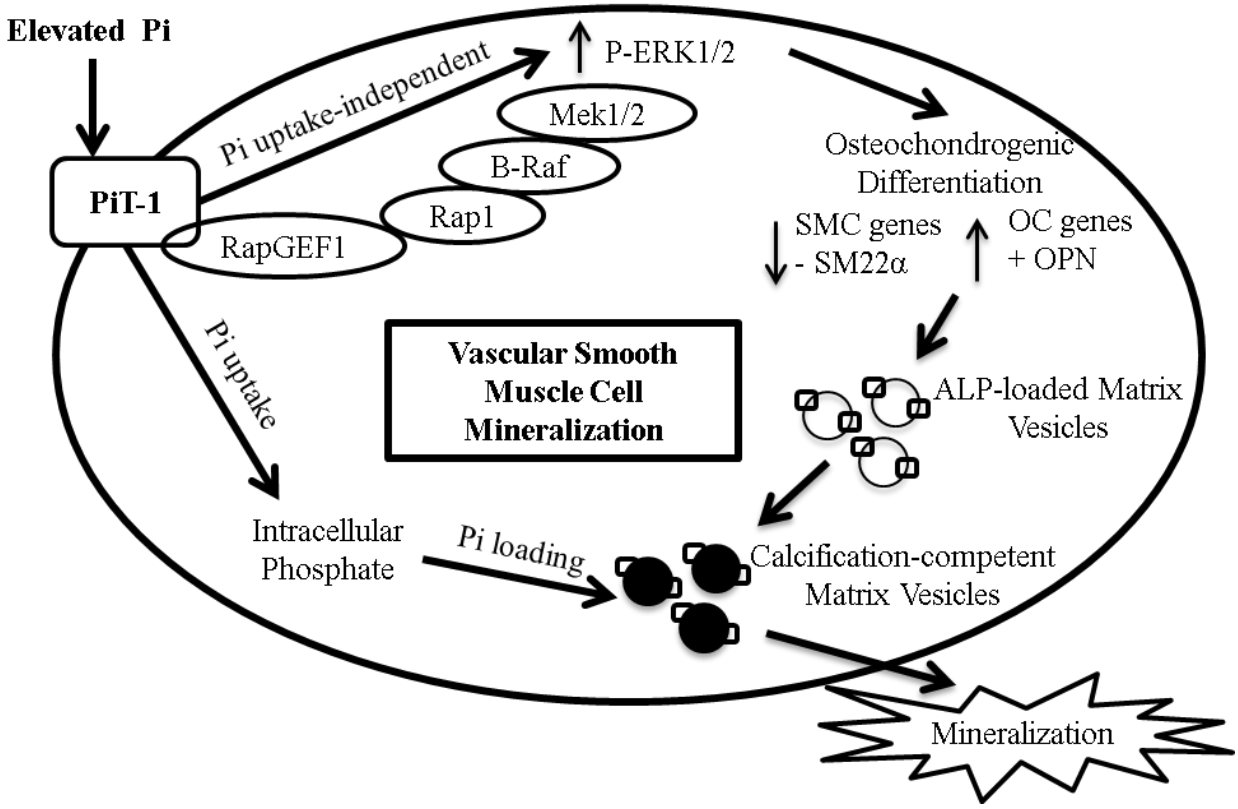

Figure 5.1. Visual conclusions.

5.3 Notes to Chapter 5

1 Sprague GF, Bell RM, Cronan JE. A mutant of Escherichia coli auxotrophic for organic phosphates: Evidence for two defects in inorganic phosphate transport. *MGG Mol Gen Genet* 1975; 143:71–77.

2 Oshima Y, Tohe A, Matsumoto K. [Regulatory circuits for gene expression: the metabolism of galactose and phosphate in Saccharomyces cerevisiae]. *Tanpakushitsu Kakusan Koso* 1984; 29:14–28.

3 Bergwitz C, Jüppner H. Phosphate Sensing. *Adv Chronic Kidney Dis* 2011; 18:132–144.

4 Miyamoto K, Haito-Sugino S, Kuwahara S, Ohi A, Nomura K, Ito M, *et al.* Sodium-dependent phosphate cotransporters: lessons from gene knockout and mutation studies. *J Pharm Sci* 2011; 100:3719–30 ST – Sodium–dependent phosphate cotranspo.

5 Tatsumi S, Segawa H, Morita K, Haga H, Kouda T, Yamamoto H, *et al.* Molecular cloning and hormonal regulation of PiT-1, a sodium-dependent phosphate cotransporter from rat parathyroid glands. *Endocrinology* 1998; 139:1692–9.

6 Nguyen AT, Gomez D, Bell RD, Campbell JH, Clowes AW, Gabbiani G, *et al.* Smooth muscle cell plasticity: fact or fiction? *Circ Res* 2013; 112:17–22.

7 Gomez D, Owens GK. Smooth muscle cell phenotypic switching in atherosclerosis. *Cardiovasc Res* 2012; 95:156–64.

8 Salaün C, Maréchal V, Heard JM. Transport-deficient Pit2 phosphate transporters still modify cell surface oligomers structure in response to inorganic phosphate. *J Mol Biol* 2004; 340:39–47.

9 Giral H, Lanzano L, Caldas Y, Blaine J, Verlander JW, Lei T, *et al.* Role of PDZK1

Protein in Apical Membrane Expression of Renal Sodium-coupled Phosphate Transporters. *J Biol Chem* 2011; 286:15032–15042.

10 Giral H, Cranston D, Lanzano L, Caldas Y, Sutherland E, Rachelson J, *et al.* NHE3 Regulatory Factor 1 (NHERF1) Modulates Intestinal Sodium-dependent Phosphate Transporter (NaPi-2b) Expression in Apical Microvilli. *J Biol Chem* 2012; 287:35047–35056.

11 El-Abbadi MM, Pai AS, Leaf EM, Yang H-Y, Bartley BA, Quan KK, *et al.* Phosphate feeding induces arterial medial calcification in uremic mice: role of serum phosphorus, fibroblast growth factor-23, and osteopontin. *Kidney Int* 2009; 75:1297–307.

BIBLIOGRAPHY

Adeney KL, Siscovick DS, Ix JH, Seliger SL, Shlipak MG, Jenny NS, et al. Association of serum phosphate with vascular and valvular calcification in moderate CKD. J Am Soc Nephrol 2009; 20:381–7.

Ahmed AK, Kamath NS, El Kossi M, El Nahas AM. The impact of stopping inhibitors of the renin-angiotensin system in patients with advanced chronic kidney disease. Nephrol Dial Transplant 2010; 25:3977–82.

Alexander MR, Owens GK. Epigenetic control of smooth muscle cell differentiation and phenotypic switching in vascular development and disease. Annu Rev Physiol 2012; 74:13–40.

Allison MA, Criqui MH, Wright CM. Patterns and Risk Factors for Systemic Calcified Atherosclerosis. Arterioscler Thromb Vasc Biol 2004; 24:331–336.

Arai A, Nosaka Y, Kohsaka H, Miyasaka N, Miura O, Hynes R, et al. CrkL activates integrin-mediated hematopoietic cell adhesion through the guanine nucleotide exchange factor C3G. Blood 1999; 93:3713–22.

BEADENKOPF WG, DAOUD AS, LOVE BM. CALCIFICATION IN THE CORONARY ARTERIES AND ITS RELATIONSHIP TO ARTERIOSCLEROSIS AND MYOCARDIAL INFARCTION. Am J Roentgenol Radium Ther Nucl Med 1964; 92:865–71.

Beck L, Leroy C, Salaün C, Margall-Ducos G, Desdouets C, Friedlander GC-P. Identification of a novel function of PiT1 critical for cell proliferation and independent of its phosphate transport activity. J Biol Chem 2009; 284:31363–74.

Bergwitz C, Jüppner H. Phosphate Sensing. Adv Chronic Kidney Dis 2011; 18:132–144.

Bhandari S, Ives N, Brettell EA, Valente M, Cockwell P, Topham PS, et al. Multicentre randomized controlled trial of angiotensin-converting enzyme inhibitor/angiotensin receptor blocker withdrawal in advanced renal disease: the STOP-ACEi trial. Nephrol Dial Transplant 2016; 31:255–61.

Bild DE, Detrano R, Peterson D, Guerci A, Liu K, Shahar E, et al. Ethnic differences in coronary calcification: the Multi-Ethnic Study of Atherosclerosis (MESA). Circulation 2005; 111:1313–20.

Block GA, Hulbert-Shearon TE, Levin NW, Port FK. Association of serum phosphorus and calcium x phosphate product with mortality risk in chronic hemodialysis patients: a national study. Am J Kidney Dis 1998; 31:607–17.

Block GA, Klassen PS, Lazarus JM, Ofsthun N, Lowrie EG, Chertow GM. Mineral metabolism, mortality, and morbidity in maintenance hemodialysis. J Am Soc Nephrol 2004; 15:2208–18.

Bohr DF, Webb RC. Vascular Smooth Muscle Function and Its Changes in Hypertension. Am J Med 1984; 77:3–16.

Bos JL. Linking Rap to cell adhesion. Curr Opin Cell Biol 2005; 17:123–128.

Bøttger P, Pedersen LC-P. Mapping of the minimal inorganic phosphate transporting unit of human PiT2 suggests a structure universal to PiT-related proteins from all kingdoms of life. BMC Biochem 2011; 12:21.

Bourgine A, Pilet P, Diouani S, Sourice S, Lesoeur J, Beck-Cormier S, et al. Mice with hypomorphic expression of the sodium-phosphate cotransporter PiT1/Slc20a1 have an unexpected normal bone mineralization. PLoS One 2013; 8:e65979.

Burke AP, Farb A, Malcom GT, Liang Y, Smialek JE, Virmani R, et al. Plaque Rupture and Sudden Death Related to Exertion in Men With Coronary Artery Disease. JAMA 1999; 281:921.

Burke AP, Taylor A, Farb A, Malcom GT, Virmani R. Coronary calcification: insights from sudden coronary death victims. Zeitschrift für Kardiol 2000; 89 Suppl 2:49–53.

Burnett S-AM, Gunawardene SC, Bringhurst FR, Jüppner H, Lee H, Finkelstein JS. Regulation of C-Terminal and Intact FGF-23 by Dietary Phosphate in Men and Women. J Bone Miner Res 2006; 21:1187–1196.

Butany J, Collins MJ, Demellawy DEI, Nair V, Israel N, Leong SW, et al. Morphological and clinical findings in 247 surgically excised native aortic valves. Can J Cardiol 2005; 21:747–55.

Cargnello M, Roux PP. Activation and function of the MAPKs and their substrates, the MAPK-activated protein kinases. Microbiol Mol Biol Rev 2011; 75:50–83.

Casas JP, Chua W, Loukogeorgakis S, Vallance P, Smeeth L, Hingorani AD, et al. Effect of inhibitors of the renin-angiotensin system and other antihypertensive drugs on renal outcomes: systematic review and meta-analysis. Lancet 2005; 366:2026–2033.

Chavkin NW, Chia JJ, Crouthamel MH, Giachelli CM. Phosphate uptake-independent signaling functions of the type III sodium-dependent phosphate transporter, PiT-1, in vascular smooth muscle cells. Exp Cell Res 2015; 333:39–48.

Cross HS, Debiec H, Peterlik M. Mechanism and regulation of intestinal phosphate absorption. Miner Electrolyte Metab 1990; 16:115–24.

Crouthamel MH, Lau WL, Leaf EM, Chavkin NW, Wallingford MC, Peterson DF, et al. Sodium-Dependent Phosphate Cotransporters and Phosphate-Induced Calcification of Vascular Smooth Muscle Cells: Redundant Roles for PiT-1 and PiT-2. Arterioscler Thromb Vasc Biol 2013; 33:2625–2632.

Cruzalegui FH, Cano E, Treisman R. ERK activation induces phosphorylation of Elk-1 at multiple S/T-P motifs to high stoichiometry.

Cupisti A, Gallieni M, Rizzo MA, Caria S, Meola M, Bolasco P. Phosphate Control in Dialysis. *Int J Nephrol Renovasc Dis* 2013; 6:193–205.

Davies MJ, Thomas AC. Plaque fissuring--the cause of acute myocardial infarction, sudden ischaemic death, and crescendo angina. Br Heart J 1985; 53:363–73.

Detrano R, Guerci AD, Carr JJ, Bild DE, Burke G, Folsom AR, et al. Coronary calcium as a predictor of coronary events in four racial or ethnic groups. N Engl J Med 2008; 358:1336–45.

Dhingra R, Sullivan LM, Fox CS, Wang TJ, D'Agostino Sr. RB, Gaziano JM, et al. Relations of serum phosphorus and calcium levels to the incidence of cardiovascular disease in the community. Arch Intern Med 2007; 167:879–85.

Ducy P, Zhang R, Geoffroy V, Ridall AL, Karsenty G. Osf2/Cbfa1: A Transcriptional Activator of Osteoblast Differentiation. Cell 1997; 89:747–754.

Dujardin KS, Enriquez-Sarano M, Schaff H V, Bailey KR, Seward JB, Tajik AJ. Mortality and morbidity of aortic regurgitation in clinical practice. A long-term follow-up study. Circulation 1999; 99:1851–7.

El-Abbadi MM, Pai AS, Leaf EM, Yang H-Y, Bartley BA, Quan KK, et al. Phosphate feeding induces arterial medial calcification in uremic mice: role of serum phosphorus, fibroblast growth factor-23, and osteopontin. Kidney Int 2009; 75:1297–307.

Everhart JE, Pettitt DJ, Knowler WC, Rose FA, Bennett PH. Medial arterial calcification and its association with mortality and complications of diabetes. Diabetologia 1987; 31:16–23.

Festing MH, Speer MY, Yang H-Y, Giachelli CM. Generation of mouse conditional and null alleles of the type III sodium-dependent phosphate cotransporter PiT-1. Genesis 2009; 47:858–63.

Fitzgerald PJ, Ports TA, Yock PG. Contribution of localized calcium deposits to dissection after angioplasty. An observational study using intravascular ultrasound. Circulation 1992; 86:64–70.

Foley RN, Parfrey PS, Sarnak MJ. Clinical epidemiology of cardiovascular disease in chronic renal disease. Am J Kidney Dis 1998; 32:S112–9.

Forand A, Beck L, Leroy C, Rousseau A, Boitez V, Cohen I, et al. EKLF-driven PIT1 expression is critical for mouse erythroid maturation in vivo and in vitro. Blood 2013; 121:666–78.

Ge C, Xiao G, Jiang D, Yang Q, Hatch NE, Roca H, et al. Identification and Functional Characterization of ERK/MAPK Phosphorylation Sites in the Runx2 Transcription Factor. J Biol Chem 2009; 284:32533–32543.

Giral H, Cranston D, Lanzano L, Caldas Y, Sutherland E, Rachelson J, et al. NHE3 Regulatory Factor 1 (NHERF1) Modulates Intestinal Sodium-dependent Phosphate Transporter (NaPi-2b) Expression in Apical Microvilli. J Biol Chem 2012; 287:35047–35056.

Giral H, Lanzano L, Caldas Y, Blaine J, Verlander JW, Lei T, et al. Role of PDZK1 Protein in Apical Membrane Expression of Renal Sodium-coupled Phosphate Transporters. J Biol Chem 2011; 286:15032–15042.

Goldsmith DJ, Covic A, Sambrook PA, Ackrill P. Vascular calcification in long-term haemodialysis patients in a single unit: a retrospective analysis. Nephron 1997; 77:37–43 ST – Vascular calcification in long–term ha.

Gomez D, Owens GK. Smooth muscle cell phenotypic switching in atherosclerosis. Cardiovasc Res 2012; 95:156–64.

Gotoh T, Hattori S, Nakamura S, Kitayama H, Noda M, Takai Y, et al. Identification of Rap1 as a target for the Crk SH3 domain-binding guanine nucleotide-releasing factor C3G. Mol Cell Biol 1995; 15:6746–6753.

Gross L, Epstein EZ, Kugel MA. Histology of the Coronary Arteries and their Branches in the Human Heart. Am J Pathol 1934; 10:253–274.7.

Guérin AP, Pannier B, Métivier F, Marchais SJ, London GM. Assessment and significance of arterial stiffness in patients with chronic kidney disease. Curr Opin Nephrol Hypertens 2008; 17:635–641.

Hruska KA, Mathew S, Lund R, Qiu P, Pratt R. Hyperphosphatemia of chronic kidney disease. Kidney Int 2008; 74:148–57.

Hutchison AJ, Smith CP, Brenchley PEC. Pharmacology, efficacy and safety of oral phosphate binders. Nat Rev Nephrol 2011; 7:578–89.

Hunt JL, Fairman R, Mitchell ME, Carpenter JP, Golden M, Khalapyan T, *et al.* Bone formation in carotid plaques: a clinicopathological study. *Stroke* 2002; 33:1214–9.

Isakova T, Wahl P, Vargas GS, Gutiérrez OM, Scialla J, Xie H, et al. Fibroblast growth factor 23 is elevated before parathyroid hormone and phosphate in chronic kidney disease. Kidney Int 2011; 79:1370–8.

Ito M, Haito S, Furumoto M, Uehata Y, Sakurai A, Segawa H, et al. Unique uptake and efflux systems of inorganic phosphate in osteoclast-like cells. Am J Physiol Cell Physiol 2007; 292:C526–34.

Johann S V, Gibbons JJ, O'Hara BC-P. GLVR1, a receptor for gibbon ape leukemia virus, is homologous to a phosphate permease of Neurospora crassa and is expressed at high levels in the brain and thymus. J Virol 1992; 66:1635–40 ST – GLVR1, a receptor for gibbon ape leu.

Jono S, McKee MD, Murry CE, Shioi a., Nishizawa Y, Mori K, et al. Phosphate Regulation of Vascular Smooth Muscle Cell Calcification. Circ Res 2000; 87:e10–e17.

Kapustin AN, Chatrou MLL, Drozdov I, Zheng Y, Davidson SM, Soong D, et al. Vascular Smooth Muscle Cell Calcification Is Mediated by Regulated Exosome Secretion. Circ Res 2015; 116:1312–1323.

Kapustin AN, Davies JD, Reynolds JL, McNair R, Jones GT, Sidibe A, et al. Calcium regulates key components of vascular smooth muscle cell-derived matrix vesicles to enhance mineralization. Circ Res 2011; 109:e1–12.

Kapustin AN, Shanahan CM. Calcium Regulation of Vascular Smooth Muscle Cell-Derived Matrix Vesicles. Trends Cardiovasc Med Published Online First: 15 August 2012. doi:10.1016/j.tcm.2012.07.009

Kavanaugh MP, Kabat D. Identification and characterization of a widely expressed phosphate transporter/retrovirus receptor family. Kidney Int 1996; 49:959–63 ST – Identification and characterization o.

Kawai-Kowase K, Owens GK. Multiple repressor pathways contribute to phenotypic switching of vascular smooth muscle cells. Am J Physiol Cell Physiol 2007; 292:C59–69.

Kestenbaum B, Belozeroff V. Mineral metabolism disturbances in patients with chronic kidney disease. Eur J Clin Invest 2007; 37:607–22.

Kestenbaum BR, Adeney KL, de Boer IH, Ix JH, Shlipak MG, Siscovick DS. Incidence and progression of coronary calcification in chronic kidney disease: the Multi-Ethnic Study of Atherosclerosis. Kidney Int 2009; 76:991–8.

Khoshniat S, Bourgine A, Julien M, Weiss P, Guicheux J, Beck L. The emergence of phosphate as a specific signaling molecule in bone and other cell types in mammals. Cell Mol Life Sci 2011; 68:205–18 ST – The emergence of phosphate as a speci.

Kimata M, Michigami T, Tachikawa K, Okada T, Koshimizu T, Yamazaki M, et al. Signaling of extracellular inorganic phosphate up-regulates cyclin D1 expression in proliferating chondrocytes via the Na+/Pi cotransporter Pit-1 and Raf/MEK/ERK pathway. Bone 2010; 47:938–947.

Koh N, Fujimori T, Nishiguchi S, Tamori A, Shiomi S, Nakatani T, et al. Severely reduced production of klotho in human chronic renal failure kidney. Biochem Biophys Res Commun 2001; 280:1015–20.

Koos R, Mahnken AH, Dohmen G, Brehmer K, Günther RW, Autschbach R, et al. Association of aortic valve calcification severity with the degree of aortic regurgitation after transcatheter aortic valve implantation. Int J Cardiol 2011; 150:142–145.

Kullo IJ, Bielak LF, Turner ST, Sheedy PF, Peyser PA. Aortic Pulse Wave Velocity Is Associated With the Presence and Quantity of Coronary Artery Calcium: A Community-Based Study. Hypertension 2006; 47:174–179.

LeGeros RZ. Formation and transformation of calcium phosphates: relevance to vascular calcification. Zeitschrift Kardiol 2001; 90:III116–III124.

Leskinen Y, Salenius JP, Lehtimäki T, Huhtala H, Saha H. The prevalence of peripheral arterial disease and medial arterial calcification in patients with chronic renal failure: Requirements for diagnostics. Am J Kidney Dis 2002; 40:472–479.

Levin A, Bakris GL, Molitch M, Smulders M, Tian J, Williams LA, et al. Prevalence of abnormal serum vitamin D, PTH, calcium, and phosphorus in patients with chronic kidney disease: results of the study to evaluate early kidney disease. Kidney Int 2007; 71:31–8.

Li X, Yang H-YY, Giachelli CM. Role of the sodium-dependent phosphate cotransporter, Pit-1, in vascular smooth muscle cell calcification. Circ Res 2006; 98:905–12.

Liu L, Sánchez-Bonilla M, Crouthamel M, Giachelli C, Keel S. Mice lacking the sodium-dependent phosphate import protein, PiT1 (SLC20A1), have a severe defect in terminal erythroid differentiation and early B-cell development. Exp Hematol Published Online First: 30 January 2013. doi:10.1016/j.exphem.2013.01.004

Lomashvili KA, Garg P, Narisawa S, Millan JL, O'Neill WC. Upregulation of alkaline phosphatase and pyrophosphate hydrolysis: potential mechanism for uremic vascular calcification. Kidney Int 2008; 73:1024–30.

London GM, Guérin AP, Marchais SJ, Métivier F, Pannier B, Adda H. Arterial media calcification in end-stage renal disease: impact on all-cause and cardiovascular mortality. Nephrol Dial Transplant 2003; 18:1731–40.

Loria CM, Liu K, Lewis CE, Hulley SB, Sidney S, Schreiner PJ, et al. Early Adult Risk Factor Levels and Subsequent Coronary Artery Calcification. The CARDIA Study. J Am Coll Cardiol 2007; 49:2013–2020.

Maldonado N, Kelly-Arnold A, Vengrenyuk Y, Laudier D, Fallon JT, Virmani R, et al. A mechanistic analysis of the role of microcalcifications in atherosclerotic plaque stability: potential implications for plaque rupture. Am J Physiol Heart Circ Physiol 2012; 303:H619–28.

Maréchal C, Coche E, Goffin E, Dragean A, Schlieper G, Nguyen P, et al. Progression of Coronary Artery Calcification and Thoracic Aorta Calcification in Kidney Transplant Recipients. Am J Kidney Dis Published Online First: 2011. doi:S0272-6386(11)01195-4 [pii] 10.1053/j.ajkd.2011.07.019 LA - ENG

Mathews SJ, de Las Fuentes L, Podaralla P, Cabellon A, Zheng S, Bierhals A, et al. Effects of sodium thiosulfate on vascular calcification in end-stage renal disease: a pilot study of

feasibility, safety and efficacy. Am J Nephrol 2011; 33:131–8 ST – Effects of sodium thiosulfate on vascu.

Meaume S, Benetos A, Henry OF, Rudnichi A, Safar ME. Aortic Pulse Wave Velocity Predicts Cardiovascular Mortality in Subjects >70 Years of Age. Arterioscler Thromb Vasc Biol 2001; 21:2046–2050.

Meloche S, Pouysségur J. The ERK1/2 mitogen-activated protein kinase pathway as a master regulator of the G1- to S-phase transition. Oncogene 2007; 26:3227–39.

Miyamoto K, Haito-Sugino S, Kuwahara S, Ohi A, Nomura K, Ito M, et al. Sodium-dependent phosphate cotransporters: lessons from gene knockout and mutation studies. J Pharm Sci 2011; 100:3719–30 ST – Sodium–dependent phosphate cotranspo.

Moe S, Drüeke T, Cunningham J, Goodman W, Martin K, Olgaard K, et al. Definition, evaluation, and classification of renal osteodystrophy: A position statement from Kidney Disease: Improving Global Outcomes (KDIGO). Kidney Int 2006; 69:1945–1953.

Moe SM, O'Neill KD, Duan D, Ahmed S, Chen NX, Leapman SB, et al. Medial artery calcification in ESRD patients is associated with deposition of bone matrix proteins. Kidney Int 2002; 61:638–47.

Mohler ER, Gannon F, Reynolds C, Zimmerman R, Keane MG, Kaplan FS. Bone formation and inflammation in cardiac valves. *Circulation* 2001; 103:1522–8.

Murer H, Hernando N, Forster I, Biber J. Regulation of Na/Pi transporter in the proximal tubule. Annu Rev Physiol 2003; 65:531–42.

Murphy RA, Herlihy JT, Megerman J. Force-Generating Capacity and Contractile Protein Content of Arterial Smooth Muscle. J Gen Physiol 1974; 64:691–705.

Nguyen AT, Gomez D, Bell RD, Campbell JH, Clowes AW, Gabbiani G, et al. Smooth muscle cell plasticity: fact or fiction? Circ Res 2013; 112:17–22.

Noordzij M, Korevaar JC, Bos WJ, Boeschoten EW, Dekker FW, Bossuyt PM, et al. Mineral metabolism and cardiovascular morbidity and mortality risk: peritoneal dialysis patients compared with haemodialysis patients. Nephrol Dial Transpl 2006; 21:2513–20 ST – Mineral metabolism and cardiovascula.

Ohba Y, Ikuta K, Ogura A, Matsuda J, Mochizuki N, Nagashima K, et al. Requirement for C3G-dependent Rap1 activation for cell adhesion and embryogenesis. EMBO J 2001; 20:3333–3341.

Oshima Y, Tohe A, Matsumoto K. [Regulatory circuits for gene expression: the metabolism of galactose and phosphate in Saccharomyces cerevisiae]. Tanpakushitsu Kakusan Koso 1984; 29:14–28.

Otto CM, Burwash IG, Legget ME, Munt BI, Fujioka M, Healy NL, et al. Prospective study of asymptomatic valvular aortic stenosis. Clinical, echocardiographic, and exercise predictors of outcome. Circulation 1997; 95:2262–70.

Otto CM, Lind BK, Kitzman DW, Gersh BJ, Siscovick DS. Association of Aortic-Valve Sclerosis with Cardiovascular Mortality and Morbidity in the Elderly. http://dx.doi.org/101056/NEJM199907153410302 1999.

Owens GK, Kumar MS, Wamhoff BR. Molecular Regulation of Vascular Smooth Muscle Cell Differentiation in Development and Disease. 2004; :767–801.

Pai A, Leaf EM, El-Abbadi M, Giachelli CM. Elastin degradation and vascular smooth muscle cell phenotype change precede cell loss and arterial medial calcification in a uremic mouse model of chronic kidney disease. Am J Pathol 2011; 178:764–73.

Pasch A, Schaffner T, Huynh-Do U, Frey BM, Frey FJ, Farese S. Sodium thiosulfate prevents vascular calcifications in uremic rats. Kidney Int 2008; 74:1444–53 ST – Sodium thiosulfate prevents vascular.

Peach MJ. Renin-Angiotensin System: Biochemistry and Mechanisms of Action. *Physiol REVIE ws* 1977; 57.

Penido MGMG, Alon US. Phosphate homeostasis and its role in bone health. Pediatr Nephrol 2012; 27:2039–48.

Proudfoot D, Skepper JN, Hegyi L, Bennett MR, Shanahan CM, Weissberg PL. Apoptosis regulates human vascular calcification in vitro: evidence for initiation of vascular calcification by apoptotic bodies. Circ Res 2000; 87:1055–62.

Qunibi W, Moustafa M, Muenz LR, He DY, Kessler PD, Diaz-Buxo JA, et al. A 1-Year Randomized Trial of Calcium Acetate Versus Sevelamer on Progression of Coronary Artery Calcification in Hemodialysis Patients With Comparable Lipid Control: The Calcium Acetate Renagel Evaluation-2 (CARE-2) Study. Am J Kidney Dis 2008; 51:952–965.

Raggi P, Boulay A, Chasan-Taber S, Amin N, Dillon M, Burke SK, et al. Cardiac calcification in adult hemodialysis patients. J Am Coll Cardiol 2002; 39:695–701.

Reimer RJ. SLC17: a functionally diverse family of organic anion transporters. Mol Aspects Med 2013; 34:350–9.

Reynolds JL, Joannides AJ, Skepper JN, McNair R, Schurgers LJ, Proudfoot D, et al. Human vascular smooth muscle cells undergo vesicle-mediated calcification in response to changes in extracellular calcium and phosphate concentrations: a potential mechanism for accelerated vascular calcification in ESRD. J Am Soc Nephrol 2004; 15:2857–67.

Reynolds JL, Skepper JN, McNair R, Kasama T, Gupta K, Weissberg PL, et al. Multifunctional roles for serum protein fetuin-a in inhibition of human vascular smooth muscle cell calcification. J Am Soc Nephrol 2005; 16:2920–30.

Roskoski R. ERK1/2 MAP kinases: Structure, function, and regulation. Pharmacol Res 2012; 66:105–143.

Russo D, Miranda I, Ruocco C, Battaglia Y, Buonanno E, Manzi S, et al. The progression of coronary artery calcification in predialysis patients on calcium carbonate or sevelamer. Kidney Int 2007; 72:1255–61 ST – The progression of coronary artery c.

Salaün C, Leroy C, Rousseau A, Boitez V, Beck L, Friedlander GC-P. Identification of a novel transport-independent function of PiT1/SLC20A1 in the regulation of TNF-induced apoptosis. J Biol Chem 2010; 285:34408–18.

Salaün C, Maréchal V, Heard JM. Transport-deficient Pit2 phosphate transporters still modify cell surface oligomers structure in response to inorganic phosphate. J Mol Biol 2004; 340:39–47.

Sarnak MJ. Cardiovascular complications in chronic kidney disease. Am J Kidney Dis 2003; 41:11–17.

Shanahan CM, Crouthamel MH, Kapustin A, Giachelli CM. Arterial calcification in chronic kidney disease: key roles for calcium and phosphate. Circ Res 2011; 109:697–711 ST – Arterial calcification in chronic ki.

Shroff RC, McNair R, Figg N, Skepper JN, Schurgers L, Gupta A, et al. Dialysis accelerates medial vascular calcification in part by triggering smooth muscle cell apoptosis. Circulation 2008; 118:1748–57.

Shulman NB, Ford CE, Hall WD, Blaufox MD, Simon D, Langford HG, et al. Prognostic value of serum creatinine and effect of treatment of hypertension on renal function. Results from the hypertension detection and follow-up program. The Hypertension Detection and Follow-up Program Cooperative Group. Hypertens (Dallas, Tex 1979) 1989; 13:I80–93.

Solbu MD, Jardine AG. "To block or not to block"; whether to continue renin–angiotensin–aldosterone system blockade in advanced chronic kidney disease. Nephrol Dial Transplant 2015; 31:gfv351.

Speer MY, Li X, Hiremath PG, Giachelli CMC-P 2895022. Runx2/Cbfa1, but not loss of myocardin, is required for smooth muscle cell lineage reprogramming toward osteochondrogenesis. J Cell Biochem 2010; 110:935–47.

Speer MY, Yang H-YY, Brabb T, Leaf E, Look A, Lin W-LL, et al. Smooth muscle cells give rise to osteochondrogenic precursors and chondrocytes in calcifying arteries. Circ Res 2009; 104:733–41.

Sprague GF, Bell RM, Cronan JE. A mutant of Escherichia coli auxotrophic for organic phosphates: Evidence for two defects in inorganic phosphate transport. MGG Mol Gen Genet 1975; 143:71–77.

Stenvinkel P, Heimbürger O, Paultre F, Diczfalusy U, Wang T, Berglund L, et al. Strong association between malnutrition, inflammation, and atherosclerosis in chronic renal failure. Kidney Int 1999; 55:1899–1911.

Sutton-Tyrrell K, Najjar SS, Boudreau RM, Venkitachalam L, Kupelian V, Simonsick EM, et al. Elevated aortic pulse wave velocity, a marker of arterial stiffness, predicts cardiovascular events in well-functioning older adults. Circulation 2005; 111:3384–90.

Tatsumi S, Segawa H, Morita K, Haga H, Kouda T, Yamamoto H, et al. Molecular cloning and hormonal regulation of PiT-1, a sodium-dependent phosphate cotransporter from rat parathyroid glands. Endocrinology 1998; 139:1692–9.

Tentori F, Blayney MJ, Albert JM, Gillespie BW, Kerr PG, Bommer J, et al. Mortality risk for dialysis patients with different levels of serum calcium, phosphorus, and PTH: the Dialysis Outcomes and Practice Patterns Study (DOPPS). Am J Kidney Dis 2008; 52:519–30.

Tonelli M, Curhan G, Pfeffer M, Sacks F, Thadhani R, Melamed ML, et al. Relation between alkaline phosphatase, serum phosphate, and all-cause or cardiovascular mortality. Circulation 2009; 120:1784–92.

Tonelli M, Sacks F, Pfeffer M, Gao Z, Curhan G. Relation between serum phosphate level and cardiovascular event rate in people with coronary disease. Circulation 2005; 112:2627–33.

Toussaint ND, Lau KK, Strauss BJ, Polkinghorne KR, Kerr PG. Associations between vascular calcification, arterial stiffness and bone mineral density in chronic kidney disease. Nephrol Dial Transplant 2008; 23:586–93.

Villa-Bellosta R, Bogaert YE, Levi M, Sorribas V. Characterization of phosphate transport in rat vascular smooth muscle cells: implications for vascular calcification. Arterioscler Thromb Vasc Biol 2007; 27:1030–6.

Villa-Bellosta R, Levi M, Sorribas V. Vascular smooth muscle cell calcification and SLC20 inorganic phosphate transporters: effects of PDGF, TNF-alpha, and Pi. Pflugers Arch 2009; 458:1151–61.

Virkki L V, Biber J, Murer H, Forster IC. Phosphate transporters: a tale of two solute carrier families. Am J Physiol Renal Physiol 2007; 293:F643–54.

Vliegenthart R, Hollander M, Breteler MMB, van der Kuip DAM, Hofman A, Oudkerk M, et al. Stroke is associated with coronary calcification as detected by electron-beam CT: the Rotterdam Coronary Calcification Study. Stroke 2002; 33:462–5.

Voss AK, Gruss P, Thomas T. The guanine nucleotide exchange factor C3G is necessary for the formation of focal adhesions and vascular maturation. Development 2003; 130:355–67.

Vossler MR, Yao H, York RD, Pan M-G, Rim CS, Stork PJ. cAMP Activates MAP Kinase and Elk-1 through a B-Raf- and Rap1-Dependent Pathway. Cell 1997; 89:73–82.

Wada T, Penninger JM. Mitogen-activated protein kinases in apoptosis regulation. Oncogene 2004; 23:2838–49.

Wallingford MC, Chia J, Leaf EM, Borgeia S, Chavkin NW, Sawangmake C, *et al.* SLC20A2 deficiency in mice leads to elevated phosphate levels in cerbrospinal fluid and glymphatic pathway-associated arteriolar calcification, and recapitulates human idiopathic basal ganglia calcification. *Brain Pathol* Published Online First: 29 January 2016. doi:10.1111/bpa.12362

Wallingford MC, Gammill HS, Giachelli CM. Slc20a2 deficiency results in fetal growth restriction and placental calcification associated with thickened basement membranes and novel CD13 and lamininα1 expressing cells. Reprod Biol 2016; 16:13–26.

Wang J, Huo K, Ma L, Tang L, Li D, Huang X, et al. Toward an understanding of the protein interaction network of the human liver. Mol Syst Biol 2011; 7:536.

Wang Z, Dillon TJ, Pokala V, Mishra S, Labudda K, Hunter B, et al. Rap1-Mediated Activation of Extracellular Signal-Regulated Kinases by Cyclic AMP Is Dependent on the Mode of Rap1 Activation. Mol Cell Biol 2006; 26:2130–2145.

Werner A, Dehmelt L, Nalbant P. Na+-dependent phosphate cotransporters: the NaPi protein families. J Exp Biol 1998; 201:3135–42.

Willum-Hansen T, Staessen JA, Torp-Pedersen C, Rasmussen S, Thijs L, Ibsen H, et al. Prognostic value of aortic pulse wave velocity as index of arterial stiffness in the general population. Circulation 2006; 113:664–70.

Wilson PW, Kauppila LI, O'Donnell CJ, Kiel DP, Hannan M, Polak JM, et al. Abdominal aortic calcific deposits are an important predictor of vascular morbidity and mortality. Circulation 2001; 103:1529–34.

Witteman JM, Kok F, Van Saase JCM, Valkenburg H. AORTIC CALCIFICATION AS A PREDICTOR OF CARDIOVASCULAR MORTALITY. Lancet 1986; 328:1120–1122.

Yamazaki M, Ozono K, Okada T, Tachikawa K, Kondou H, Ohata Y, et al. Both FGF23 and extracellular phosphate activate Raf/MEK/ERK pathway via FGF receptors in HEK293 cells. J Cell Biochem 2010; 111:1210–1221.

Yoshida T, Sinha S, Dandré F, Wamhoff BR, Hoofnagle MH, Kremer BE, et al. Myocardin is a key regulator of CArG-dependent transcription of multiple smooth muscle marker genes. Circ Res 2003; 92:856–64.

CURRICULUM VITAE

Education

Ph.D., Bioengineering, University of Washington — August 2016
Thesis: "Elevated Phosphate-Induced Cell Signaling through Phosphate Transporter PiT-1 in Vascular Smooth Muscle Cells" — Seattle, WA
Advisor: Cecilia Giachelli

M.S., Biomedical Engineering, University of Southern California — May 2011
Los Angeles, CA

B.S., Biomedical (Biochemical) Engineering, University of Southern California — May 2010
Los Angeles, CA

Research Experience

Graduate Student, University of Washington — June 2011 – September 2016
Advisor: Dr. Cecilia Giachelli

- Researched vascular calcification; cell signaling in vascular smooth muscle cells
- Researched the molecular mechanisms leading to hydroxyapatite deposition in the vasculature by elevated inorganic phosphate cell signaling by the phosphate transporter PiT-1 in vascular smooth muscle cells

Intelligent Optical Systems - Research Intern — January 2011 – May 2011
Advisor: Dr. Glenn Bastiaans

- Created nanoparticles to engineer optical devices that can detect cancer markers

University of Southern California – Undergrad Lab Researcher — August 2008 – May 2011
Advisor: Dr. Steven Finkel

- Researched microbial fuel cell design to turn cell energy into voltage. Involved multiparameter assessment of Shewanella species for characteristics of interest for commercial exploitation.

University of Washington - Research Assistant — Summer 2010
Advisor: Dr. Charles Chavkin

- Developed viral vectors for insertion of genes with cre-lox sequences into murine neural cells

University of Washington – Research Assistant — Summer 2008, 2009
Advisor: Dr. David Baker

- Engineered novel genes to optimize expression of a novel CO2 fixation pathway in E. coli. Involved cloning and expression of yeast genes in E. coli, characterization of the engineered strains, development of directed evolution approaches for pathway optimization, and development of new screening vectors for optimization of engineered proteins

Publications

Chavkin NW, Brooks KE, Soberg EM, Wallingford MC, Lund SM, Giachelli CM. Rap1 guanine nucleotide exchange factor, RapGEF1, is required for sodium-dependent phosphate transporter PiT-1 mediated phosphate signaling through ERK1/2 and inhibition of smooth muscle 22 alpha in vascular smooth muscle cells. In Preparation.

Chavkin NW, Chia J, Crouthamel MH, Giachelli CM. Phosphate uptake-independent signaling functions of the type III sodium-dependent phosphate transporter, PiT-1, in vascular smooth muscle cells. Exp Cell Res. 2015 Apr 10;333(1):39-48.

Wallingford MC, Chia J, Leaf EM, Borqeia S, Chavkin NW, Sawanqmake C, Marro K, Cox T, Speer M, Giachelli CM. Slc20a2 deficiency in mice leads to elevated phosphate levels in cerebrospinal fluid and glymphatic pathway-associated arteriolar calcification, and recapitulates human idiopathic basal ganglia calcification. Brain Pathology. Submitted Sept 21, 2015, accepted with minor revisions and soon to be published.

Crouthamel MH, Lau WL, Leaf EM, Chavkin NW, Wallingford MC, Peterson DF, Li X, Liu Y, Chin MT, Levi M, Giachelli CM. Sodium-dependent phosphate cotransporters and phosphate-induced calcification of vascular smooth muscle cells: redundant roles for PiT-1 and PiT-2. Arterioscler Thromb Vasc Biol. 2013 Nov;33(11):2625-32.

Scialla JJ, Lau WL, Reilly MP, Isakova T, Yang HY, Crouthamel MH, Chavkin NW, Rahman M, Wahl P, Amaral AP, Hamano T, Master SR, Nessel L, Chai B, Xie D, Kallem RR, Chen J, Lash JP, Kusek JW, Budoff MJ, Giachelli CM, Wolf M; Chronic Renal Insufficiency Cohort Study Investigators. Fibroblast growth factor 23 is not associated with and does not induce arterial calcification. Kidney Int. 2013 Jun;83(6):1159-68.

Schindler AG, Messinger DI, Smith JS, Shankar H, Gustin RM, Schattauer SS, Lemos JC, Chavkin NW, Hagan CE, Neumaier JF, Chavkin C. Stress produces aversion and potentiates cocaine reward by releasing endogenous dynorphins in the ventral striatum to locally stimulate serotonin reuptake. J Neurosci. 2012 Dec 5;32(49):17582-96.

Funding Awards

National Institute of Health Predoctoral National Research Service Award (F31 HL129649), National Heart, Lung, and Blood Institute, July 1st 2015 – June 30th 2017. Competitive grant awarded June 2015 for pre-doctoral training based on research proposal, mentor training plan, and previous experience.

American Heart Association Predoctoral Fellowship. Competitive grant awarded May 2015 for pre-doctoral training based on research proposal, mentor training plan, and previous experience. Funding could not be awarded concurrently with NIH F31.

Bioengineering Cardiovascular Training Grant (BCTG) (T32 EB001650, Dr. Michael Regnier), University of Washington, June 15th, 2013 – June 14th, 2015. Competitive application based on current research progress, mentor training plan, and future research goals for graduate funding through a T32 training grant focused on cardiovascular science and engineering.

USC Viterbi School of Engineering Merit Research Scholarship awarded for 2009/2010 academic year. Selective competitive scholarship awarded for scientific research to students who demonstrate outstanding academic progress.

Conference Presentations

Chavkin NW, Chia J, Giachelli CM. Phosphate uptake-independent cell signaling through PiT-1 promotes elevated phosphate-induced ERK1/2 phosphorylation, osteochondrogenic differentiation, and calcification in vascular smooth muscle cells. Oral Abstract Presentation and Poster Presentation. North American Vascular Biology Organization, Vascular Biology Conference, Hyannis MA, October 18th-22nd 2015.

Chavkin NW and Giachelli CM. PiT-1 Signaling through ERK1/2 Promotes Smooth Muscle Cell Osteochondrogenic Phenotype Change and Calcification. Oral Abstract Presentation. American Society of Nephrology, Kidney Week Conference, Philadelphia PA, November 11th-16th 2014.

Chavkin NW and Giachelli CM. Engineering the sodium-dependent phosphate transporter, PiT-1, in vascular smooth muscle cells to elucidate novel cell signaling mechanisms that mediate matrix mineralization. Poster Presentation. National Institute of Biomedical Imaging and Bioengineering, Training Grantees Meeting. June 5th-6th 2014.

Chavkin NW, Crouthamel MH, Giachelli CM. Phosphate Transport-Dependent and –Independent functions of the Sodium Dependent Phosphate Transporter, PiT-1, in Vascular Smooth Muscle Cell Mineralization. Oral Abstract Presentation. American Society of Nephrology, Kidney Week Conference, Atlanta GA, November 7th-10th 2013.

Chavkin NW, Crouthamel MH, Giachelli CM. Engineering PiT-1 in Vascular Smooth Muscle Cells: Role of Phosphate Uptake in Matrix Calcification. Poster Presentation. Biomedical Engineering Society, Annual Meeting, Seattle WA, September 25th-28th 2013.

Seminars/Talks

"Phosphate transporter PiT-1 and ERK1/2 signaling: Phosphate sensing and response in vascular smooth muscle cells." Bioengineering Cardiovascular Training Grant Symposium. July 25th 2014.

"Effects of PiT-1 and Inorganic Phosphate on Calcification of Vascular Smooth Muscle Cells." Bioengineering/Chemical Engineering 511 Biomaterials Seminar. October 11th 2012.

Mentor Experience

Kadin Brooks. University of Washington Undergraduate Student Researcher and Capstone Student in the Giachelli Lab, October 2013 – June 2015. I directly supervised Kadin's projects that included investigating the role of the intracellular domain of PiT-1, and engineering fluorescently-tagged PiT-1 and PiT-2 constructs for use in protein localization and FRET imaging. Kadin's awards at the University of Washington:

- Stanford Amgen Scholars Program Summer 2015: Competitive summer program awarded to undergraduate students with strong academic records, research experience, and show promise as future graduate students. Includes a nine-week research program at a lab in Stanford, GRE prep courses, and professional development courses.
- Mary Gates Research Award 2014, 2015: Competitive application awarded to students for stipend towards laboratory research at UW; awarded to Kadin twice.
- Presentations at the UW Undergraduate Research Symposium 2014, 2015. Kadin presented posters of his current work in Spring 2014 and 2015 at a symposium organized by UW to showcase undergraduate research.

Tiffany Gray. University of Washington Summer Research Student in the Giachelli Lab through the Building Bridges to Bioengineering program, Summer 2013. I directly supervised Tiffany's project that included generating point mutations in PiT-2. Although only in lab for a Summer, Tiffany learned valuable laboratory skills, including PCR, gel electrophoresis, and site-directed mutagenesis.

Teaching Experience

University of Washington – Teaching Assistant Spring 2016

- Professors Suzie Pun, Marta Scatena, and Michael Regnier
- Teaching assistant for BIOEN 345: Failure Analysis and Human Physiology
- Junior level Bioengineering course with 58 students
- Presented one lecture, designed and organized multiple lab sections, graded midterms

University of Southern California - Teacher's Assistant: Grader Fall 2010 – May 2011

- Professor Jean-Michel Maarek
- Grader for BME 405L: Senior Project Design
- Grader for BME 302L: Medical Devices